# Linking Intracellular Events to Network Reorganization in Sleep-Dependent Memory Consolidation

by
James Delorme

A dissertation submitted in partial fulfillment
of requirements for the degree of
Doctor of Philosophy
(Neuroscience)
in the University of Michigan
2020

Doctoral Committee:

Associate Professor Sara J. Aton, Chair
Professor Richard Hume
Associate Professor Ryan Mills
Professor Michael Sutton
Assistant Professor Natalie Tronson

“I believe there are techniques of the human mind whereby, in its dark deep, problems are examined, rejected or accepted. Such activities sometimes concern facets a man does not know he has. How often one goes to sleep troubled and full of pain, not knowing what causes the travail, and in the morning a whole new direction and a clearness is there…”

John Steinbeck, East of Eden

James E. Delorme
delormej@umich.edu
ORCID ID: 0000-0003-2149-4583

# Acknowledgments

My thesis would not have been possible without the support of my family, friends, and mentors (past and present). I thank you all.

To Sruti, you are my person. I love you tremendously and I'm thankful for all of the support and love you've given me through this process.

To my parents, this has been quite the ride. From Delaware, to Switzerland, and now to Michigan you guys have supported and trusted me in my academic pursuit. I love you both and it means the world to me that you're driving up to watch me defend my thesis even through COVID.

To my boss Sara. You are going to be the best boss I ever work for and I hate realizing that this early in my career. Through all of this you've always found time to chat with me about new ideas and directions and supported me in all my graduate and post-graduate endeavors. Thank you times a million.

To Sha. It has been an honor to work next to you over the past five years. Your daily optimism, kindness, and friendship has meant the world to me and I cannot imagine making it through my PhD without you. Thank you.

To Varna, my brilliant undergrad who is now going to get her MPH and eventually will run the world, you have been an amazing research assistant. I was continually in awe at how quickly you picked up new techniques and how hard you were willing to work. It was truly great getting to know you and I genuinely can't wait to see what you do next.

To all the members of the Aton lab, thank you for making lab so much fun! I will miss all of you (past and present).

# Table of Contents

# List of Figures

# List of Abbreviations

| | |
|---|---|
| **CNO** | Clozapine-N-Oxide |
| **CFC** | Contextual Fear Conditioning |
| **DG** | Dentate Gyrus |
| **DREADDs** | Designer Receptor Exclusively Activated By Designer Drugs |
| **EMG** | Electromyogram |
| **IEG** | Immediate-Early Gene |
| **LFP** | Local Field Potential |
| **LTP** | Long Term Potentiation |
| **MB** | Membrane-bound |
| **NREM** | Non-Rapid Eye Movement |
| **PCA** | Principal Component Analysis |
| **REM** | Rapid Eye Movement |
| **SWS** | Slow Wave Sleep |
| **SWR** | Sharp Wave Ripple |
| **SST** | Somatostatin |
| **SD** | Sleep Deprivation |
| **TRAP** | Translating Ribosome Affinity Purification |
| **PVALB** | Parvalbumin |
| **ZT0** | Zeitgeber Time Zero (Lights On) |

# Abstract

Research in animal and human subjects has found that sleep loss profoundly disrupts the consolidation of hippocampus-dependent memories. One leading hypothesis regarding how sleep consolidates memories is by increasing protein synthesis, thereby translating any synaptic plasticity transcripts expressed during wakefulness. Still it remains unclear how translational processes or differences in hippocampal activity are modulated during sleep or which transcripts are necessary for memory consolidation. The studies outlined in this dissertation aim to address this question in the context of a well-studied form of sleep-dependent memory consolidation in mice, contextual fear memory (CFM). CFM is disrupted by sleep loss in the first few hours following CFM.

To describe the contributions of sleep and learning on hippocampal protein translation, we modified existing translating ribosome affinity purification (TRAP) techniques to immunoprecipitate ribosome-bound mRNAs from multiple hippocampal cell populations in the same tissue and isolate transcripts from different subcellular fractions. Our protocol allowed us to quantify differences in ribosome-bound mRNAs from excitatory and ‘activated’ neurons, as well mRNA from whole hippocampal homogenate from the same mice. To further characterize differences in translation based on ribosomes intracellular localization, we separated free-floating from membrane-bound (MB)

ribosomes and analyzed them separately. Our results identified divergent effects of SD and learning on cytosolic and MB ribosomes, respectively. At cytosolic ribosomes, SD increased the expression of synaptic plasticity genes and occluded the sparse expression of CFC-related genes in excitatory hippocampal neurons. In MB ribosomes, CFC induced overlapping cellular pathways in both sleep permitted and SD mice. However we also detected ribosome-associated enrichments of transcripts for components of bioenergetic pathways not observed in sleeping mice. These results reveal how SD differentially impairs CFC-related protein translation in two distinct subcellular compartments.

Since sleep deprivation impairs protein synthesis and hippocampus-dependent memory tasks, we analyzed the phosphorylation of the ribosomal S6 protein (pS6) in mice following CFC and subsequent sleep or SD. S6 is phosphorylated in response to increased neuronal activity, and pS6 is correlated with elevated translational regulation. We characterized expression of pS6 the major subregions of the hippocampus (DG, CA1, & CA3) using immunohistochemistry. We found that 3 h of SD alone reduced S6 phosphorylation across all subregions whereas prior learning (CFC) increased pS6 expression in the DG. Furthermore, depriving mice of sleep following CFC selectively impaired pS6 expression in the DG and CA1, suggesting that memory processing during sleep invokes cellular circuits distinct from experimentally naïve mice. To characterize cell populations affected by SD, we used translating ribosome affinity purification (TRAP) to isolate cell type-specific transcripts associated with pS6-ribosomes in active neurons. Our results identified DG hilar somatostatin (SST+) interneurons to be highly enriched with pS6 during SD and express intracellular markers of plasticity and activity. Increasing

SST+ interneuron activity during post-CFC sleep using pharmacogenetics reduced the number of activated neurons in the DG and impaired memory consolidation, suggesting that this interneuron population dampens network activity and potentially intracellular signaling events. To determine the aspect of sleep influencing SST activity, we tested reducing cholinergic input to the hippocampus following CFC and observed increased DG cFos+ neurons as well as improved memory retention 24 h later. Our research has identified a hippocampal SST microcircuit that serves to dampen hippocampal activity during SD and may contribute to disruptions in memory consolidation extended wakefulness.

# Introduction

## 1.1 The neurobiology of sleep

Every night as we lay down for bed, we close our eyes and drop out of consciousness. Defenseless against predators, and unable to forage for food or find a mate, sleep has survived evolutionary pressures across diverse animal species [1]. The defining behavioral features of sleep include behavioral inactivity, increased sensory thresholds, and homeostatic regulation. Homeostatic regulation refers to the increased drive to sleep following extended bouts of wakefulness. Considering sleep has been conserved across multiple phyla coupled with its homeostatic regulation (or drive to sleep) suggests that sleep serves critical biological functions [2, 3].

With the advent of the electroencephalogram (EEG) in the 1920s, researchers were surprised to observe dramatically altered brain rhythms present during sleep [4]. Brain rhythms measured in the EEG reflect synchronized neuronal activity. Recordings from the human scalp found unsynchronized low-voltage, high frequency signals dominated the EEG during wakefulness but as participants fell asleep, highly synchronous and large-amplitude EEG oscillations emerged (in a state now referred to as Slow-Wave Sleep or NREM) [5]. After a few hours, NREM oscillations gave way to low-voltage, fast-oscillating activity reminiscent of rhythms observed during wake, while subjects experienced muscular atonia and rapid eye movements (which give the state of

REM sleep its name). During REM sleep dreams allow us to imagine ourselves flying or moving about the world while lower brainstem pathways tonically inactivate motor neurons in the spine, preventing us from acting out their dreams [6]. Over the course of the night, an average young adult enters NREM sleep and begins cycling transitions into REM once every 90 minutes [2].

Transitioning into and out of NREM and REM sleep is a nightly occurrence and reflects shifts in brain states. Changes in neural firing patterns are often preceded by key changes in the activity of neuromodulatory pathways, responsible for coordinating network-level transitions. For example, during wake, forebrain projecting cholinergic, monoamine (norepinephrine, serotonin, histamine, and dopamine), and hypocretin-releasing neurons in the brainstem and hypothalamus fire actively but become completely quiescent during NREM sleep. Interestingly, in the dreaming REM state, cholinergic neurons' activity increases while monoamine and hypocretin-releasing neurons' activity remains low [7].

## 1.2 Sleep-dependent memory consolidation

Scientists have long agreed that sleep supports memory functions in the brain, but to date, there has been much debate on sleep-dependent mechanisms for this. Memory functions comprise three major subprocesses (encoding, consolidation, and retrieval). During encoding, incoming information is stored in the brain as a labile memory trace susceptible to interference or decay (forgetting). During consolidation, the memory trace is gradually stabilized, enabling long-term storage of the memory. During retrieval, the stored memory can be accessed and utilized in context-specific forms [8]. A general

consensus in the field is that the encoding of new information occurs during wakefulness while sleep acts to integrate and consolidate the resulting memory trace [9].

Behavioral data has been instrumental in demonstrating the necessity of sleep for memory consolidation. This seems to be particularly true for spatial and episodic memories, which are dependent on the hippocampus. For example, after training human subjects to learn a specific route on a computer maze, participants allowed subsequent sleep showed improved recall when tested 24 h later. Measuring cerebral blood flow (CBF) as an indicator of neuronal activity, participants trained on the maze displayed elevated activity in their hippocampi during subsequent NREM sleep - this increased brain activity correlated with their performance on the task [10]. Subsequent investigations have shown that boosting NREM slow-wave oscillations by transcranial stimulation improves consolidation of hippocampus-dependent declarative memories in human subjects, while failing to improve non-declarative, non-hippocampus-dependent memories [11] .

### 1.3 Hippocampal mechanisms of long-term memory consolidation

Human lesion studies have found that hippocampal damage results in anterograde and temporally graded retrograde amnesia. Because patients are unable to form new memories and have difficulty recalling recent memories, the hippocampus has come to be viewed as a processing station for newly acquired information [12]. Researchers have come to view the standard two-stage model of consolidation as the basis to conceptualize the role sleep plays in memory stabilization. The model proposes that there are two modes of memory storage driving memory consolidation. The first occurs during wakefulness and allows learning to proceed quick rate but only holding information

temporarily. The second proceeds at a slower rate (hours to years) and serves to selectively store memories for long-term storage [13].

At the level of neural circuits and cells, wakefulness permits rapid learning through the selective strengthening or weakening of synapses (“synaptic consolidation”). Events experienced during wakefulness are encoded in parallel in the hippocampus and neocortex. During subsequent periods of sleep, recently acquired memory traces are repeatedly reactivated and gradually transferred to the cortex [14]. As time goes on, recalling memories becomes less reliant on the hippocampus as it is stored in the neocortex. The process of reallocating memories to extra-hippocampal circuits for permanent storage is referred to generally as “systems consolidation” [15] (**Figure 1.1**). Despite general agreement over the mechanisms governing learning and consolidation, there is still significant debate over the interactions between systems and synaptic consolidation.

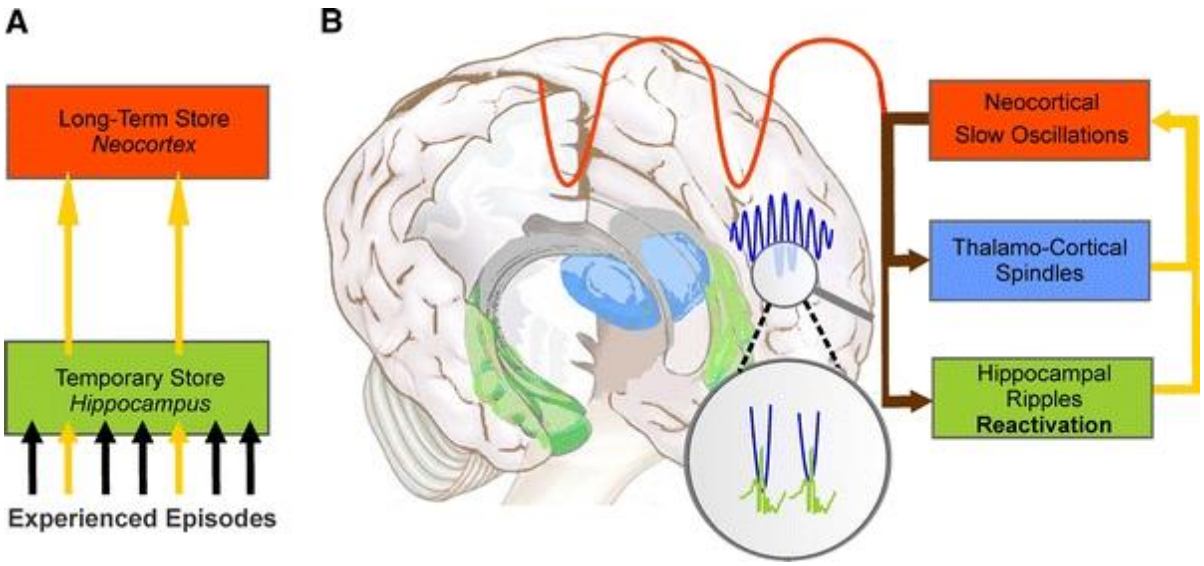


**Figure 1.1 Active system consolidation during sleep [14]**

Research in rodents has been critical in elucidating the underlying systems- and cellular- level events necessary for sleep-dependent memory consolidation [16]. The hippocampus is comprised of three major subregions including in the dentate gyrus (DG), CA1, and CA3. Recordings from the rat hippocampus (CA1) have found that neurons which were sequentially activated while mice traversed a maze were sequentially reactivated or 'replayed' during NREM sleep [17]. Researchers later clarified that reactivation occurs preferentially during sharp-wave ripples (SWRs). SWRs are short bursts (40-120ms) of high frequency (140-200 Hz) oscillations that occur in CA1, driven by activity in CA3 [18]. Reactivations have been observed in other brain regions such as the striatum and neocortex but are believed to originate in the hippocampus [14]. Inhibiting SWRs consistently leads to slower learning on hippocampus-dependent spatial memory tasks [19] and impaired recall of previously learned fear memory [20]. Research from our lab has shown that CA1 parvalbumin-expressing (PV+) interneurons are necessary for propagating SWRs and orchestrating synchronous firing activities during sleep. Furthermore, inhibiting PV+ interneurons during sleep impairs consolidation of the contextual fear conditioning (CFC) [21]. Together these findings highlight the importance of hippocampal network-level activities involved in memory consolidation during sleep.

Contextual fear conditioning (CFC) is one of best studied behavioral paradigms for memory formation and storage in rodents. CFC is initiated by placing an animal in a novel chamber and allowing the animal to freely explore the unique spatial, olfactory, and visual details of the new context. After a period of free exploration, the animal is delivered a mild foot shock through the grid floor of the chamber, then returned to its homecage. The pairing of the foot shock (unconditioned stimulus) and novel environment (conditioned

stimulus) reflects the initial *encoding* stage of contextual fear memory (CFM). Once the animal returns to its home-cage, the memory of CFM continues stabilize over-time (*consolidation*). To test the animal's ability to recall the shock/context association, the animal is placed back into the same context and assessed for the time it spends 'freezing' (*recall*). Freezing refers to a state of alert immobility and the percent time an animal spends freezing is used as a metric of CFM. Early studies established the importance of the hippocampus in processing contextual fear memory, demonstrating that hippocampal lesions impaired CFC encoding while leaving other forms of memory intact (cued fear conditioning)[22]. Similarly, pharmacologically inhibiting the dorsal hippocampus in the hours following CFC disrupts CFM consolidation [23]. Later experiments found that depriving mice of sleep over the first five hours following CFC similarly impaired recall 24-hrs later while leaving non-hippocampus dependent tasks intact [24]. Importantly, depriving mice of sleep 5-10hrs following CFC failed to impair recall, suggesting an early post-training window where hippocampus-dependent tasks are susceptible to sleep deprivation. Together these data suggest a critical window (within the first few hours following learning) for sleep-associated hippocampal activity for consolidating CFM.

### 1.4 Cellular consequences of sleep-deprivation

Scientists generally agree that memories are formed through changes in the connectivity between neurons. Therefore, to enable persistent, long-lasting memories, neurons must adjust their intracellular gene expression to produce proteins to support changes in synaptic connections. Research into the neural correlates of learning and memory have used long-term potentiation (LTP) as a model to study the gene and protein changes neurons undergo as their synapses 'strengthen' or increase in efficacy in

response to activity. Like memory, LTP exhibits a transient early phase (E-LTP) followed by a late (L-LTP) – with the latter dependent on transcription of new mRNAs and translation of new proteins [25]. Through coordinated waves of gene transcription and translation, neurons are capable of strengthening or weakening their connectivity. Less well understood is how memory traces genetic programs are modified during sleep and wake.

Early studies measuring genes differentially transcribed during sleep and wake found that ~5% of all genes were altered by sleep. Transcripts upregulated during wakefulness support high energy demand, elevated transcriptional activity, and synaptic potentiation. Meanwhile, transcripts associated with sleep increased expression of genes coding for regulators of protein synthesis [26]. These findings combined with similar results observed in the hippocampus [27] has led to the hypothesis that learning while awake induces *de novo* gene transcripts which are later translated into proteins during sleep [9]. Converging lines of evidence support this hypothesis finding that only five hours of sleep deprivation (SD) is sufficient to reduce total protein synthesis in the hippocampus and the activity of key regulators of protein translation [28]. Still it is unclear how SD impairs translation or which transcripts are preferentially translated during sleep

## 1.5 Outline

The aim of this thesis is to explore the system and cellular mechanisms of sleep-dependent hippocampal memory consolidation. Using a combination of behavioral assays, molecular biology techniques, RNA-sequencing, computational analyses, and

pharmacogenetic manipulations, we have discovered new circuit- and cell-level mechanisms that facilitate memory consolidation during sleep.

In **Chapter 2,** we investigate the differences in *Arc* mRNA expression measured by quantitative PCR (qPCR) and *in situ* hybridization. Following 3 h of SD, *Arc* mRNA increased in whole hippocampus as anticipated from previous reports. In contrast, newly transcribed *Arc* pre-mRNA was not affected by SD. Using *in situ* hybridization for *Arc* mRNA and immunohistochemistry for Arc protein in dorsal hippocampus, we unexpectedly observed more Arc+ neurons in the DG of mice permitted to sleep. This work was published in *Neurobiology of Learning and Memory* in 2019 [29].

In **Chapter 3** we aimed to identify differences in learning-related ribosome-associated mRNAs in sleep permitted or SD mice. We assessed gene expression across three cell populations by developing a translating ribosome affinity purification (TRAP) technique to profile transcripts from hippocampal excitatory neurons (Camk2a+), highly-active neurons expressing phosphorylated ribosomal subunit S6 (pS6+), and total hippocampal mRNA (Input). To profile any putative differences in translation based on a ribosomes subcellular localization in the neuron, we collected samples from both supernatant and pellet fractions from each cell population. Our sequencing results revealed that separating supernatant and pellet fractions reliably enriched for cytosolic-enriched genes (ex: transcription factors, kinases) whereas pellet fractions enriched for trafficked and secretory pathway genes (e.g., transmembrane receptor, endoplasmic reticulum, and synaptic genes). Comparing the effects of sleep-deprivation and learning (single-trial contextual fear conditioning [CFC]), we find that CFC elevates a few sparsely expressed transcript isoforms (e.g., *ΔFosb* and *Homer1a*) which are detectable in

cytosolic fractions of activated neurons (pS6+) and total hippocampal mRNA (Input). Interestingly, CFC-driven transcript changes at ribosomes in excitatory neurons were occluded by 3 h or 5 h of subsequent SD. This suggests that activity-dependent transcripts expressed on ribosomes during wakefulness occlude CFC-related gene expression. Furthermore, our data show that mRNAs associated with membrane-bound ribosomes – but not cytosolic ribosomes - are dramatically affected by CFC. Moreover, mRNAs representing different biochemical pathways are induced when CFC is followed by sleep vs. SD. Because SD during this time window profoundly disrupts hippocampus-dependent consolidation of contextual fear memory (CFM), these findings are currently in submission for publication, suggest new cellular mechanisms for sleep facilitation of memory consolidation. These findings have recently been submitted for peer review.

In **Chapter 4**, we further characterized differences in hippocampal activity measured by pS6. Compared to three hours of SD, rodents allowed to sleep displayed increased S6 phosphorylation in the major subregions of the dorsal hippocampus. To measure transcripts differentially associated with phosphorylated ribosomes, we immunoprecipitated pS6 ribosomes and performed RNA-seq after a period of sleep or SD. Unexpectedly, SD increased pS6 ribosomes with transcripts enriched in neuromodulatory (cholinergic/hypocretin) and interneuron (somatostatin) cell populations among pS6+ neurons. Profiling ribosome-associated mRNAs in somatostatin-expressing (SST) interneurons, we discovered that activity-dependent transcripts were elevated following 3 h of SD. Together our data suggest that SD selectively activated this hippocampal interneuron population, which gates activity in the remaining hippocampal circuit. Pharmacogenetically elevating activity in this cell population in freely-sleeping

mice following CFC impaired fear recall the next day. This suggests that reduced SST activity during sleep is a necessary component for CFM consolidation. These finding are in preparation for a forthcoming publication.

## 1.6 References


1. Jointer, W.J. (2016). Unraveling the Evolutionary Determinants of Sleep. 26 *20*.

2. Allada, R., and Siegel, J.M. (2008). Unearthing the Phylogenetic Roots of Sleep. Curr Biol *18*.

3. Tobler, I. (1995). Is sleep fundamentally different between mammalian species? Behav Brain Res *69*, 35-41.

4. McKenna, J.T., Zielinski, M.R., and McCarley, R.W. (2017). Neurobiology of REM Sleep, NREM Sleep Homeostasis, and Gamma Band Oscillations. In Sleep Disorders Medicine. pp. 55-77.

5. Scammell, T.E., Arrigoni, E., and Lipton, J. (2017). Neural Circuitry of Wakefulness and Sleep. Neuron *93*, 747-765.

6. Fuller, P.M., Saper, C.B., and Lu, J. (2007). The pontine REM switch: past and present. J Physiol *584*, 735-741.

7. Holst, S.C., and Landolt, H.-P. (2018). Sleep-Wake Neurochemistry RSS Sleep Medicine Clinics *13*, 137-146.

8. McGaugh, J.L. (2000). Memory--a century of consolidation. Science *287*, 248-251.

9. Seibt, J., and Frank, M.G. (2019). Primed to Sleep: The Dynamics of Synaptic Plasticity Across Brain States. Front Systems Neurosci.

10. Peigneux, P., Laureys, S., Fuchs, S., Collette, F., Perrin, F., Reggers, J., Phillips, C., Degueldre, C., Del Fiore, G., Aerts, J., et al. (2004). Are spatial memories strengthened in the human hippocampus during slow wave sleep? Neuron *44*, 535-545.

11. Marshall, L., Helgadottir, H., Molle, M., and Born, J. (2006). Boosting slow oscillations during sleep potentiates memory. Nature.

12. Joo, H.R., and Frank, L.M. (2018). The hippocampal sharp wave–ripple in memory retrieval for immediate use and consolidation. Nat Rev Neurosci *19*, 744-757.

13. Diekelmann, S., and Born, J. (2010). The memory function of sleep. Nat Rev Neurosci *11*, 114-126.

14. Born, J., and Wilhelm, I. (2012). System consolidation of memory during sleep. Psychol Res *76*, 192-203.

15. Klinzing, J.G., Niethard, N., and Born, J. (2019). Mechanisms of systems memory consolidation during sleep. Nature Neuroscience *22*, 1598-1610.

16. Abel, T., Havekes, R., Saletin, J.M., and Walker, M.P. (2013). Sleep, plasticity and memory from molecules to whole-brain networks. Curr Biol *23*, R774-788.

17. Wilson, M.A., and McNaughton, B.L. (1994). Reactivation of hippocampal ensemble memories during sleep. Science *265*, 676-682.

18. Buzsaki, G., Buhl, D.L., Harris, K.D., Csicsvari, J., Czeh, B., and Morozov, A. (2003). Hippocampal network patterns of activity in the mouse. Neuroscience *116*, 201-211.

19. Girardeau, G., Benchenane, K., Wiener, S.I., Buzsaki, G., and Zugaro, M.B. (2009). Selective suppression of hippocampal ripples impairs spatial memory. Nat Neurosci *12*, 1222-1223.

20. Wang, D.V., Yau, H.-J., Broker, C.J., Tsou, J.-H., Bonci, A., and Ikemoto, S. (2015). Mesopontine median raphe regulates hippocampal ripple oscillation and memory consolidation. Nat Neurosci *18*, 728-735.

21. Ognjanovski, N., Schaeffer, S., Mofakham, S., Wu, J., Maruyama, D., Zochowski, M., and Aton, S.J. (2017). Parvalbumin-expressing interneurons coordinate hippocampal network dynamics required for memory consolidation. Nature Communications *8*, 15039.

22. Phillips, R.G., and LeDoux, J.E. (1992). Differential Contribution of Amygdala and Hippocampus to Cued and Contextual Fear Conditioning. Behav Neurosci *106*, 274-285.

23. Daumas, S., Halley, H., Frances, B., and Lassalle, J.M. (2005). Encoding, consolidation, and retrieval of contextual memory: differential involvement of dorsal CA3 and CA1 hippocampal subregions. Learn Mem *12*, 375-382.

24. Graves, L.A., Heller, E.A., Pack, A.I., and Abel, T. (2003). Sleep deprivation selectively impairs memory consolidation for contextual fear conditioning. Learn. Mem. *10*, 168-176.

25. Costa-Mattioli, M., Sossin, W.S., Klann, E., and Sonenberg, N. (2009). Translational Control of Long-Lasting Synaptic Plasticity and Memory. Neuron *61*, 10-26.

26. Cirelli, C., Gutierrez, C.M., and Tononi, G. (2004). Extensive and divergent effects of sleep and wakefulness on brain gene expression. Neuron *41*, 35-43.

27. Vecsey, C.G., Peixoto, L., Choi, J.H., Wimmer, M., Jaganath, D., Hernandez, P.J., Blackwell, J., Meda, K., Park, A.J., Hannenhalli, S., et al. (2012). Genomic analysis of sleep deprivation reveals translational regulation in the hippocampus. Physiol Genomics *44*, 981-991.

28. Tudor, J.C., Davis, E.J., Peixoto, L., Wimmer, M.E., van Tilborg, E., Park, A.J., Poplawski, S.G., Chung, C.W., Havekes, R., Huang, J., et al. (2016). Sleep deprivation impairs memory by attenuating mTORC1-dependent protein synthesis. Sci Signal *9*, ra41.

29. Delorme, J.E., Kodoth, V., and Aton, S.J. (2019). Sleep loss disrupts Arc expression in dentate gyrus neurons. Neurobiol Learn Mem *160*, 73-82.

# Chapter II. Sleep Loss Disrupts Arc Expression in Dentate Gyrus Neurons

This chapter includes the manuscript: Delorme J, Kodoth V, & Aton SJ. (2019) Sleep loss disrupts Arc expression in dentate gyrus neurons. Neurobiol Learn Mem. 2019; 160: 73-82. doi:10.1016/j.nlm.2018.04.006

## 2.1 Abstract

Sleep loss affects many aspects of cognition, and memory consolidation processes occurring in the hippocampus seem particularly vulnerable to sleep loss. The immediate-early gene Arc plays an essential role in both synaptic plasticity and memory formation, and its expression is altered by sleep. Here, using a variety of techniques, we have characterized the effects of brief (3-h) periods of sleep vs. sleep deprivation (SD) on the expression of Arc mRNA and Arc protein in the mouse hippocampus and cortex. By comparing the relative abundance of mature Arc mRNA with unspliced pre-mRNA, we see evidence that during SD, increases in Arc across the cortex, but not hippocampus, reflect de novo transcription. Arc increases in the hippocampus during SD are not accompanied by changes in pre-mRNA levels, suggesting that increases in mRNA stability, not transcription, drives this change. Using in situ hybridization (together with behavioral observation to quantify sleep amounts), we find that in the dorsal hippocampus, SD minimally affects Arc mRNA expression, and decreases the number of dentate gyrus (DG) granule cells expressing Arc. This is in contrast to neighboring cortical areas, which show large increases in neuronal Arc expression after SD. Using immunohistochemistry, we find that Arc protein expression is also differentially affected

in the cortex and DG with SD - while larger numbers of cortical neurons are Arc+, fewer DG granule cells are Arc+, relative to the same regions in sleeping mice. These data suggest that with regard to expression of plasticity-regulating genes, sleep (and SD) can have differential effects in hippocampal and cortical areas. This may provide a clue regarding the susceptibility of performance on hippocampus-dependent tasks to deficits following even brief periods of sleep loss.

## 2.2 Introduction

Over the past century, numerous studies have shown that following memory encoding, sleep promotes information storage in the brain. This has led to numerous theories of how sleep could facilitate plasticity of synapses between neurons involved in memory formation (Puentes-Mestril et al, 2017). Memory processes relying on neural circuits in the hippocampus (e.g., the formation of new episodic and spatial memories) seem particularly susceptible to disruption by post-encoding sleep loss (Prince and Abel, 2013).

One strategy for understanding sleep's role in brain function has been to determine how sleep and sleep loss affect gene expression in the brain. Expression of the immediate-early gene *Arc* is consistently increased in various mammalian brain structures following a period of sustained wake, relative to a similar period of *ad lib* sleep (Cirelli et al., 2004; Mackiewicz et al., 2007; Vecsey et al., 2012). Arc protein function is linked to various types synaptic plasticity, with loss of *Arc* leading to deficits in long term depression (LTD) (Waung et al., 2008), late phase long term potentiation (LTP) (Messaoudi et al., 2007; Plath et al., 2006), and homeostatic plasticity (Gao et al., 2010; Shepherd et al., 2006). *Arc* mRNA and Arc protein expression are induced in specific brain circuits *in vivo*

by increased neuronal activity (Miyashita et al., J Neurosci 2009) or by prior learning (Carter et al., 2015; Czerniawski et al., 2011; Fellini and Morellini, 2013; Guzowski et al., 2001). *Arc* mutants also show deficits in both hippocampus-dependent long-term memory consolidation (Plath et al., 2006) and experience-dependent plasticity in sensory cortex (McCurry et al., 2010). The level of expression of *Arc* mRNA in the hippocampus immediately following training on a hippocampus-dependent task is a predictor of subsequent memory performance (Guzowski et al., 2001).

Together the available data suggest a causal role for Arc in both synaptic plasticity and long-term memory formation. Thus a parsimonious interpretation of prior gene expression studies, showing sleep-dependent decreases in *Arc* expression (Cirelli et al., 2004; Mackiewicz et al., 2007; Vecsey et al., 2012), is that synaptic plasticity is generally decreased during sleep vs. wake. However, recent data have suggested that both functional and structural plasticity in the dorsal hippocampus are disrupted by sleep deprivation (Havekes et al., 2016; Vecsey et al., 2009). Other studies have shown that expression of various immediate early genes can actually be augmented (rather than reduced) in the hippocampus during post-learning sleep (Calais et al., 2015; Ribeiro et al., 1999; Ulloor and Datta, 2005). Furthermore, dorsal hippocampal network activity patterns (e.g. oscillations) associated with sleep promote both changes in functional connectivity following learning, and long-term memory formation (Ognjanovski et al., 2014; Ognjanovski et al., 2017). It is unclear whether these changes are unique to the hippocampus, the dorsal hippocampus, or perhaps to specific areas within the dorsal hippocampal circuit. To further clarify this issue, we assessed the effects of sleep and

sleep loss on *Arc* mRNA expression and Arc protein levels in the hippocampus and cortex, using multiple techniques.

## 2.3 Materials & Methods

***Mouse handling and husbandry:*** All animal husbandry and surgical/experimental procedures were approved by the University of Michigan Institutional Animal Care and Use Committee (PHS Animal Welfare Assurance number D16-00072 [A3114-01]). All mice were individually housed in standard caging with beneficial environmental enrichment (nesting material and/or manipulanda) throughout all procedures. Lights were maintained on a 12 h:12 h light: dark cycle (lights on at 8 AM), and food and water were provided *ad lib*. At age 3 months, C57BL/6J mice (IMSR_JAX:000664, Jackson) were habituated to handling over 5 days, for 4 min each day. Following habituation, and beginning at lights-on (ZT0), mice either were allowed *ad lib* sleep in their home cage (Sleep) or were sleep deprived by gentle handling (SD). In the Sleep group, sleep behavior was scored based on visual observation, at 5-min intervals, throughout the 3-h *ad lib* sleep period. Criteria for sleep were immobility and a stereotyped sleep posture. Such criteria have been used (and validated against EEG-based sleep assessments) in previous studies to quantify sleep behavior in mice (Fisher et al., 2012; Pack et al., 2007). Sleep amounts across the *ad lib* sleep period are shown for individual mice in **Figure 2.2**. Based on these scoring criteria, all Sleep mice slept > 50% of the 3-h sleep period (avg = 79%, SEM= 4%). At ZT3, mice were sacrificed by cervical dislocation under isoflurane anesthesia.

***Quantitative real-time PCR (qPCR):*** Whole hippocampi (and for comparison, whole cerebral cortices) from individual mice in Sleep ($n$ = 5) and SD ($n$ = 5) groups were

dissected in PBS, flash frozen in liquid nitrogen, and stored at -80 °C. RNA purification was performed using an RNeasy Mini Kit (Qiagen) and coupled with a DNAse digestion

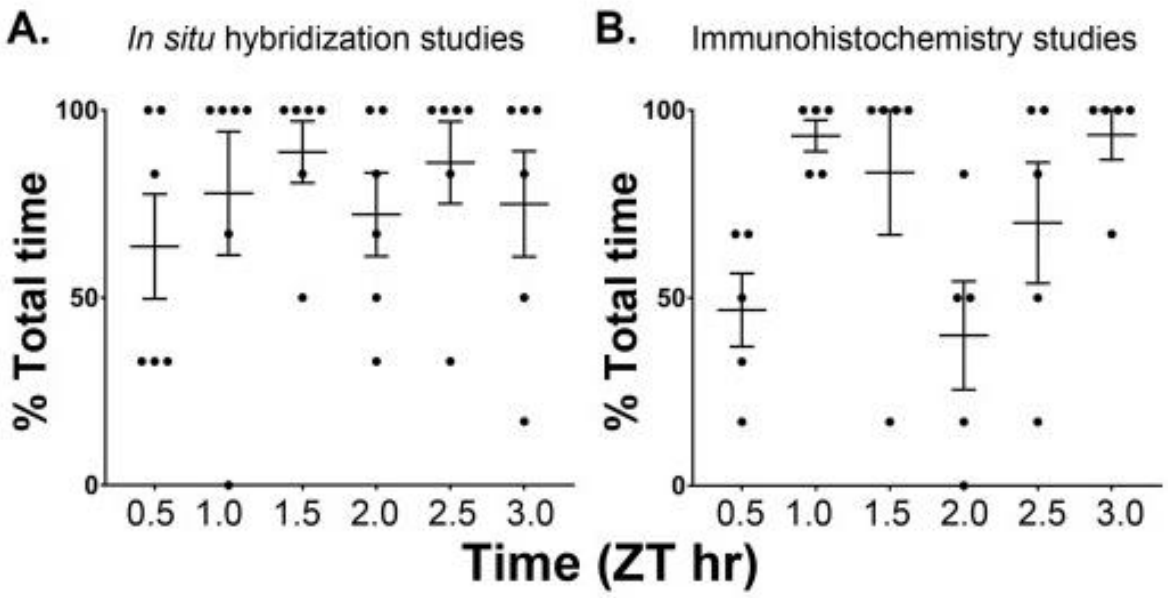


**Figure 2.2 Total sleep time in mice allowed ad lib sleep from ZT0-3.** Amount of time during which Sleep mice were observed to be inactive and in stereotyped sleep posture across the 3-h ad lib sleep period. Values are expressed as a percentage of total time, in 30-min intervals. Data are shown for mice used for in situ hybridization studies in A and for mice used for immunohistochemistry studies in B.

step (Qiagen); RNA concentration and purity were quantified with spectrophotometry (Nanodrop Lite; ThermoFisher). 0.5 µg of RNA was used to synthesize cDNA using iScript cDNA Synthesis Kit (Bio-Rad) and cDNA was diluted 1:10 for mature *Arc* mRNA quantification and, due to the low expression of pre-mature Arc mRNA transcript, cDNA was diluted 1:5. qPCR reactions were measured using a CFX96 Real-Time System, in 96-well reaction plates (Bio-Rad). Three technical replicates were used for each sample. Primer specificity was confirmed using NIH Primer Blast while primer efficiency was measured by calculating primer amplification efficiency (AE) and coefficient of correlation for a standard curve ($R_2$) for each primer set (data and sequences shown in **Table 1**). All primers utilized had amplification efficiency values within 90-110%, $R_2$ values greater than 0.98, and standard deviations < 0.20 among 5 replicates. Expression data for *Arc* primer sets were normalized to gamma actin (*Actg1*). Expression of *Actg1* itself was not affected by SD (raw CT values: Sleep = 23.91 ± 0.15 vs. SD = 23.89 ± 0.11, *N.S.*, Student's t-test). *Actg1* expression levels were also normalized to the housekeeping genes *Tuba4a* (Sleep = 1.00 ± 0.035 vs. SD = 1.05 ± 0.035, *N.S.*, Student's t-test) and *Gapdh* (Sleep = 1.02 ± 0.093 vs. SD = 1.04 ± 0.096, *N.S.*, Student's t-test) and were similar between groups. For comparison with previous studies, values for SD mice were expressed as fold changes normalized to the mean values for mice in the Sleep group. Values were calculated using the delta delta Ct method.

***RNAScope in situ hybridization:*** *In situ* hybridization was performed on 12-µm sections taken from fresh-frozen brains containing dorsal hippocampus, from mice in Sleep ($n$ = 6) and SD ($n$ = 5) groups. The RNAscope Multiplex Fluorescent Reagent Kit v2 (323100-USM, Advanced Cell Diagnosis) was used to image *Arc* expression. Prior to probe

incubation, slices were pretreated with hydrogen peroxide (10 min, room temperature), Target Retrieval Reagent (5 min, 99°C), and RNAscope protease III (30 min, 40°C). Slices were incubated with 20 custom-synthesized *Arc* mRNA probes (316911-C3, Advanced Cell Diagnostics) targeting regions between bases 23 and 1066 within the open reading frame and hybridized to Opal 690 (PerkinElmer FP1497001KT) for visualization. Positive and negative control probes were used in parallel experiments to confirm specificity of hybridization.

***Immunohistochemistry:*** For immunohistochemical quantification of Arc protein expression, mice in Sleep ($n$ = 5) and SD ($n$ = 5) groups were sacrificed and perfused with PBS followed by 4% paraformaldehyde. 40-µm brain sections were blocked with normal goat serum for 2-hours and incubated overnight with a polyclonal guinea pig Arc antibody (Synaptic Systems, 156 004, 1:500) at 4°C. The following day, sections were stained with goat anti-guinea pig IgG H&L, Alexa Fluor® 594 (Abcam, ab150188, 1:200). Stained sections were coverslipped in ProLong Gold Antifade Reagent (ThermoFisher, P36930). Fluorescence intensity was used to identify Arc protein-expressing (Arc+) cells in the dentate gyrus granule cell layer in sections containing either dorsal (-1.5 to -2.3 mm posterior to bregma) or intermediate (-2.9 to -3.2 mm posterior to bregma) hippocampus, and Arc+ neurons in posterior parietal and primary somatosensory cortical areas overlying dorsal hippocampus (1.5-3.0 mm lateral, -1.5 to -2.1 mm posterior to bregma), using the automated protocol described below.

***Imaging and Quantification****.* RNAscope probe fluorescence signals were captured using a 10x objective lens on a Leica 3D STED SP8 while immunohistochemical sections

were imaged on a Leica SP5 laser scanning confocal microscope. Settings were fixed for each imaging session. Fluorescence images were analyzed using MIPAR image analysis software in their raw grayscale format (Sosa et al., 2014). Mean fluorescence intensity values (0-255) were quantified within posterior parietal and primary somatosensory cortical areas overlying the dorsal hippocampus, across granule (dentate gyrus) or pyramidal (CA1, CA3) cell layers (layer borders were delineated using a freehand tool by a scorer blind to experimental condition). In addition to layer-specific mean intensity measures, in the case of the dentate gyrus and cortex (where cell bodies were sparsely labelled with intense fluorescence), Arc-immunopositive (Arc+) cell bodies were counted by a blind scorer using an automated protocol and normalized to the area of the DG or cortical area in each section (in $mm^2$). Because the borders of the DG granule cell layer were difficult to distinguish in IHC sections, Arc+ cell numbers were normalized to linear distance, using a line drawn along the hilus bordering the DG. Briefly, a non-local means filter was used to reduce image noise, and an adaptive threshold was used to identify areas >30 µm whose mean pixel intensity was 200% of its surroundings. Four images per region (two per hemisphere) were quantified for each animal.

### 2.4 Arc mRNA expression, but not Arc transcription rates, are increased in the hippocampus during brief sleep deprivation.

To investigate how sleep and sleep deprivation affect *Arc* transcription in the hippocampus, we first quantified expression of both *Arc* pre-mRNA and mature mRNA in samples obtained from whole (dorsal + ventral) hippocampus using qPCR. Animals were habituated to daily handling, and starting at lights-on the day of tissue collection they were either were allowed 3 h of *ad lib* sleep (Sleep) or were sleep deprived for 3 h by gentle handling (SD). Consistent with previous findings from the mouse hippocampus following

longer (i.e., 5-h) sleep or SD intervals (Vecsey et al., 2012), qPCR results measuring the mature Arc transcript **(Figure 2.1A, B**) indicated that 3-h SD increased *Arc* mRNA expression ~1.5-fold in the hippocampus (Sleep = 1.02 ± 0.11 vs. SD = 1.56 ± 0.05, $p < 0.01$, Student's t-test).

Because steady-state *Arc* mRNA levels are modulated by both transcription and degradation rates, the mechanism for *Arc* mRNA accumulation during SD is unknown. The mature *Arc* transcript is derived from a pre-mRNA containing two short introns within the 3' UTR, which are removed during mRNA maturation (Rao et al., 2006; Saha et al., 2011). The mature mRNA has a half-life of approximately 45 minutes *in vivo* (Rao et al., 2006), and is thought to be degraded rapidly after translation, via translation-dependent decay (Farris et al., 2014; Ninomiya et al., 2016). To determine whether observed increases in *Arc* mRNA expression with SD were due to increased *de novo* synthesis or mature mRNA stabilization, we designed primers which spanned the first intron of the *Arc* pre-mRNA transcript. Previous *in vitro* studies using similar primers have demonstrated that *Arc* pre-mRNA expression increases 5-10 min prior to mature *Arc* mRNA (Saha et al., 2011). Using these primers (**Figure 2.1A**) we found no significant effect of SD on hippocampal *Arc* pre-mRNA levels (**Figure 2.1B**), which were nearly identical in Sleep and SD mice (Sleep = 1.07 ± 0.20 vs. SD = 1.10 ± 0.07, *N.S.*, Student's t-test). This suggests that increased expression of mature *Arc* mRNA after SD may not result from increased *de novo Arc* transcription during the wake state, as previously assumed. Rather, increased mature mRNA levels could be driven by reduced translation-dependent mRNA decay during SD.

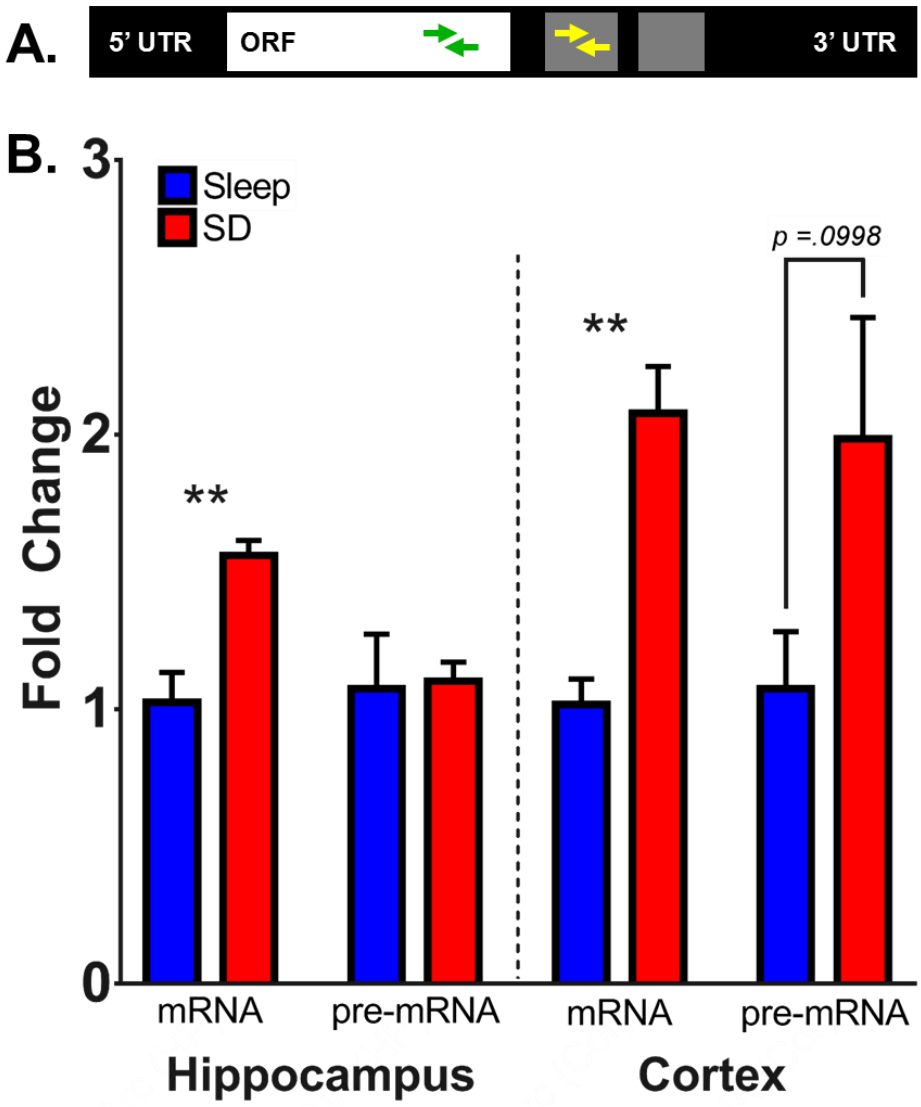


**Figure 2.1 Expression of mature and pre-mRNA Arc transcripts in hippocampus and cerebral cortex of sleep deprived animals. A.** Arc transcript structure and quantitative polymerase chain reaction (qPCR) primer design. To quantify de novo Arc transcription, Arc primers were designed to target either the transcript's open reading frame (green) or the first intron on its 3' UTR (yellow). These primer sets were aimed at amplifying mature and pre-mRNA, respectively. **B.** Expression of Arc mRNA and pre-mRNA in samples of whole hippocampus or whole cerebral cortex, normalized to expression of gamma actin (Actg1). Gene expression data in samples taken from mice after 3 h of ad lib sleep (Sleep) and sleep deprivation (SD) were normalized as a fold change relative to mean values from the Sleep group. Values indicate mean ± SEM; n = 5 mice/group; ** indicate $p < 0.01$, *** indicate $p < .001$, Student's t-test.

For comparison with changes seen in the hippocampus, we also used qPCR to measure *Arc* pre-mRNA and mature mRNA in cerebral cortical samples taken from the same Sleep and SD mice (**Figure 2.1B**). Consistent with the findings of others (Cirelli et al., 2004; Mackiewicz et al., 2007; Vecsey et al., 2012), we found that mature *Arc* mRNA was increased approximately two-fold in the cortex following SD (Sleep = 1.02 ± 0.09 vs. SD = 2.08 ± 0.17, $p < 0.001$, Student's t-test). In contrast to pre-mRNA levels in the hippocampus, which were identical in mice from SD and Sleep groups, pre-mRNA levels in cortex measured with both primer sets were elevated following SD (Sleep = 1.07 ± 0.21 vs. SD = 1.98 ± 0.44). While this change did not reach statistical significance ($p = 0.1$), it was similar in magnitude (i.e., twofold) to the increase in mature mRNA seen in cortex with SD (**Figure 2.1B**).

## 2.5 Sleep selectively increases Arc mRNA expression among neurons in the dentate gyrus

To clarify where in the hippocampal circuit *Arc* mRNA expression is regulated, we used RNAscope fluorescence *in situ* hybridization (Wang et al., 2012) to visualize the mature *Arc* transcript. To do this, we utilized predesigned Arc RNAScope probes targeting the bases 23 to 1066 in the Arc ORF. To ensure their specificity, positive control probes targeting the housekeeping gene *Hprt1* and negative control probes targeting *DapB* (a gene expressed in *bacillus subtilis*) were run alongside the *Arc* probes (**Figure 2.3**). Once the specificity of the probes were confirmed, multiple hippocampal subregions (dentate gyrus [DG], CA3, and CA1) were imaged from brain sections containing the dorsal hippocampus which were taken from mice in Sleep ($n = 6$) and SD ($n = 5$) groups. Across each area, mean fluorescence signal intensity was first quantified in pyramidal (or granule) cell body layers, and in adjacent molecular layers (i.e., in pyramidal/granule cell

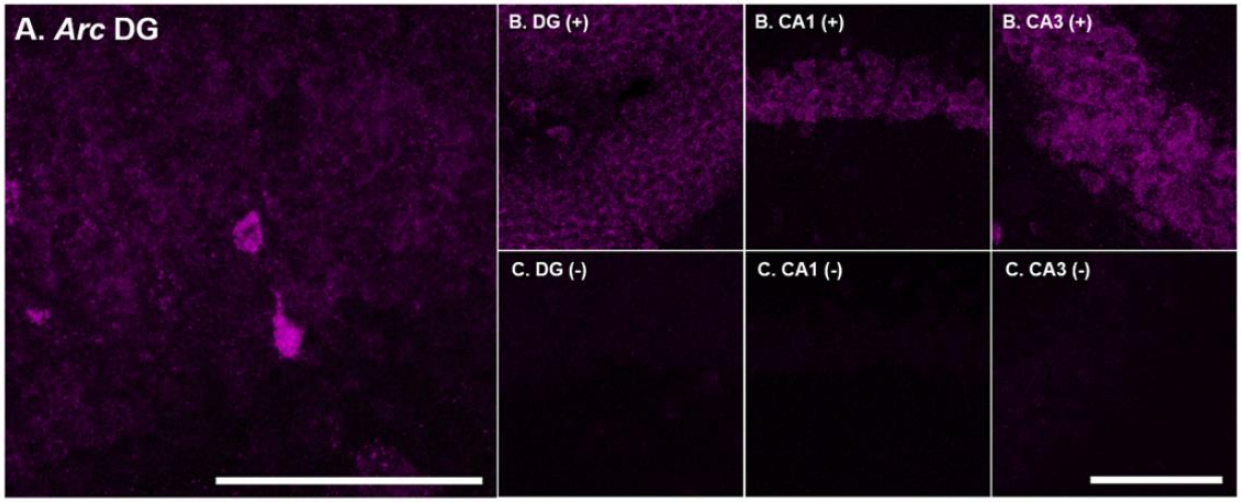


**Figure 2.3 Validation of Arc mRNA probes for RNAscope fluorescence in situ hybridization. A.** RNAscope in situ hybridization of mouse dentate gyrus (DG) section. Violet color represents Arc mRNA probe hybridization. **B.** Positive control probes for in situ hybridization, targeting mRNA for the ubiquitously-expressed housekeeping gene Hprt1; images show representative signal in DG, CA1, and CA3. **C.** Negative control probes targeting mRNA for DapB, a gene expressed in bacillus subtilis, shown in the same regions. Scale bars indicate 100 µm.

dendritic fields). As shown in **Figure 2.4**, there were no significant changes in *Arc* expression with SD in either pyramidal cell or molecular layers, in either CA1, CA3, or DG. For comparison with hippocampal expression values, we measured *Arc* mRNA expression in cortical areas (i.e., posterior parietal/ primary somatosensory cortex) overlying dorsal hippocampus. As shown in **Figure 2.4B**, mean intensity (measured across all cortical layers) was slightly, but not significantly, higher following SD.

In DG and in cortex, *Arc*+ neuronal labeling was sparse, allowing comparisons of *Arc*+ neuronal density in these regions between Sleep and SD. As shown in **Figure 2.5A-B**, we observed twice as many *Arc*+ neurons in the DG granule cell layer of mice from the Sleep group than were seen in the DG of mice from the SD group (87.44 ± 3.70 vs. 39.40 ± 7.59 cells/$mm^2$, $p < 0.001$, Student's t-test). No differences in the background mean fluorescence intensity (measured within the granule cell layer, with fluorescence intensity values of Arc+ cell bodies subtracted) were observed in DG between mice in Sleep and SD groups (data not shown, Sleep = 43.39 ± 5.32 vs. SD = 45.34 ± 4.69, *N.S.*, Student's t-test). This suggests that in contrast to areas CA1 and CA3 (where *Arc* mRNA expression levels are largely unchanged after SD), expression of *Arc* among DG granule cells is significantly greater following a period of *ad lib* sleep. However, DG *Arc* expression levels for individual animals were not correlated with sleep amounts across the 3-h *ad lib* sleep period prior to sacrifice (*N.S.*, Pearson correlation, **Figure 2.5C**).

In contrast to what was seen in DG (and consistent with qPCR data from whole cortical RNA samples), *Arc*+ labeling in the cortex indicated a ~3-fold increase in *Arc*+ neuronal density after SD (**Figure 2.5D-E**; Sleep = 43.17 ± 10.76 cells/$mm^2$ vs. SD = 149.9 ± 19.14 cells/$mm^2$, $p < 0.001$, Student's t-test). Among freely-sleeping mice, the

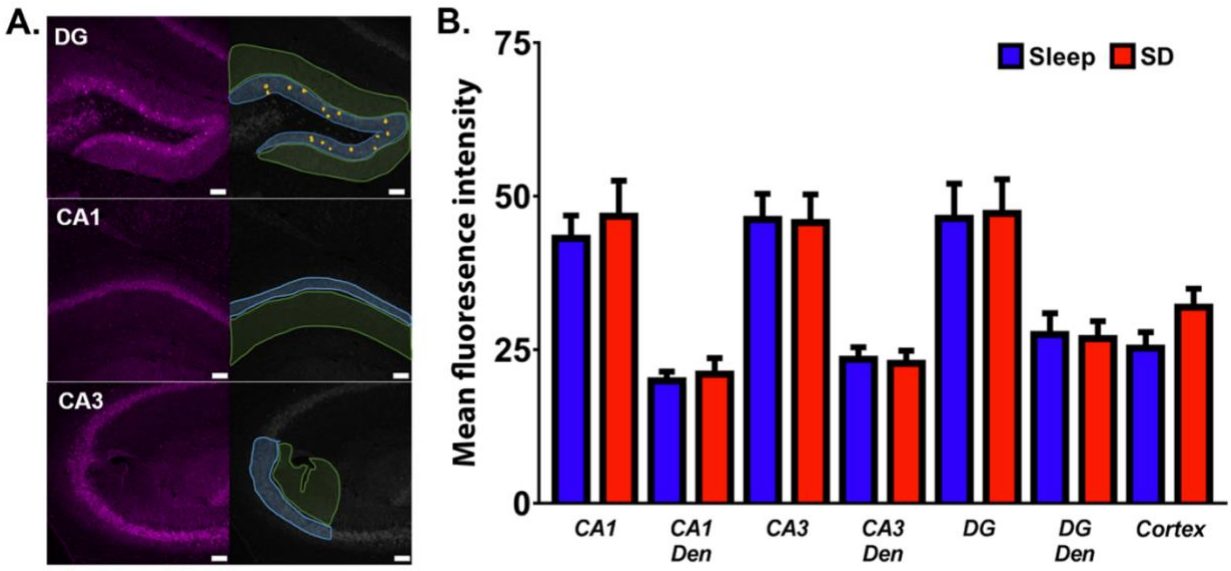


**Figure 2.4 Mean fluorescence intensity values for in situ hybridization data for Arc mRNA in dorsal hippocampus and cortex. A.** Strategy for measuring mean fluorescence intensity in pyramidal cell and dendritic (Den) layers in dorsal hippocampal subregions. Selection of granule cell layer of the dentate gyrus and pyramidal cell layer of CA1/CA3 are shown in blue. Estimated dendritic regions adjacent to cell layers are shown in green. For Arc cellular quantification in the DG, an automated protocol (see Methods) detected Arc+ cells in the DG (yellow) and counted the number of Arc+ cells/mm2 within the granule cell layer (blue). **B.** Mean fluorescence values did not significantly differ between Sleep (n = 6 mice) and SD (n = 5 mice) conditions in any area. Scale bars indicate 100 µm.

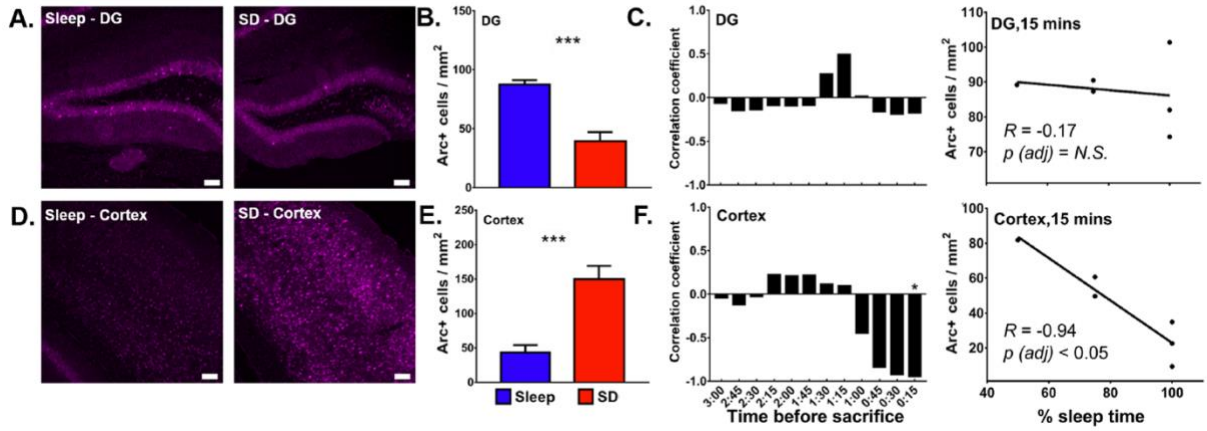


**Figure 2.5 Sleep deprivation simultaneously decreases Arc+ cells in the DG, and increases Arc+ cells in the cortex. A.** Representative images showing Arc+ cells in the DG following 3 h of ad lib Sleep (n = 6 mice) or SD (n = 5 mice). Scale bars indicate 100 µm. **B.** The number of Arc+ cells/mm2 was reduced in the DG of mice following SD mice relative to mice allowed ad lib Sleep. Values indicate means ± SEM for each condition; *** indicates $p < 0.001$, Student's t-test. **C.** Pearson correlation coefficients for Arc+ cells/mm2 in DG vs. sleep time integrated over various intervals prior to sacrifice, based on sleep amounts from individual mice in the Sleep condition. **D.** Representative images from Sleep and SD mice, showing Arc+ cells in primary somatosensory cortex overlying dorsal hippocampus. Scale bars indicate 100 µm. **E.** The number of Arc+ cells/mm2 in the cortex was increased after SD. *** indicates $p < 0.001$, Student's t-test. **F.** Pearson correlation coefficients for cortical Arc+ cells/mm2 vs. total sleep time, integrated over various intervals prior to sacrifice. Negative relationships between sleep time and Arc+ cell numbers were present over the final 45-minutes of the experiment (* indicates $p < 0.05$ after Bonferroni correction).

number of *Arc*+ neurons in the cortex of individual mice was predicted by the amount of time spent awake vs. asleep over the final fifteen minutes prior to sacrifice (**Figure 2.5F**; Pearson $R = 0.94$, Bonferroni corrected $p$ value $< 0.05$).

## 2.6 Sleep increases Arc protein expression in the dorsal and intermediate dentate gyrus

To determine whether brain region-specific changes in *Arc* mRNA expression were mirrored by changes Arc protein levels after SD, we used immunohistochemistry to measure differences in Arc translation. As observed in the *in situ* hybridization experiments, no significant changes in the mean fluorescence intensity were recorded following SD in hippocampal subregions CA1 and CA3 (**Figure 2.6**). In contrast, as shown in **Figure 2.7A-B,** in both dorsal (Sleep = 16.46 ± 1.84 cells/mm vs. SD = 10.96 ± 0.80 cells/mm), $p < 0.05$, Student's t-test) and intermediate (Sleep = 10.48 ± 0.69 cells/mm vs. SD = 3.22 ± 1.06 cells/mm, $p < 0.001$, Student's t-test) DG, the number of granule cells expressing Arc protein was decreased in SD mice. Among mice in the Sleep group, in both dorsal and intermediate DG, the number of Arc+ cells tended to be highest in animals that had slept the most over the last 1.25 h prior to sacrifice (Pearson $R = 0.86$ and 0.93, respectively, Bonferroni-corrected $p$ value *N.S.*) (**Figure 2.7C**). This suggests that appropriately-timed sleep may promote the translation of Arc protein among DG neurons.

For comparison, we also quantified expression of Arc protein in primary somatosensory and posterior parietal cortex. As was true for *Arc* mRNA, following SD, mice showed a ~5-fold increase in the number of Arc+ cells across all layers of the cortex (Sleep = 25.18 ± 17.49 cells/$mm^2$ vs. SD = 122.90 ± 27.29 cells/$mm^2$, $p < 0.05$, Student's t-test). Similar to results observed in the cortex, among sleeping mice, Arc protein

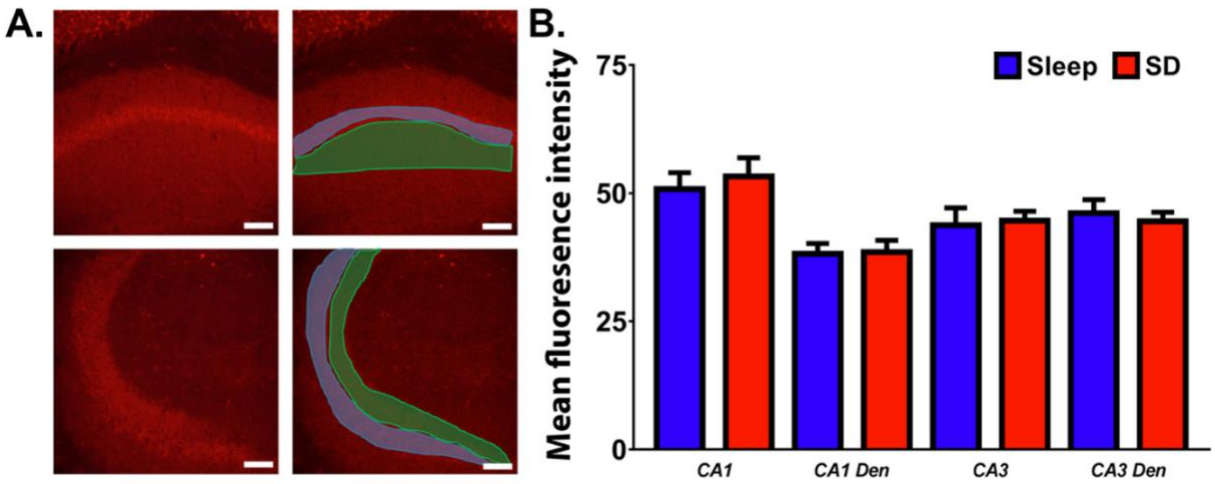


**Figure 2.6 Sleep deprivation does not significantly alter Arc protein levels in hippocampal areas CA3 or CA1. A.** Strategy for measuring mean fluorescence intensity in pyramidal cell and dendritic (Den) layers in dorsal hippocampal subregions. Selection of the pyramidal cell layer in CA1/CA3 are shown in blue. Estimated dendritic regions adjacent to cell layers are shown in green. **B.** Mean fluorescence values did not significantly differ between Sleep (n = 5 mice) and SD (n = 5 mice) conditions in any area. Scale bars indicate 100 µm.

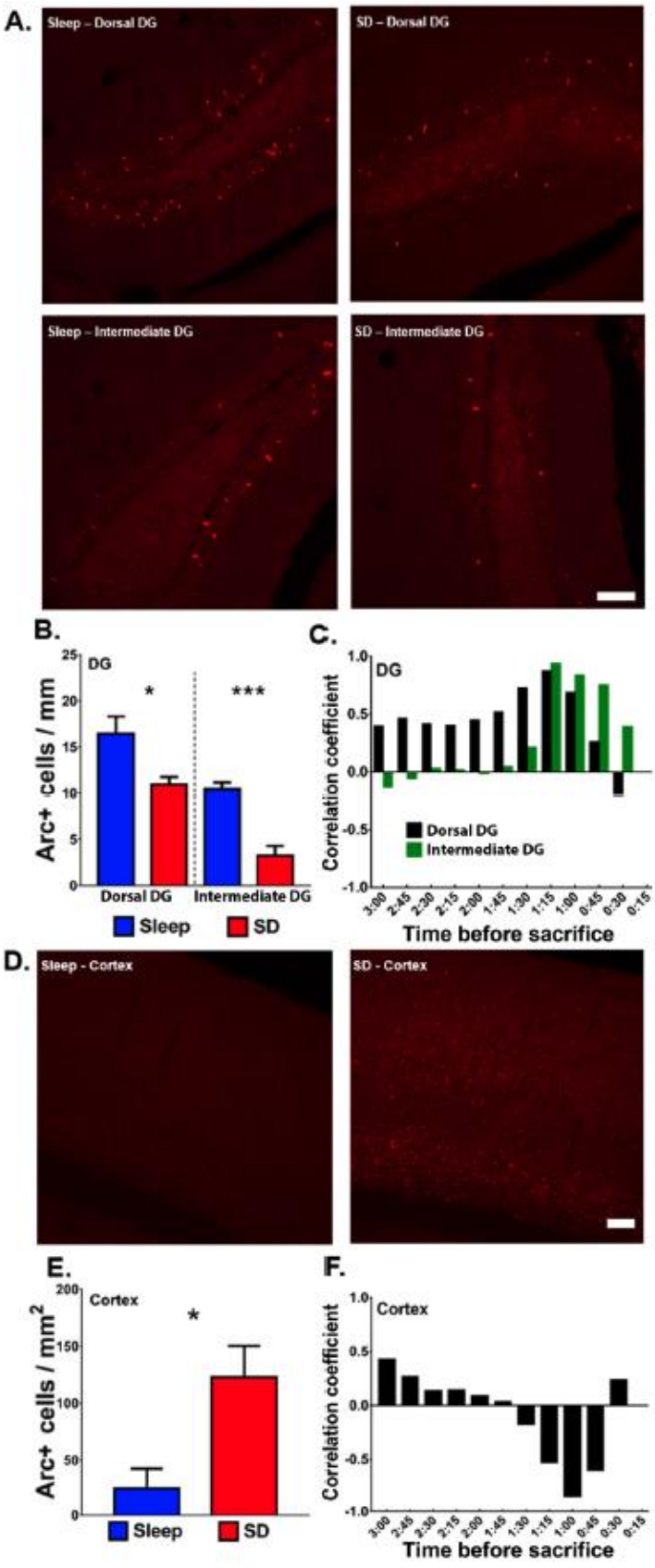


**Figure 2.7 Sleep deprivation simultaneously decreases Arc protein expression among DG cells, and increases Arc expression among cortical cells. A.** Representative images of immunohistochemical staining for Arc in dorsal and intermediate DG following 3 h of ad lib Sleep (n = 5 mice) or SD (n = 5 mice). **B.** Arc+ cells/mm were decreased in both dorsal and intermediate DG. Data indicate mean ± SEM for each condition; * indicates $p < 0.05$, *** indicates $p < 0.001$, Student's t-test. **C.** Pearson correlation coefficients for cortical Arc+ cells/mm in dorsal (black bars) and intermediate (green bars) DG vs. sleep time integrated over various intervals prior to sacrifice. **D.** Representative images from Sleep and SD mice, showing Arc+ cells in primary somatosensory cortex overlying dorsal hippocampus. Scale bar indicates 100 µm. **E.** The number of Arc+ cells/mm2 in the cortex was increased after SD. * indicates $p < 0.05$, Student's t-test. **F.** Pearson correlation coefficients for cortical Arc+ cells/mm2 vs. sleep time integrated over various intervals prior to sacrifice. Negative relationships between total sleep time and Arc+ cell numbers were present over the final hour of the experiment.

expression showed a tendency to be reduced in animals sleeping more over the last hour prior to sacrifice (Pearson *R* = -0.84, Bonferroni-corrected *p* value *N.S.*).

## 2.7 Discussion

Here, we show that sleep- and SD-associated *Arc* mRNA and protein expression patterns vary between the hippocampus and cortex. We find that expression levels measured in samples of whole hippocampus (or cortex) increase in a manner consistent with previous reports (Cirelli et al., 2004; Mackiewicz et al., 2007; Thompson et al., 2010; Vecsey et al., 2012). By comparing the relative levels of pre-mRNA and mature mRNA in Sleep and SD conditions, we find new (immature) *Arc* transcripts in the hippocampus are unchanged across SD, while in the cortex, increases in pre-mRNA parallel increases in mature *Arc* mRNA. This suggests that previously-reported increases in *Arc* mRNA in cortex following SD (Cirelli et al., 2004; Mackiewicz et al., 2007) reflect *de novo* transcription.

Previous work has shown that in the hippocampus, stimulus-induced expression of mature *Arc* mRNA lags expression of its pre-mRNA by only 5-10 min (Saha et al., 2011). Our surprising finding of an increase in mature *Arc* in the hippocampus *without* a corresponding increase in pre-mRNA suggests that a non-transcriptional mechanism must increase *Arc* levels across SD. One mechanism which could plausibly affect the ratio of pre-mRNA to mature RNA is an altered rate of pre-mRNA splicing. Here, we would expect an increase in the splicing rate in the hippocampus with SD. While splicing rates can be altered *in vitro* (for example, through phosphorylation of the C-terminal of RNA polymerase II (Millhouse and Manley, 2005), the rate of splicing *in vivo* is tightly coupled

with polymerase recruitment, and thus the rate of transcription (Saldi et al., 2016). Furthermore, expression of genes required for RNA splicing are reportedly downregulated in the hippocampus across a period of SD (Vecsey et al., 2012), making this an unlikely explanation for our results. In contrast, selective increases in levels of mature mRNA could be explained by increased mRNA stability. There is abundant evidence that following translation, mature *Arc* transcripts undergo rapid degradation; thus the half-life of new hippocampal *Arc* transcripts is ~45 min (Rao et al., 2006). One possibility is that during SD (and specifically in the hippocampus), the activity- and translation-dependent mechanisms which mediate Arc mRNA degradation (Farris et al., 2014; Ninomiya et al., 2016) are suppressed. Prior data have suggested that translation rates are decreased throughout the brain during spontaneous wake relative to slow wave sleep (Ramm and Smith, 1990), and that SD suppresses protein synthesis in the hippocampus (Tudor et al., 2016; Vecsey et al., 2012). Further, sleep promotes, and SD reduces, the expression of genes involved in protein synthesis (Mackiewicz et al., 2007). Thus a parsimonious explanation of our current findings is that in the hippocampus, SD does not increase the rate of *Arc* transcription, but slows its translation and subsequent degradation. Our immunohistochemical results are consistent with this interpretation; expression of Arc protein in the DG is reduced after just 3 h of SD.

*Arc* is an immediate early gene which is rapidly transcribed in the hippocampus response to increasing neural activity (Rao et al., 2006) and learning (Guzowski et al., 2001). SD in the hours following learning is known to disrupt memory consolidation for tasks that are selectively dependent on the dorsal hippocampus (Graves et al., 2003; Vecsey et al., 2009). Thus we assessed how SD affected *Arc* mRNA expression among

neurons in specific subregions of the dorsal hippocampus and in overlying neocortex, using fluorescence *in situ* hybridization. Surprisingly, we found that no significant changes in overall expression levels with SD in any of these regions. Mean intensity values were nearly identical in Sleep and SD conditions in CA1, CA3, and DG, and while expression tended to be higher in the cortex following SD, intensity differences between Sleep and SD were not statistically significant. We attribute the lack of statistical significance for changes in overall *in situ* fluorescence (when changes were detected using qPCR) to two plausible issues. First, the quantified areas were necessarily subsampled for *in situ* hybridization, while qPCR quantified expression in whole brain structures. Second, the differential outcomes may be the result of differences in the sensitivity of detection using the two techniques. In contrast, by counting the density of *Arc*+ neurons in DG and cortex, we found substantial differences in expression between Sleep and SD conditions. In cortex, these changes mirrored changes in cortical *Arc* mRNA expression levels measured using qPCR - with higher numbers of neurons labeled with *Arc* probes after SD. Arc protein expression follows the same pattern in the cortex, with significantly higher expression following SD, and a negative relationship between sleep time and the number of Arc-expressing neurons. In stark contrast, significantly fewer DG granule cells were *Arc*+ in the SD condition. Together these data suggest that sleep, but not extended wake, supports *Arc* expression in the DG; further, this relationship between sleep and *Arc* expression may be unique to DG granule cells. Our immunohistochemical quantification of Arc protein in the DG supports this idea - we find that Arc protein-expressing granule cells are also more numerous following a 3-h interval of *ad lib* sleep that following SD,

and that expression levels showed a strong tendency to be higher in animals that had spent more time sleeping.

Ours is not the first study to link DG *Arc* expression to sleep. Recently, Renouard et al. demonstrated that following a prolonged (multi-day) period of REM sleep deprivation, *Arc* expression is reduced in the hippocampus (and increased in the cortex); during subsequent recovery sleep (which contains relatively high amounts of REM) *Arc* levels increase and decrease, respectively, in hippocampus and cortex. The same study demonstrated immunohistochemically that the number of Arc+ neurons in DG decreased with REM sleep deprivation, and increased with recovery sleep (Renouard et al., 2015). The authors attributed these changes to differing amounts of REM in the various experimental conditions. However, another possibility is that these changes were related to differences in the amount of non-REM (NREM) sleep and wake, which were significantly decreased and increased, respectively, as a result of REM sleep deprivation (Renouard et al., 2015). While mice in our present study were not instrumented for polysomnographic quantification of REM and NREM sleep, we would expect (based on prior studies of *ad lib* sleep in instrumented C57Bl6/J mice) that REM constitutes roughly 5-10% of total recording time at ZT0-3, while NREM constitutes 50-70% of the same time period (Huber et al., 2000; Koehl et al., 2006; Meerlo et al., 2001; Wimmer et al., 2013). The limited REM sleep time expected for mice in our current study (which we estimate would amount to 9-18 minutes, total, prior to sacrifice) suggest that either REM sleep can induce expression of Arc in the DG very efficiently and quickly, or that NREM sleep may also be important for Arc expression. While future studies will be required to address this

issue, it is clear from our present findings that even brief periods of sleep loss disrupt DG Arc expression.

How might increased DG expression of Arc during sleep impact hippocampal function? In the absence of Arc expression, various forms of synaptic plasticity are disrupted, including homeostatic plasticity, LTD, and LTP (Gao et al., 2010; Messaoudi et al., 2007; Plath et al., 2006; Shepherd et al., 2006; Waung et al., 2008). In the DG, Arc plays a role in synaptic structure as well as function. Disruption of Arc in the DG leads to reduced phosphorylation of the actin depolymerization factor cofilin, and reduced synaptic filamentous actin (F-actin) (Messaoudi et al., 2007). Since SD appears to disrupt *Arc* transcription and translation among granule cells in a similar manner, one might expect reduced synaptic spine density in DG after SD. Indeed, in this same issue, Raven et al. show that spine density in DG granule cells is reduced after 5 h of SD (Raven et al., In press). Prior work has shown that SD also reduces cofilin phosphorylation, leading to reduced spine numbers (Havekes et al., 2016). Taken together, the available data suggest that SD disrupts Arc-dependent regulation of the actin cytoskeleton in the DG, and that this leads to reduced dendritic spine numbers among granule cells. Because DG granule cells play a critical role in the recall of spatial, episodic, and contextual memories (Bernier et al., 2017; Liu et al., 2012; Morris et al., 2013; Niewoehner et al., 2007; Yokoyama and Matsuo, 2016), it is plausible that deficits in hippocampally-mediated cognitive functions after SD are mediated in part by effects on Arc expression in DG.

A final unresolved question is why Arc expression is reduced in DG, while simultaneously being increased in cortex, following brief SD. Previous studies, using longer periods of SD (up to 24 h), have shown differential effects on dendritic spines in

other areas of hippocampus (e.g., CA1) vs. cortex (Acosta-Pena et al., 2015; Havekes et al., 2016). We have proposed previously that sleep may have differing effects on intracellular pathways required for synaptic plasticity, either downregulating or upregulating their activity, depending on prior experience during wake (Puentes-Mestril and Aton, 2017). This idea is based on experimental findings from studies carried out using animal models over the past two decades. For example, following a learning experience, immediate early genes *Egr1, Fos, and Arc* (Calais et al., 2015; Ribeiro et al., 1999) and Arc protein (Ulloor and Datta, 2005) expression are increased in the hippocampus during subsequent sleep. Data from our own lab suggest that both sleep-associated network activity patterns (Aton et al., 2013; Aton et al., 2014; Durkin et al., 2017; Durkin and Aton, 2016; Ognjanovski et al., 2014; Ognjanovski et al., 2017) and sleep-associated activation of cellular signaling pathways involved in synaptic plasticity (Aton et al., 2009) vary as a function of prior learning experience.

Multiple lines of evidence suggest that DG synaptic plasticity, in particular, may be augmented preferentially during sleep. It has long been known that following spatial task performance, DG place cell reactivation occurs selectively during NREM sleep (Shen et al., 1998). Since the DG appears to play a continuous role in encoding and storing spatial, temporal, and contextual aspects of the animal's environment (Kesner, In Press), it seems likely that mechanisms underlying synaptic- and systems-level memory consolidation (including those mediated by Arc) would be active in this structure during sleep, even under "baseline" conditions. DG granule cells integrate inputs from cortical, hippocampal, and septal structures (Kesner, In Press), all of which show sleep-associated changes in activity (Puentes-Mestril and Aton, 2017). Recent studies support the idea that cortical

input to the DG is altered, and possibly augmented, during sleep. For example, spikes of highly synchronous DG activity occur frequently during NREM sleep, and that these spikes are temporally associated with inter-regional cortical up-states (Headley et al., 2017). Theta (7-12 Hz) and slow oscillatory (~1 Hz) activity patterns (associated with REM and NREM, respectively) differentially modulate input to the DG via the lateral and medial perforant pathway (Schall and Dickson, 2010). Finally, during NREM sleep, DG evoked firing rate responses to input are higher than during wake (Winson and Abzug, 1978). Based on our present data and these prior findings, we hypothesize that the unique network connectivity of the DG leads to activity-driven plastic changes - mediated, at least in part, by Arc - in this structure during sleep.

## 2.8 References


Acosta-Pena, E., Camacho-Abrego, I., Megarejo-Gutierrez, M., Flores, G., Drucker-Colin, R., and Garcia-Garcia, F. (2015). Sleep deprivation induces differential morphological changes in the hippocampus and prefrontal cortex in young and old rats. Synapse *69*, 15-25.

Aton, S.J., Broussard, C., Dumoulin, M., Seibt, J., Watson, A., Coleman, T., and Frank , M.G. (2013). Visual experience and subsequent sleep induce sequential plastic changes in putative inhibitory and excitatory cortical neurons. Proc Natl Acad Sci U S A *110*, 3101-3106.

Aton, S.J., Seibt, J., Dumoulin, M., Jha, S.K., Steinmetz, N., Coleman, T., Naidoo, N., and Frank, M.G. (2009). Mechanisms of sleep-dependent consolidation of cortical plasticity. Neuron *61*, 454-466.

Aton, S.J., Suresh, A., Broussard, C., and Frank, M.G. (2014). Sleep promotes cortical response potentiation following visual experience. Sleep *37*, 1163-1170.

Bernier, B.E., Lacagnina, A.F., Ayoub, A., Shue, F., Zemelman, B.V., Krasne, F.B., and Drew, M.R. (2017). Dentate Gyrus Contributes to Retrieval as well as Encoding: Evidence from Context Fear Conditioning, Recall, and Extinction. J Neurosci *37*, 6359-6371.

Calais, J.B., Ojopi, E.B., Morya, E., Sameshima, K., and Ribeiro, S. (2015). Experience-dependent upregulation of multiple plasticity factors in the hippocampus during early REM sleep. Neurobiol Learn Mem *122*, 19-27.

Carter, S.D., Mifsud, K.R., and Reul, J.M. (2015). Distinct epigenetic and gene expression changes in rat hippocampal neurons after Morris water maze training. Front Behav Neurosci *9*, 156.

Cirelli, C., Gutierrez, C.M., and Tononi, G. (2004). Extensive and divergent effects of sleep and wakefulness on brain gene expression. Neuron *41*, 35-43.

Czerniawski, J., Ree, F., Chia, C., Ramamoorthi, K., Kumata, Y., and Otto, T.A. (2011). The importance of having Arc: expression of the immediate-early gene Arc is required for hippocampus-dependent fear conditioning and blocked by NMDA receptor antagonism. J Neurosci *31*, 11200-11207.

Durkin, J., Suresh, A.K., Colbath, J., Broussard, C., Wu, J., Zochowski, M., and Aton, S.J. (2017). Cortically coordinated NREM thalamocortical oscillations play an essential, instructive role in visual system plasticity. Proceedings National Academy of Sciences *114*, 10485-10490.

Durkin, J.M., and Aton, S.J. (2016). Sleep-dependent potentiation in the visual system is at odds with the Synaptic Homeostasis Hypothesis. Sleep.

Farris, S., Lewandowski, G., Cox, C.D., and Steward, O. (2014). Selective localization of arc mRNA in dendrites involves activity- and translation-dependent mRNA degradation. J Neurosci *34*, 4481-4493.

Fellini, L., and Morellini, F. (2013). Mice create what-where-when hippocampus-dependent memories of unique experiences. J Neurosci *33*, 1038-1043.

Fisher, S.P., Godinho, S.I.H., Pothecary, C.A., Hankins, M.W., Foster, R.G., and Peirson, S.N. (2012). Rapid assessment of sleep/wake behaviour in mice. J Biol Rhythms *27*, 48-58.

Gao, M., Sossa, K., Song, L., Errington, L., Cummings, L., Hwang, H., Kuhl, D., Worley, P., and Lee, H.K. (2010). A specific requirement of Arc/Arg3.1 for visual experience-induced homeostatic synaptic plasticity in mouse primary visual cortex. J Neurosci *30*, 7168-7178.

Graves, L.A., Heller, E.A., Pack, A.I., and Abel, T. (2003). Sleep deprivation selectively impairs memory consolidation for contextual fear conditioning. Learn Mem *10*, 168-176.

Guzowski, J.F., Setlow, B., Wagner, E.K., and McGaugh, J.L. (2001). Experience-dependent gene expression in the rat hippocampus after spatial learning: a comparison of the immediate-early genes Arc, c-fos, and zif268. J Neurosci *21*, 5089-5098.

Havekes, R., Park, A.J., Tudor, J.C., Luczak, V.G., Hansen, R.T., Ferri, S.L., Bruinenberg, V.M., Poplawski, S.G., Day, J.P., Aton, S.J.*, et al.* (2016). Sleep deprivation causes memory deficits by negatively impacting neuronal connectivity in hippocampal area CA1. eLife *5*, pii: e13424.

Headley, D.B., Kanta, V., and Pare, D. (2017). Intra- and interregional cortical interactions related to sharp-wave ripples and dentate spikes. J Neurophysiol *117*, 556-565.

Huber, R., Deboer, T., and Tobler, R. (2000). Effects of sleep deprivation on sleep and sleep EEG in three mouse strains: empirical data and simulations. Brain Research *857*, 8-19.

Kesner, R.P. (In Press). An analysis of dentate gyrus function (an update). Behav Brain Res.

Koehl, M., Battle, S., and Meerlo, P. (2006). Sex Differences in Sleep: the Response to Sleep Deprivation and Restraint Stress in Mice. Sleep *29*, 1224-1231.

Liu, X., Ramirez, S., Pang, P.T., Puryear, C.B., Govindarajan, A., Diesseroth, K., and Tonegawa, S. (2012). Optogenetic stimulation of a hippocampal engram activates fear memory recall. Nature *484*, 381-385.

Mackiewicz, M., Shockley, K.R., Romer, M.A., Galante, R.J., Zimmerman, J.E., Naidoo, N., Baldwin, D.A., Jensen, S.T., Churchill, G.A., and Pack, A.I. (2007). Macromolecule biosynthesis - a key function of sleep. Physiol Genomics *31*, 441-457.

McCurry, C.L., Shepherd, J.D., Tropea, D., Wang, K.H., Bear, M.F., and Sur, M. (2010). Loss of Arc renders the visual cortex impervious to the effects of sensory experience or deprivation. Nat Neurosci *13*, 450-457.

Meerlo, P., Easton, A., Bergmann, B.M., and Turek, F. (2001). Restraint increases prolactin and REM sleep in C57BL/6J mice but not in BALB/cJ mice. Am J Comp Physiol *281*, R846-854.

Messaoudi, E., Kanhema, T., Soule, J., Tiron, A., Dagyte, G., da Silva, B., and Bramham, C.R. (2007). Sustained Arc/Arg3.1 synthesis controls long-term potentiation consolidation through regulation of local actin polymerization in the dentate gyrus in vivo. J Neurosci *27*, 10455-10455.

Millhouse, S., and Manley, J.L. (2005). The C-terminal domain of RNA polymerase II functions as a phosphorylation-dependent splicing activator in a heterologous protein. Mol Cell Biol *25*, 533-544.

Morris, A.M., Curtis, B.J., Chruchwell, J.C., Maasberg, D.W., and Kesner, R.P. (2013). Temporal associations for spatial events: the role of the dentate gyrus. Behav Brain Res *256*, 250-256.

Niewoehner, B., Single, F.N., Hvalby, O., Jensen, V., Meyer zum Alten Borgloh, S., Seeburg, P.H., Rawlins, J.N., Sprengel, R., and Bannerman, D.M. (2007). Impaired spatial working memory but spared spatial reference memory following functional loss of NMDA receptors in the dentate gyrus. Eur J Neurosci *25*, 837-846.

Ninomiya, K., Ohno, M., and Kataoka, N. (2016). Dendritic transport element of human arc mRNA confers RNA degradation activity in a translation-dependent manner. Genes Cells *21*, 1263-1269.

Ognjanovski, N., Maruyama, D., Lashner, N., Zochowski, M., and Aton, S.J. (2014). CA1 hippocampal network activity changes during sleep-dependent memory consolidation. Front Syst Neurosci *8*, 61.

Ognjanovski, N., Schaeffer, S., Mofakham, S., Wu, J., Maruyama, D., Zochowski, M., and Aton, S.J. (2017). Parvalbumin-expressing interneurons coordinate hippocampal network dynamics required for memory consolidation. Nature Communications *8*, 15039.

Pack, A.I., R.J., G., Maislin, G., Cater, J., Metaxas, D., Lu, S., Zhang, L., Von Smith, R., Kay, T., Lian, J.*, et al.* (2007). Novel method for high-throughput phenotyping of sleep in mice. Physiol Genomics *28*, 232-238.

Plath, N., Ohana, O., Dammermann, B., Errington, M.L., Schmitz, D., Gross, C., Mao, X., Engelsberg, A., Mahlke, C., Welzl, H.*, et al.* (2006). Arc/Arg3.1 is essential for the consolidation of synaptic plasticity and memories. Neuron *52*, 437-444.

Prince, T.M., and Abel, T. (2013). The impact of sleep loss on hippocampal function. Learn Mem *20*, 558-569.

Puentes-Mestril, C., and Aton, S.J. (2017). Linking network activity to synaptic plasticity during sleep: hypotheses and recent data. Frontiers in Neural Circuits *11*, doi: 10.3389/fncir.2017.00061.

Ramm, P., and Smith, C.T. (1990). Rates of cerebral protein synthesis are linked to slow-wave sleep in the rat. PhysiolBehav *48*, 749-753.

Rao, V.R., Pintchovski, S.A., Chin, K., Peebles, C.L., Mitra, S., and Finkbeiner, S. (2006). AMPA receptors regulate transcription of the plasticity-related immediate-early gene Arc. Nat Neurosci *9*, 887-895.

Raven, F., Meerlo, P., Van der Zee, E.A., Abel, T., and Havekes, R. (In press). A brief period of sleep deprivation causes spine loss in the dentate gyrus of mice. Neurobiology of Learning and Memory.

Renouard, L., Billwiller, F., Ogawa, K., Clement, O., Camargo, N., Abdelkarim, M., Gay, N., Scote-Blachon, C., Toure, R., Libourel, P.A.*, et al.* (2015). The supramammillary nucleus and the claustrum activate the cortex during REM sleep. Sci Adv *1*, e1400177.

Ribeiro, S., Goyal, V., Mello, C.V., and Pavlides, C. (1999). Brain gene expression during REM sleep depends on prior waking experience. Learn Mem *6*, 500-508.

Saha, R.N., Wissink, E.M., Bailey, E.R., Zhao, M., Fargo, D.C., Hwang, J.Y., Daigle, K.R., Fenn, J.D., Adelman, K., and Dudek, S.M. (2011). Rapid activity-induced transcription of Arc and other IEGs relies on poised RNA polymerase II. Nat Neurosci *14*, 848-856.

Saldi, T., Cortazar, M.A., Sheridan, R.M., and Bentley, D.L. (2016). Coupling of RNA Polymerase II Transcription Elongation with Pre-mRNA Splicing. J Mol Biol *428*, 2623-2635.

Schall, K.P., and Dickson, C.T. (2010). Changes in hippocampal excitatory synaptic transmission during cholinergically induced theta and slow oscillation states. Hippocampus *20*, 279-292.

Shen, J., Kudrimoti, H.S., McNaughton, B.L., and Barnes, C.A. (1998). Reactivation of neuronal ensembles in hippocampal dentate gyrus during sleep after spatial experience. J Sleep Res *7*, 6-16.

Shepherd, J.D., Rumbaugh, G., Wu, J., Chowdhury, S., Plath, N., Kuhl, D., Huganir, R.L., and Worley, P.F. (2006). Arc/Arg3.1 mediates homeostatic synaptic scaling of AMPA receptors. Neuron *52*, 475-484.

Thompson, C.L., Wisor, J.P., Lee, C.-K., Pathak, S.D., Gerashchenko, D., Smith, K.A., Fischer, S.R., Kuan, C.L., Sunkin, S.M., Ng, L.L.*, et al.* (2010). Molecular and Anatomical Signatures of Sleep Deprivation in the Mouse Brain. Front Neurosci *4*.

Tudor, J.C., Davis, E.J., Peixoto, L., Wimmer, M.E., van Tilborg, E., Park, A.J., Poplawski, S.G., Chung, C.W., Havekes, R., Huang, J.*, et al.* (2016). Sleep deprivation impairs memory by attenuating mTORC1-dependent protein synthesis. Sci Signal *9*.

Ulloor, J., and Datta, S. (2005). Spatio-temporal activation of cyclic AMP response element-binding protein, activity-regulated cytoskeletal-associated protein and brain-derived nerve growth factor: a mechanism for pontine-wave generator activation-dependent two-way active-avoidance memory processing in the rat. Journal of Neurochemistry *95*, 418-428.

Vecsey, C.G., Baillie, G.S., Jaganath, D., Havekes, R., Daniels, A., Wimmer, M., Huang, T., Brown, K.M., Li, X.Y., Descalzi, G.*, et al.* (2009). Sleep deprivation impairs cAMP signalling in the hippocampus. Nature *461*, 1122-1125.

Vecsey, C.G., Peixoto, L., Choi, J.H., Wimmer, M., Jaganath, D., Hernandez, P.J., Blackwell, J., Meda, K., Park, A.J., Hannenhalli, S.*, et al.* (2012). Genomic analysis of sleep deprivation reveals translational regulation in the hippocampus. Physiol Genomics *44*, 981-991.

Wang, F., Flanagan, J., Su, N., Wang, L.C., Bui, S., Nielson, A., Wu, X., Vo, H.T., Ma, X.J., and Luo, Y. (2012). RNAscope: a novel in situ RNA analysis platform for formalin-fixed, paraffin-embedded tissues. J Mol Diagn *14*, 22-29.

Waung, M.W., Pfeiffer, B.E., Nosyreva, E.D., Ronesi, J.A., and Huber, K.M. (2008). Rapid translation of Arc/Arg3.1 selectively mediates mGluR-dependent LTD through persistent increases in AMPAR endocytosis rate. Neuron *59*, 84-97.

Wimmer, M., Rising, J., Galante, R.J., Wyner, A., and Abel, T. (2013). Aging in Mice Reduces the Ability to Sustain Sleep/Wake States. PLoS ONE *8*, e81880.

Winson, J., and Abzug, C. (1978). Neuronal transmission through hippocampal pathways dependent on behavior. J Neurophysiol *41*, 716-732.

# Chapter III. Learning and Sleep Have Divergent Effects on Cytosolic and Membrane-Associated Ribosomal mRNA Profiles in Hippocampal Neurons

## 3.1 Abstract

The hippocampus plays an essential role in consolidating transient experiences into long-lasting memories. Memory consolidation can be facilitated by post-learning sleep, although the underlying cellular mechanisms are undefined. Here, we addressed this question using a mouse model of hippocampally-mediated, sleep-dependent memory consolidation (contextual fear memory; CFM), which is known to be disrupted by post-learning sleep loss. We used translating ribosome affinity purification (TRAP) to quantify ribosome-associated RNAs in different subcellular compartments (cytosol and membrane) and in different hippocampal cell populations (either whole hippocampus, Camk2a+ excitatory neurons, or highly active neurons expressing phosphorylated ribosomal subunit S6 [pS6+]). Using RNA-seq, we examined how these transcript profiles change as a function of sleep vs. sleep deprivation (SD), and as a function of prior learning (contextual fear conditioning; CFC). To our surprise, we found that while many mRNAs on cytosolic ribosomes were altered by sleep loss, almost none were altered by learning. Of the few changes in cytosolic ribosomal transcript abundance following CFC, almost all were occluded by subsequent SD. This effect was particularly pronounced in pS6+ neurons with the highest level of neuronal activity following CFC, suggesting SD-induced disruption of post-learning transcript changes in putative “engram” neurons. In

striking contrast, far fewer transcripts on membrane-bound (MB) ribosomes were altered by SD, and many more mRNAs (and lncRNAs) were altered MB ribosomes as a function of prior learning. For hippocampal neurons, cellular pathways most significantly affected by CFC were involved in structural remodeling. Comparisons of post-CFC transcript profiles between freely-sleeping and SD mice implicated changes in cellular metabolism in Camk2a+ neurons, and increased protein synthesis capacity in pS6+ neurons, as biological processes disrupted by post-learning sleep loss.

## 3.2 Introduction

The role of sleep in promoting synaptic plasticity and memory storage (consolidation) in the brain is an enduring mystery (Puentes-Mestril and Aton, 2017). For the past two decades, transcriptomic (Cirelli et al., 2004; Mackiewicz et al., 2007; Vecsey et al., 2012) and proteomic (Cirelli et al., 2009; Noya et al., 2019; Poirrier et al., 2008; Ren et al., 2016) profiling of the mammalian brain after sleep vs. experimental sleep deprivation (SD) have provided insights regarding the general functions of sleep for the brain. For example, observed increases in the abundance of transcripts for immediate early genes and some synaptic proteins after SD were the initial basis for the synaptic homeostasis hypothesis for sleep function (Cirelli et al., 2004). The hypothesis proposes that synapses are broadly “downscaled” during sleep. However, the function of such a process in memory consolidation, and it’s occurrence during post-learning sleep, are a matter of debate (Havekes and Aton, 2020). On the other hand, observations from in vivo electrophysiology in the sleeping brain has led to conclusion that specific patterns of activity present during learning experiences may be replayed during subsequent sleep. Such a mechanism would be instructive with regard to memory storage (i.e., selectively

affecting only highly active “engram neurons” engaged during prior experience and their postsynaptic partners). However, determining whether replay is necessary for memory consolidation has been difficult (Puentes-Mestril and Aton, 2017; Puentes-Mestril et al., 2019), and it is unknown how this process (and other features of brain physiology associated with sleep) would affect intracellular pathways (e.g. those involved in synaptic plasticity).

More recently, transcriptomic and proteomic profiling of synaptic or axonal organelles has been used to better understand the effects of learning (Ostroff et al., 2019) or of sleep vs. wake (Noya et al., 2019) on synaptic function. However, to date, there has been no experimental work aimed at characterizing cellular changes during sleep-dependent memory consolidation - i.e. those occurring as a function of post-learning sleep. Here, we use a well-established mouse model of sleep-dependent memory consolidation - contextual fear memory (CFM) - to study this process. CFM can be encoded in a single learning trial (contextual fear conditioning; CFC), and is consolidated via hippocampus-dependent mechanisms over the next few hours. Critically, CFM consolidation can be disrupted by sleep deprivation (SD) within the first 5-6 h following CFC (Graves et al., 2003; Ognjanovski et al., 2018). Over this same post-CFC time interval, disruption of either neuronal activity (Daumas et al., 2005), transcription (Igaz et al., 2002; Pereira et al., 2019), or translation (Gafford et al., 2011; Tudor et al., 2016) in the dorsal hippocampus can likewise disrupt consolidation. This suggests that an activity- and sleep-dependent mechanism, impinging on biosynthetic pathways in the hippocampus, is essential for consolidation.

To shed light on this putative mechanism, we characterized changes to ribosome-associated mRNAs from different hippocampal cell populations (including Camk2a+ excitatory neurons and highly active neurons expressing phosphorylated S6 [pS6+]) as a function of both sleep vs. SD and prior CFC. By quantifying mRNA profiles on ribosomes differentially localized to the cytosol and cellular membranes, we find that while the majority of changes to transcripts on cytosolic ribosomes vary as a function of sleep vs. wake, the majority of transcript changes on membrane-bound (MB) ribosomes vary as a function of learning. Our findings reveal new subcellular functions for post-learning sleep, and suggest new cellular mechanisms by which sleep could selectively promote memory storage.

## 3.3 Materials & Methods

### Mouse Husbandry, Handling, and Behavioral Procedures

All animal husbandry and experimental procedures were approved by the University of Michigan Institutional Animal Care and Use Committee (PHS Animal Welfare Assurance number D16-00072 [A3114-01]). For all studies, mice were maintained on a 12:12h light/dark cycle (lights on at 8 AM) with food and water provided *ad lib*. B6.Cg-Tg(Camk2a-cre)T29-1Stl/J mice (Jackson) were crossed to B6N.129-Rpl22$^{tm1.1Psam}$/J mice (Jackson) to express HA-tagged Rpl22 protein in Camk2a+ neurons.

Mice were individually housed with beneficial enrichment for one week prior to experiments, and were habituated to handling (5 min/day) for five days prior to experiments. Mice were randomly assigned to one of four groups: HC + Sleep ($n$ = 8), HC + SD ($n$ = 7), CFC + Sleep ($n$ = 8), CFC + SD ($n$ = 7). Beginning at lights-on (8 AM),

half of the mice underwent single-trial contextual fear conditioning (CFC) as described previously (Ognjanovski et al., 2018; Ognjanovski et al., 2014; Ognjanovski et al., 2017). Briefly, mice were placed in a novel conditioning chamber (Med Associates), and were allowed 2.5 min of free exploration time prior to delivery a 2-s, 0.75 mA foot shock through the chamber's grid floor. After 3 min total in the chamber, mice were returned to their home cage (HC). As a control for the effects of learning, HC controls remained in their home cage during this time. HC + SD or CFC + SD mice were then kept awake continuously by gentle handling (SD; consisting of cage tapping, nest disturbance, and if necessary, stroking with a cotton-tipped applicator) over the next 3 h (for all RNA seq studies) or 5 h (for all qPCR experiments). HC + Sleep and CFC + Sleep mice were permitted *ad lib* sleep in their home cage for the same time interval.

**Translating Ribosome Affinity Purification (TRAP)**

RiboTag TRAP was performed as previously described (Sanz et al., 2009) by indirect conjugation (Jiang et al., 2015), separating membrane-bound and free-floating ribosomes (Kratz et al., 2014). Briefly, following 3 h *ad lib* sleep or SD, mice were sacrificed with an overdose of pentobarbital (Euthasol). Brains were extracted and hippocampi dissected in ice cold dissection buffer (1x HBSS, 2.5 mM HEPES [pH 7.4], 4 mM $NaHCO_3$, 35 mM glucose, 100ug/ml cycloheximide). Tissue was then transferred to glass dounce column containing 1 ml homogenization buffer (10 mM HEPES [pH 7.4], 150 mM KCl, 10 mM $MgCl_2$, 2 mM DTT, 0.1 cOmplete™ Protease Inhibitor Cocktail [Sigma-Aldrich, 11836170001], 100 U/mL RNasin® Ribonuclease Inhibitors [Promega, N2111], and 100 µg/mL cycloheximide) and manually homogenized on ice. Homogenate

was transferred to 1.5 ml LoBind tubes (Eppendorf) and centrifuged at 4°C at 1000 g for 10 min. The resulting supernatant (cytosolic fraction) was transferred to a new LoBind tube while the pellet (MB fraction) was resuspended in homogenization buffer. 10% NP40 was then added to the samples and incubated 5 min on ice, after which both MB and cytosolic fractions were centrifuged at 4°C at maximum speed for 10 min. The resulting supernatant from both MB and cytosolic fractions was then separated into Input (~50µL), Camk2a+ (~400µL), and pS6+ fractions (~500µL). For isolating ribosomes from Camk2a+ populations, fractions were incubated with 1:40 anti-HA antibody (Abcam, ab9110)(Shigeoka et al., 2018). To isolate ribosomes from highly active (pS6+) neurons fractions were incubated with 1:25 anti-pS6 244-247 (ThermoFisher 44-923G)(Knight et al., 2012). Antibody binding of the homogenate-antibody solution occurred over 1.5 h at 4°C with constant rotation.

For affinity purification, 200 µl/sample of Protein G Dynabeads (ThermoFisher, 10009D) were washed 3 times in 0.15M KCl IP buffer (10 mM HEPES [pH 7.4], 150 mM KCl, 10 mM $MgCl_2$, 1% NP-40) and incubated in supplemented homogenization buffer (+10% NP-40). Following this step, supplemented buffer was removed, homogenate-antibody solution was added directly to the Dynabeads, and the solution was incubated for 1 h at 4°C with constant rotation. After incubation, the RNA-bound beads were washed four times in 900µL of 0.35M KCl (10mM HEPES [pH 7.4], 350 mM KCl, 10 mM $MgCl_2$, 1% NP40, 2 mM DTT, 100 U/mL RNasin® Ribonuclease Inhibitors [Promega, N2111], and 100 µg/mL cycloheximide). During the final wash, beads were placed onto the magnet and moved to room temperature. After removing the supernatant, RNA was

eluted by vortexing the beads vigorously in 350 µl RLT (Qiagen, 79216). Eluted RNA was purified using RNeasy Micro kit (Qiagen).

**Quantitative Real-Time PCR (qPCR)**

For qPCR, RNA from each sample was converted into cDNA using the SuperScript IV Vilo Master Mix (Invitrogen 11756050). qPCR was performed on diluted cDNA that employed either Power SYBR Green PCR Mix (Invitrogen 4367659) or TaqMan Fast Advanced Master Mix (Invitrogen 4444557). For TRAP enrichment values, each sample was normalized to the geometric mean of *Pgk1* and *Gapdh* housekeeping transcripts and then normalized to the corresponding Input sample (TRAP Enrichment = 2^(ΔCt_target - ΔCt_housekeeping). Effects of SD were assessed by normalizing all groups' expression to the HC + Sleep group. Effects of CFC were quantified by normalizing CFC + Sleep to HC + Sleep and normalizing CFC + SD to HC + SD. Primers for mRNAs quantified are listed below.

| | Forward Primer | Reverse Primer |
|---|---|---|
| Gapdh | GTGTTTCCTCGTCCCGTAGA | AATCCGTTCACACCGACCTT |
| Pgk1 | TCGTGATGAGGGTGGACTTC | ACAGCAGCCTTGATCCTTTG |
| Arc | CCAGATCCAGAACCACATGAA | GAGAGTGTACCCTCACTGTATTG |
| cFos | GAAGAGGAAGAGAAACGGAGAAT | CTTGGAGTGTATCTGTCAGCTC |

| | | |
|---|---|---|
| Homer1a | GCATTGCCATTTCCACATAGG | ATGAACTTCCATATTTATCCACCTTACTT |
| Glua1 | AGTGACGCTCGGGACCACAC | CTCTGGAAGGCCTCCGCCAT |
| Bdnf | GGTCACAGCGGCAGATAAA | TCAGTTGGCCTTTGGATACC |
| Hspa5 | CCGAGAACACGGTCTTCGAT | ATTCCAAGTGCGTCCGATGA |
| Grin2a | CGTAGAGGATGCCTTGGTCA | CCATAGCCTGTGGTGGCAAA |
| Grin2b | CGGCCTGAGTGACAAGAAGT | TCCTCTCTGTGCTGCCATTG |
| Vglut1 | CCAGCATCTCTGAGGAGGAG | GGCTGAGAGATGAGGAGCAG |
| Parv | GTCGATGACAGACGTGCTCA | TTGTGGTCGAAGGAGTCTGC |
| Sst | CTCGGACCCCAGACTCCGTC | CTCGGGCTCCAGGGCATCAT |
| Mbp | CCTTGACTCCATCGGGCGCT | CTTCTGGGGCAGGGAGCCAT |
| Gfap | TCCTGGAACAGCAAAACAAG | CAGCCTCAGGTTGGTTTCAT |

| | Catalog # for ThermoFisher Taqman Probes |
|---|---|
| Gapdh | Mm99999915_g1 |
| Pgk1 | Mm00435617_m1 |
| FosB | Mm00500401_m1 |
| FosB | Custom-AP47Y2V |

| | |
|---|---|
| Homer1 | Mm01282664_m1 |
| Homer1a | Custom-APT2DGG |
| Atf3 | Mm00476033_m1 |
| Egr3 | Mm00516979_m1 |
| 1700016P03Rik | Mm01253067_m1 |

**RNA-Seq and Expression Analysis**

RNA-Seq was carried out at the University of Michigan's DNA Sequencing Core. Amplified cDNA libraries were prepared using Takara's SMART-seq v4 Ultra Low Input RNA Kit (Takara 634888) and sequenced on Illumina's NovaSeq 6000 platform. Sequencing reads (50 bp, paired end) were mapped to *Mus musculus* using Star v2.6.1a and quality checked with Multiqc (v1.6a0). Reads mapped to unique transcripts were counted with featureCounts (Liao et al., 2013).

Differential expression analyses were run with Deseq2 (Love et al., 2014). Analyses were run with an initial filtering step (removing rows with < 10 counts) and with betaPrior = False. To test differences between subcellular fractions within their respective cell population, the design of the GLM was set to compare differences between supernatant and pellet-enriched transcripts. Camk2a+, pS6+, and Input samples were analyzed separately (e.g., Camk2a+[supernatant/pellet]). To quantify effects of SD and CFC on expression, the design was switched and each cell population and subcellular fraction was analyzed separately. The same two-factor design was used to analyze the effects of an animal's state (Sleep or SD) and learning (CFC or HC) on RNA expression.

The design compared the effects of SD alone by combining HC and CFC animals. In contrast, the effect of learning (CFC) was assessed separately in CFC + Sleep and CFC + SD mice.

To characterize the differences between the effects of SD and CFC, significantly altered transcripts were analyzed using Ingenuity's Pathway Analysis (IPA). GO analyses were performed in IPA and DAVID's Functional Annotation tool. For subcellular fraction comparisons, 2000 of the top cytosolic (Log2FC > 0) and MB (Log2FC < 0) enriched transcripts (ranked by adjusted *p* values) were run through IPA's Canonical Pathways analysis. To characterize differences in common metabolic pathways between cytosolic and MB fractions, hierarchical clustering was used to visualize the most differentially-expressed transcripts. Since signaling pathways were less overlapping between the MB and cytosolic fraction, they were ranked by enrichment *p* values. Those transcripts were then run through DAVID's Functional Annotation tool, selecting for cellular composition to describe the cellular compartment the corresponding protein relates to. Data were plotted in Fragments Per Million (FPM) and their correlation value (R) calculated in the ViDger R package (McDermaid et al., 2019).

**Immunohistochemistry**

To characterize HA and pS6 expression in the hippocampus, experimentally naive animals were sacrificed and perfused with 1xPBS followed by 4% paraformaldehyde. 50μM coronal sections containing dorsal hippocampus were blocked in normal goat serum for 2 h and incubated overnight using a biotin conjugated anti-HA (Biolegend 901505, 1:500), anti-pS6 244-247 (ThermoFisher 44-923G, 1:500), and anti-parvalbumin

(Synaptic Systems 195 004, 1:500) antibodies. Sections were then incubated with secondary antibodies - Streptavidin-Alexa Fluor® 647 (Biolegend 405237), Fluorescein (FITC) Goat Anti-Rabbit IgG (H+L) (Jackson 111-095-003), and Alexa Fluor® 555 Goat Anti-Guinea pig IgG H&L (Abcam ab150186). Immunostained sections were coverslipped in ProLong Gold Antifade Reagent (ThermoFisher, P36930) for imaging with a Leica SP5 laser scanning confocal microscope.

## 3.4 TRAP-Mediated Isolation of mRNAs From Hippocampal Neuron Subpopulations.

To quantify the effects of sleep and learning on hippocampal mRNA translation, we employed two translating ribosome affinity purification (TRAP) techniques. First, to quantify ribosome-associated mRNAs in excitatory neurons, B6.Cg-Tg(Camk2a-cre)T29-1Stl/J mice were crossed to the B6N.129-*Rpl22*$^{tm1.1Psam/J}$ mouse line (Sanz et al., 2019; Sanz et al., 2009). Offspring from this cross express hemmatagluttin (HA)-tagged ribosomal protein 22 (HA-Rpl22) in excitatory (Camk2a+) neurons (**Figure 3.1A, left**). Second, to quantify mRNAs associated with ribosomes in active hippocampal neurons, we used an antibody targeting the terminal phosphorylation sites (Ser244/247) of ribosomal protein S6 (pS6) (Knight et al., 2012) (**Figure 3.1A, left**). These sites are phosphorylated in neurons as the result of high neuronal activity, by mTOR-dependent kinase S6K1/2 (Biever et al., 2015). This strategy allowed us to compare mRNAs expressed in the whole hippocampus (Input) with those associated with ribosomes in either Camk2a+ or highly active (pS6+) neuronal populations from the same hippocampal tissue. To further test how mRNA translation varies as a function of ribosomes' subcellular

localization, we centrifuged our homogenized hippocampal tissue into supernatant (presumptive cytosolic) and pellet (presumptive membrane-containing) fractions (Kratz et al., 2014). From both fractions, we compared whole-hippocampus (Input) transcripts with

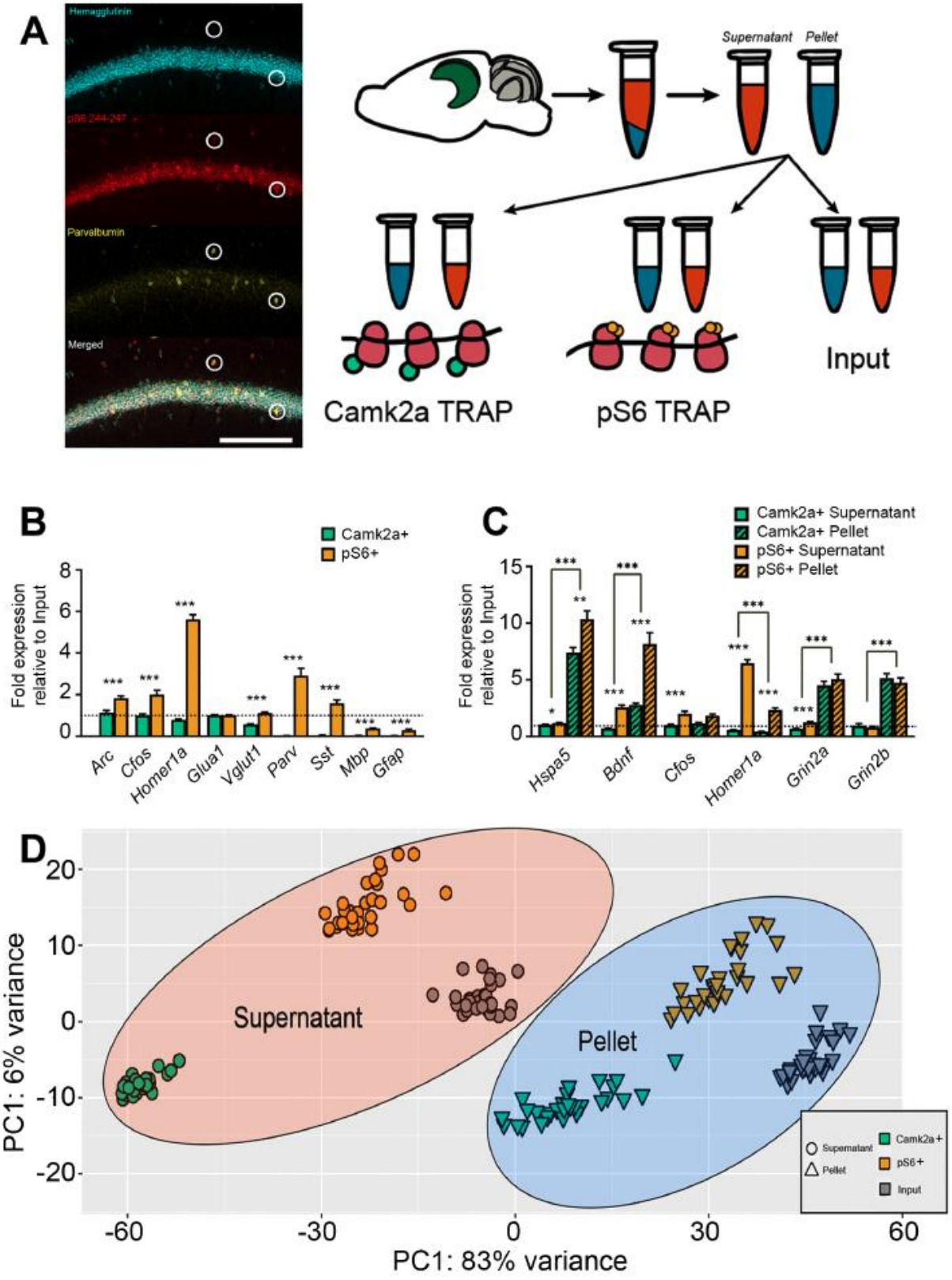


**Figure 3.1 TRAP-based profiling of hippocampal cell populations and isolation of subcellular fractions. (A) *Left*:** Confocal images showing expression of hemagglutinin (HA, Camk2a), phosphorylated S6 (pS6), and parvalbumin in area CA1 of dorsal hippocampus.

Highlighted neurons are parvalbumin+, pS6+, and HA-. Scale bar = 100 μm. ***Right:*** Schematic of protocol for isolating mRNAs from subcellular fractions and different cell populations using TRAP. **(B)** Camk2a+ (cyan) and pS6+ (orange) TRAP mRNA enrichment values were calculated (vs. Input) for activity-dependent (*Arc*, *Cfos*, *Homer1a*), excitatory neuron (*Glua1*, *Vglut1*), inhibitory neuron (*Parv*, *Sst*), and glial (*Mbp*, *Gfap*) transcripts. *** indicates $p < 0.001$ for enrichment value differences between Camk2a+ and pS6+ neuronal populations (Student's t-test, $n = 7$/group). **(C)** Camk2a+ and pS6+ TRAP enrichment in supernatant (solid bars) and pellet (hatched bars) fractions (vs. Input) for transcripts encoding secreted (*Bdnf*), transmembrane (*Grin2a, Grin2b*), endoplasmic reticulum (*Hspa5*), and cytosolic (*Cfos, Homer1a*) proteins. (Student's t-test, $n = 9$/group, * , ** , and *** indicate $p < 0.05$, $p < 0.01$, and $p < 0.001$, respectively). **(D)** PCA plot (VST, Deseq2) for RNAseq data (from $n = 30$ hippocampal samples) from the three cell populations (Input, Camk2a+ neurons, and pS6+ neurons) and two fractions (supernatant and pellet).

transcripts isolated by TRAP from excitatory (Camk2a+) and highly active (pS6+) neuron populations (**Figure 3.1A**).

Using quantitative PCR (qPCR), we validated cell type-specific gene expression from the Camk2a+ and pS6+ populations. Relative to Input mRNA, Camk2a+ mRNA displayed similar levels of *Arc*, *Cfos*, *Homer1a*, *Glua1*, and *Vglut1*, with reduced expression of interneuron and glial cell markers. Compared to Input, highly activated pS6+ neurons' mRNA profiles displayed significant enrichment in activity-dependent transcripts (*Arc, Cfos, Homer1a*) and interneuron-specific transcripts (*Pvalb, Sst*), and comparable levels of excitatory neuron-specific mRNAs (*Glua1*, *Vglut1*) (**Figure 3.1A,B**).

We next used qPCR for preliminary validation of sub-cellular enrichment of mRNAs expressed in supernatant and pellet fractions. Previous reports have found that isolating pellet ribosomes enriches for endoplasmic reticulum (ER) and dendritic localized ribosomes) (Kratz et al., 2014). To test whether fractions differently enriched genes trafficked to the ER and dendrites we first analyzed *Hspa5*. Encoding the resident ER chaperone BIP, *Hspa5* was significantly more enriched in the pellet fractions than the cytosolic fractions of both Camk2a+ and pS6+ neurons (**Figure 3.1C**; Camk2a+: supernatant - 1.03 × Input, pellet - 7.38 × Input, $p < 0.001$, Student's t-test; pS6+: supernatant - 1.17 × Input, pellet - 10.33 × Input, $p < 0.001$). Similarly, *Bdnf*, *Grin2a,* and *Grin2b* mRNAs (encoding the secreted growth factor and glutamatergic receptor subunits) were more enriched on ribosomes isolated from the pellet fraction compared to the supernatant fraction. In contrast, *Homer1a* (encoding the truncated version of the synaptic scaffolding protein Homer1, present in cytosol) was more abundant on supernatant ribosomes in both neuron populations, and *Cfos* was equally abundant in

both fractions. These results suggest that ribosome-associated transcripts observed in pellet and supernatant fractions encode proteins with predicted enrichment on cell membranes and in cytosol, respectively. We further characterized mRNAs taken from different cell populations (Camk2a+, pS6+, Input) and subcellular fractions (supernatant, pellet) using a non-biased approach - RNA-seq. PCA analysis of the full RNA-seq data set revealed six discrete clusters of mRNA expression profiles, based on the origin of the samples (**Figure 3.1D**).

## 3.5 Supernatant and Pellet Fractions Distinguish Transcripts Localized to Cytosolic and Membrane-Bound (MB) Ribosomes

To characterize transcripts that are differentially localized to the supernatant or pellet fraction, we next calculated the relative mRNA abundance in the two fractions from Camk2a+ neurons (**Figure 3.2A**), pS6+ neurons (**Figure 3.3A**), and Input (i.e., whole hippocampus, **Figure S3.1A**) using Deseq2 (Love et al., 2014). The top 2000 most differentially expressed transcripts between the two fractions (based on adjusted *p* value) were characterized using DAVID's cellular component annotation (Dennis Jr. et al., 2003). Confirming our initial validation (**Figure 3.1B**), supernatant-enriched transcripts from both neuron populations (and Input) encoded proteins with functions localized to the cytoplasm and nucleus. Pellet-enriched transcripts encoded proteins with functions localized to the plasma membrane, endoplasmic reticulum, Golgi apparatus, and synapses (**Figure 3.2B, Figure 3.3B, Figure S3.1B**). Thus for subsequent analyses, we refer to supernatant and pellet fractions as cytosolic and membrane-bound (MB), respectively. Signaling and metabolic pathways enriched among cytosolic ribosome-associated

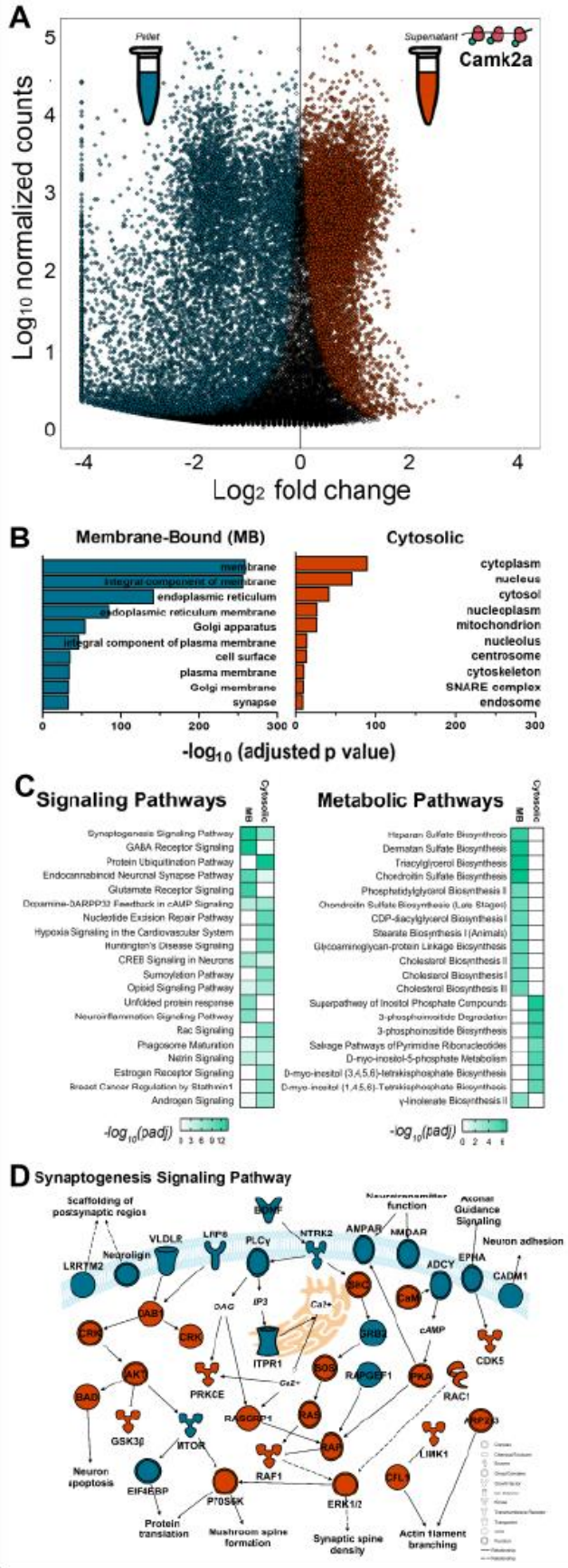


**Figure 3.2 Cytosolic and membrane protein-encoding transcripts in Camk2a+ neurons are preferentially enriched in supernatant and pellet ribosomal fractions respectively.** **(A)** Volcano plot of transcripts significantly enriched in pellet (red) and supernatant (blue) cell fractions of Camk2a+ neurons. Of the 28,071 transcripts detected, 7,651 (27%) were significantly ($p_{adj}$ < 0.1) enriched in the supernatant (cytosolic) fraction, and 10,911 (39%) were significantly enriched in the pellet (MB) fraction. **(B)** Top 10 cellular component localizations (from DAVID) of the 2000 transcripts most significantly enriched (based on adjusted *p* value) in either pellet (MB) or supernatant (cytosolic) fractions. **(C)** Top 20 most-enriched signaling and metabolic pathways represented by the 2000 most-enriched transcripts in Camk2a+ cytosolic or MB fractions. **(D)** Illustration of the synaptogenesis signaling pathway (IPA) with proteins shaded by their respective transcripts' preferential localization in cytosolic (red) and MB (blue) fractions.

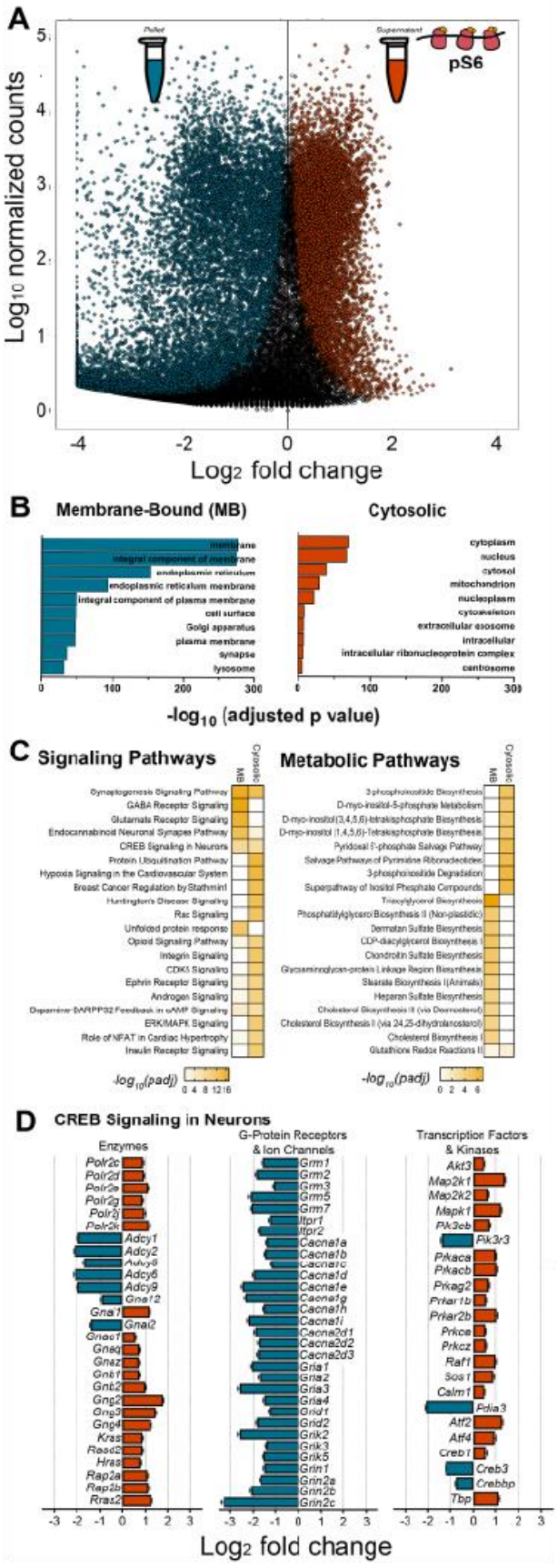


**Figure 3.3 Differential expression of mRNAs encoding intracellular signaling pathway components in cytosolic vs. MB ribosomal fractions from highly active (pS6+) neurons. (A)** Volcano plot of transcripts significantly enriched in pellet (red) and supernatant (blue) cell fractions. Of the 34,657 transcripts detected, 8,030 (23%) were significantly ($p_{adj} < 0.1$) enriched in the supernatant (cytosolic) fraction, and 14,244 (41%) were significantly enriched in the pellet (MB) fraction. **(B)** Top 10 cellular component localizations (from DAVID) of the 2000 transcripts which were most significantly enriched (based on adjusted *p* value) in either pellet (MB) or supernatant (cytosolic) fractions of pS6+ neurons. **(C)** Top 20 most-enriched signaling and metabolic pathways represented by the 2000 most-enriched transcripts in pS6+ cytosolic or MB fractions. **(D)** Log2FC values indicating enrichment of transcripts from the Creb1 signaling pathway in the cytosolic (red) or MB (blue) fractions (subcategorized by encoded protein type).

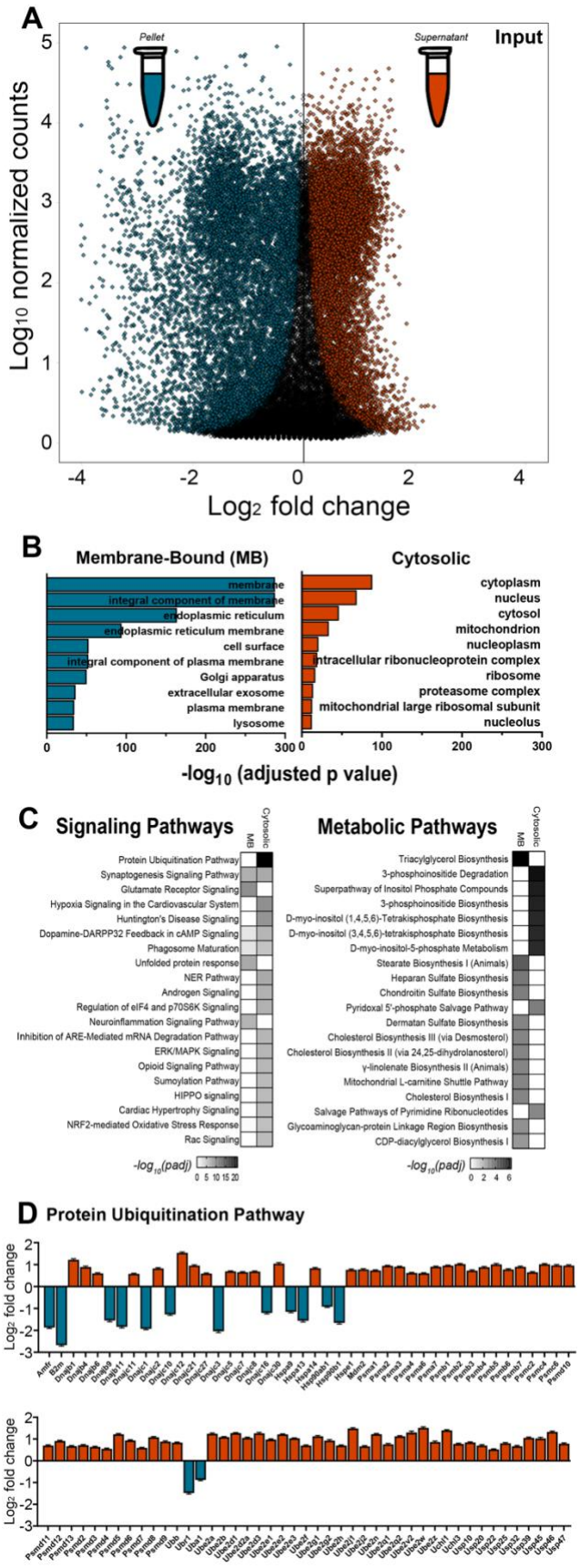


**Supplemental Figure S3.1 Transcripts enriched in cytosolic and MB fractions from Input (whole hippocampus). (A)** Volcano plot of transcripts significantly enriched in pellet (red) and supernatant (blue) cell fractions. Of the 27,773 transcripts detected, and 8310 (30%) showed significant enrichment in the supernatant (cytosolic) fraction, 9,285 (33%) showed enrichment in the pellet (MB) fraction. **(B)** Top 10 cellular component localizations (from DAVID) of the 2000 transcripts which were most significantly enriched (based on $p_{adj}$ value) in either pellet (MB) or supernatant (cytosolic) fractions. **(C)** Top 20 most-enriched signaling and metabolic pathways represented by the 2000 most-enriched transcripts in Input cytosolic or MB fractions. **(D)** Log2FC values indicating enrichment of transcripts from the ubiquitin signaling pathway in the cytosolic (red) or MB (blue) fractions.

mRNAs were assessed using Ingenuity Pathway Analysis [IPA] canonical pathways (**Figure 3.2C-D, Figure 3.3C-D**). Here, we identified cytosol-localized cellular pathways including ubiquitination, nucleotide excision repair, hypoxia signaling, and sumoylation pathways. In contrast, MB fraction-enriched transcripts represented signaling pathways involved in synaptic (GABAergic receptor, glutamatergic receptor, and endocannabinoid signaling) and endoplasmic reticulum (e.g., unfolded protein response) functions (**Figure 3.2C-D, Figure 3.3C-D**).

To further investigate subcellular localization of transcripts representing cellular pathways critically involved in hippocampal function, we examined signaling pathways enriched in both cytosolic and MB fractions. Because both learning and sleep affect synaptic structure and function (Bruning et al., 2019; Noya et al., 2019; Raven et al., 2019; Spano et al., 2019), we first focused on the synaptogenesis signaling pathway. In Camk2a+ neurons, MB-enriched transcripts encoded secreted proteins (e.g., *Bdnf*), transmembrane proteins including AMPA, NMDA, and ephrin receptors (e.g., *Gria1, Gria2, Gria3, Grin2a, Grin2b, Grin2c, Epha1, Epha2)* and membrane-associated enzymes (*Plcγ*) (**Figure 3.2D**). Cytosol-enriched mRNAs encoded intracellular complexes including adaptor proteins (*Crk, Shc)* and kinases (*Cdk5, Lmk1, Gsk3b, Mapk1, Mapk2, P70S6K*) in the synaptogenesis pathway (**Figure 3.2D**). Components of the CREB signaling pathway (another known target of both learning and sleep) (Abel et al., 1997; Kandel, 2012; Luo et al., 2013; Vecsey et al., 2009; Vecsey et al., 2007) was also differentially enriched on cytosolic vs. MB ribosomes, in both Camk2a+ and pS6+ neuronal populations (**Figure 3.2C, Figure 3.3C**). mRNAs encoding enzymes in the CREB pathway were selectively localized to ribosomes in either compartment of neuronal

populations (e.g., *Polr2c*, encoding the RNA polymerase subunit, in the cytosolic fraction; *Adcy1*, encoding adenylate cyclase, in the MB fraction). mRNAs encoding G-protein coupled receptors and ion channels (metabotropic glutamate receptors, endoplasmic reticulum $IP_3$ receptors, calcium channel subunits, AMPA and NMDA receptor subunits) localized exclusively to the MB fraction, while those encoding transcription factors and kinases localized primarily to the cytosolic fraction (**Figure 3.3D**). In contrast to Camk2a+ and pS6+ neuron populations, the CREB signaling pathway was not represented among mRNAs differentially localized to subcellular fractions of Input (i.e., whole hippocampus; **Figure S3.1**), suggesting that differential localization of mRNAs encoding CREB signaling components are more pronounced in neurons than other hippocampal cell types.

Overall, functional categories represented in the two subcellular fractions in Input RNA followed a pattern similar to that seen in Camk2a+ and pS6+ neuronal populations. However, in contrast to ribosome-associated transcript profiles from neuronal populations, the signaling pathway category that was most represented by mRNAs differentially localized between the two Input fractions was the protein ubiquitination pathway (**Figure S3.1**). This may indicate more dramatic subcellular segregation of mRNAs encoding ubiquitin pathway components in non-neuronal hippocampal cell types (i.e., glial cells).

## 3.6 Learning and Sleep Loss Have Divergent Effects on Cytosolic and MB Ribosome-Associated mRNA Profiles.

Because both learning and sleep alter hippocampal activity, intracellular signaling, and function (Havekes et al., 2016; Ognjanovski et al., 2018; Ognjanovski et al., 2014;

Vecsey et al., 2009), we next tested how cytosolic and MB ribosome-associated transcripts in different neuron types were affected by prior training on a hippocampus-dependent memory task (contextual fear conditioning [CFC]). We also tested how these transcript profiles were affected by a brief (3-h) period of subsequent sleep or sleep deprivation (which is sufficient to disrupt contextual fear memory (CFM) consolidation) (Graves et al., 2003; Ognjanovski et al., 2018; Vecsey et al., 2009). At lights on (i.e., the beginning of the rest phase), mice were either left in their home cage (HC) or underwent single-trial CFC (placement in a novel chamber followed by delivery of a foot shock). Over the next 3 h, mice in CFC and HC control groups were either permitted *ad lib* sleep (Sleep) or were sleep deprived (SD) in their home cage by gentle handling (**Figure 3.4A**). These manipulations were followed by RNA isolation and sequencing as described above. Effects of learning and sleep loss on mRNA abundance were quantified for each cell population (Camk2a+, pS6+, or Input) and subcellular fraction (cytosolic or MB; e.g., pS6+ MB) to preserve gene-level inferences made by the Deseq2 model.

We first assessed the specific effects of sleep deprivation alone (comparing SD and Sleep conditions) by combining data sets from naive (HC) and recently trained (CFC) mice (**Figure 3.4A, Yellow**). We then quantified the effects of learning (comparing CFC and HC conditions) separately in Sleeping and SD mice (**Figure 3.4A, Red[SD], Blue[Sleep]**). Venn diagrams (shown in **Figure 3.4B**) show the proportional changes in mRNAs resulting from these comparisons. SD had a relatively large effect on cytosolic ribosomal mRNAs (Camk2a+: 567 transcripts, pS6+: 913 transcripts, Input: 297 transcripts) compared to the effect of learning, which had extremely modest effects on cytosolic ribosomal transcripts. Conversely, MB ribosomal mRNAs were dramatically

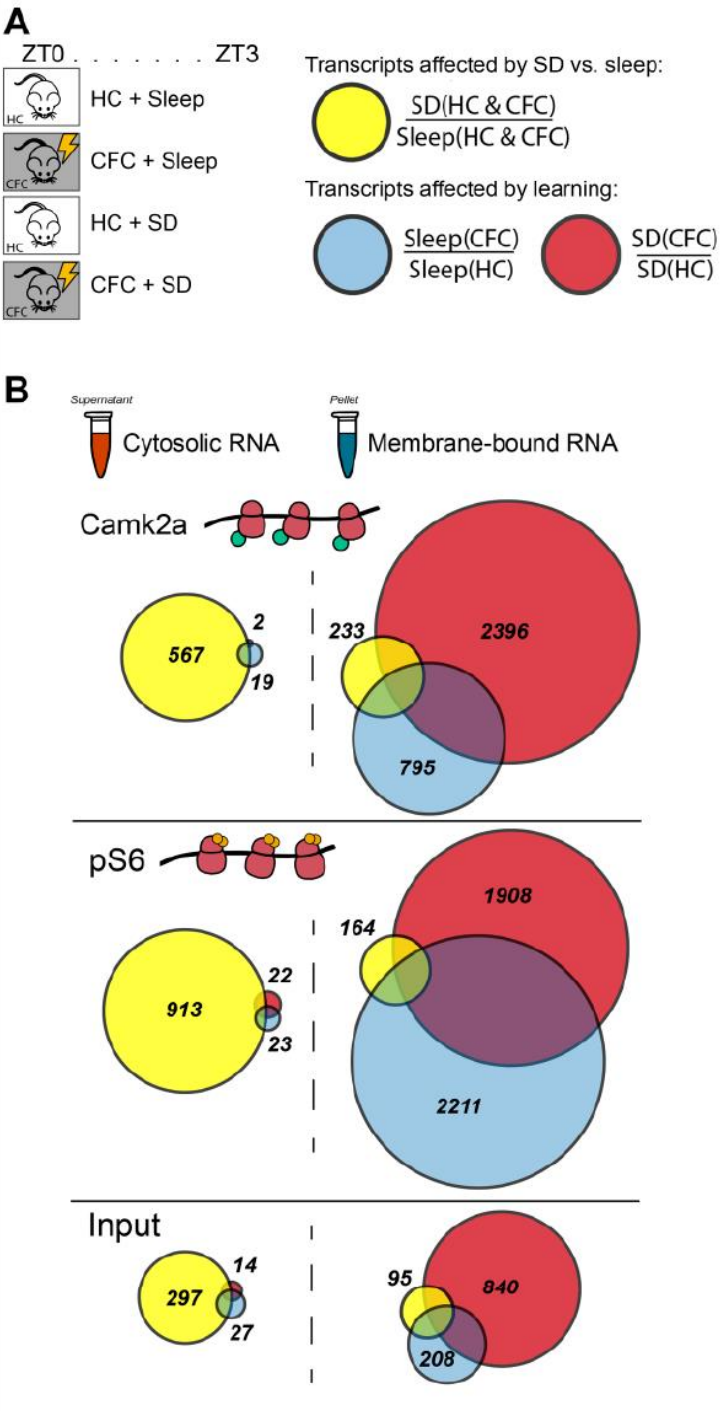


**Figure 3.4 Cytosolic ribosomal transcripts are altered primarily by SD, while MB ribosomal transcripts are altered primarily by learning. (A)** ***Left*****:** Experimental paradigm for RNA-seq experiments. At lights on, mice were either left in their home cage (HC) or underwent single-trial CFC. All mice were then either permitted *ad lib* sleep or were sleep deprived (SD) over the following 3 h. ***Right:*** Transcript comparisons for quantifying effects of SD (yellow) included both HC and CFC animals. To quantify effects of CFC, CFC + Sleep (Blue) and CFC + SD (Red) mice were analyzed separately. Following behavioral manipulations, cytosolic and MB fractions for different cell populations were isolated as described in **Figure 3.1**. **(B)** Proportional Venn diagrams reflect the number of significantly altered transcripts in each cell populations and subcellular fractions (i.e., Camk2a+/Membrane-Bound), based on comparisons shown in **A**.

altered by learning in both SD (CFC + SD - Camk2a+: 2,396 transcripts, pS6+: 1,908 transcripts, Input: 840 transcripts) and Sleep groups (CFC + Sleep - Camk2a+: 795 transcripts, pS6+: 2,211 transcripts, Input: 208 transcripts). In contrast, relatively few MB ribosomal mRNAs were altered by SD (Camk2a+: 233 transcripts, pS6+: 164 transcripts, Input: 95 transcripts). These results suggest that SD and learning differentially affect ribosomal mRNA profiles based on their subcellular localization - with SD (vs. Sleep) having more pronounced effects in the cytosol, and learning having more pronounced effects on MB ribosomes.

## 3.7 SD Primarily Affects Cytosolic Ribosomal mRNAs Involved in Transcription Regulation.

Significantly more cytosolic ribosome-associated mRNAs were altered as a function of Sleep vs. SD alone (compared with relatively few changes driven by CFC) in Camk2a+ neurons (SD: 567 transcripts, CFC: 20 transcripts), pS6+ neurons (SD: 913 transcripts, CFC: 43 transcripts), and to a lesser extent, Input (whole hippocampus) mRNA (SD: 297 transcripts, CFC: 37 transcripts) (**Figure 3.4B**). Therefore, we next sought to characterize the molecular and cellular pathways altered by SD-induced changes to cytosolic ribosome transcripts (**Figure 3.5A**). Molecular functions most affected by SD alone (based on adjusted *p* values < 0.1 for transcripts using IPA annotation) overwhelmingly favored transcriptional regulation and RNA processing in both Camk2a+ and pS6+ neurons, as well as in Input (**Figure 3.5B, Top**). Previous transcriptome analysis has shown that mRNAs encoding transcription regulators are more abundant following brief SD in the hippocampus (*Fos*, *Elk1*, *Nr4a1*, *Creb*, *Crem1*)

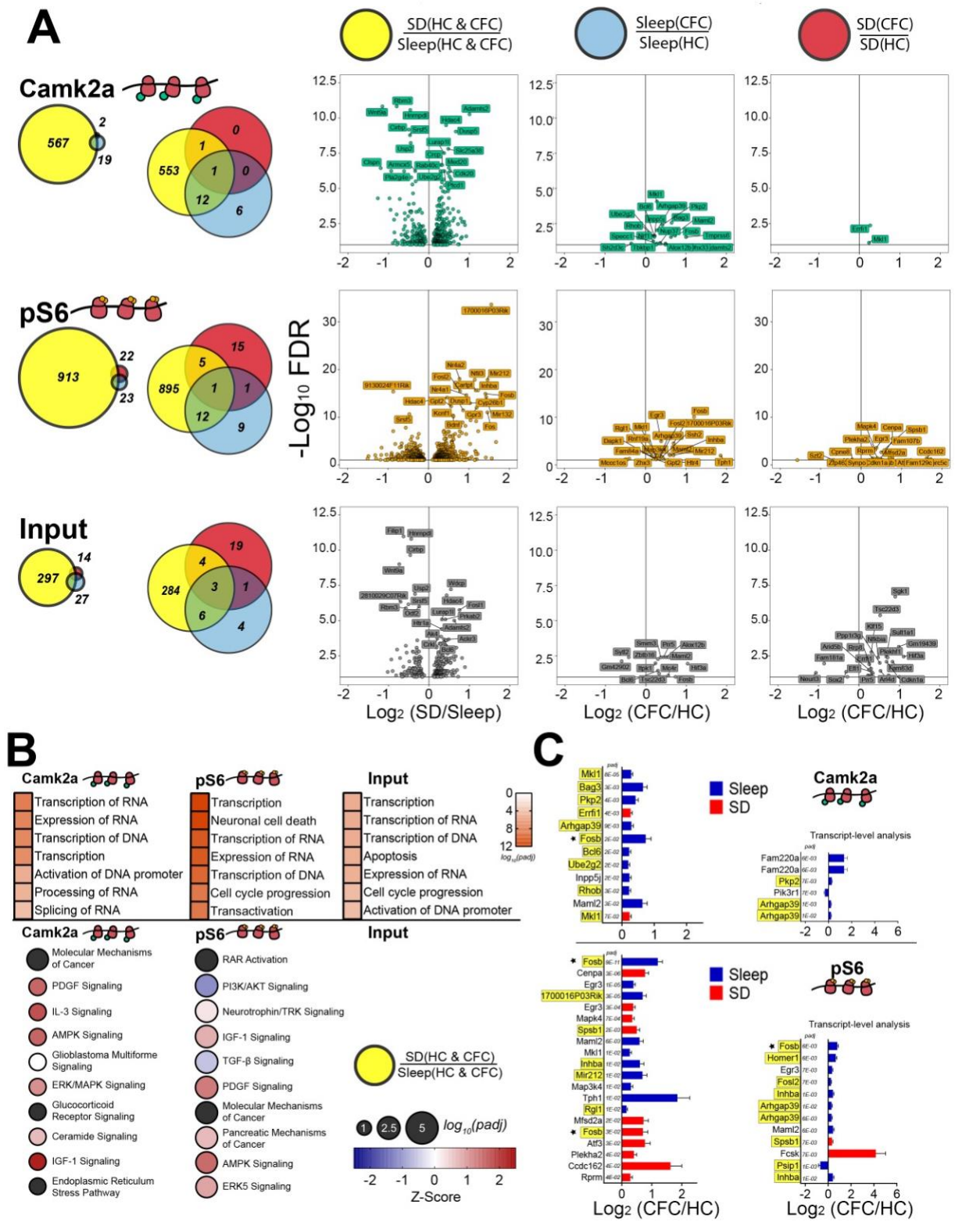


**Figure 3.5 mRNAs altered by SD on cytosolic ribosomes encode transcriptional regulators.** **(A)** ***Left*****:** Proportional and overlapping Venn diagrams of transcripts significantly altered by SD, CFC + Sleep, and CFC + SD in cytosolic fractions from Camk2a+ neurons, pS6+ neurons, and Input. ***Right:*** Volcano plots of Deseq2 results for transcripts measured in each condition. **(B)**

***Top*:** The 7 most-enriched molecular and cellular function categories (ranked by $p_{adj}$ value) for transcripts altered by SD alone in Camk2a+ neurons, pS6+ neurons, and Input. ***Bottom:*** The 10 most-enriched canonical pathways of SD-affected transcripts are listed in order $p_{adj}$ value (indicated by circle diameter), with z-scores indicating direction of pathway regulation (indicated by hue). There were no significant canonical pathways present in the Input fraction. **(C)** ***Left*:** The 10 transcripts most significantly affected in CFC + Sleep (blue) and CFC + SD (red) conditions for Camk2a+ (***top***) and pS6+ (***bottom***) neurons, ranked by $p_{adj}$ value. Transcripts that were also significantly altered as a function of SD alone are highlighted in yellow. ***Right:*** Results of transcript-level analysis (Yi et al., 2018), show transcripts for transcript isoforms altered in Camk2a+ (***top***) and pS6+ (***bottom***) neurons following CFC. Transcript isoforms that were significantly altered as a function of SD are highlighted in yellow.

(Vecsey et al., 2012) and cortex (*Per2*, *Egr1*, *Nr4a1*) (Cirelli et al., 2004). Consistent with those findings, SD increased the abundance of multiple mRNAs encoding transcription factors and upstream regulators in all cell populations, including *E2f6, Elk1, Erf, Fosl1, Fosl2, Fos, Fosb, Lmo4, Taf12, Xbp1, Atf7, Artnl2, Atoh8, Bhlhe40(Dec1), Crebl2, Crem, Egr2, Nfil3,* and *Ubp1*. Transcripts affected in Camk2a+ and pS6+ neurons overlapped partially with those reported in previous SD experiments, including components of pathways for AMPK, PDGF, ERK/MAPK, IGF-1 and endoplasmic reticulum stress signaling (**Figure 3.5B, Bottom**) (Naidoo et al., 2005; Tudor et al., 2016; Vecsey et al., 2012). However, only a small fraction (12-16%) of the 511 mRNAs previously reported to be altered by SD in whole hippocampus (Vecsey et al., 2012) overlapped with SD-affected mRNAs in cytosolic fractions of any cell population (**Figure S3.2**). In pS6+ neurons only, mRNAs encoding components of the PI3K/AKT and TGF-B signaling pathways were downregulated in the cytosolic fraction after SD (**Figure 3.5B, Bottom**), suggesting that activity in these pathways may be higher during sleep.

We next performed upstream regulator analysis to characterize transcript changes due to SD-associated transcriptional regulation. Results of this analysis provide both a *p*-value for the significance of mRNAs' regulation by a specific common upstream regulator, and a z-score indicating the direction of the regulated mRNAs' fold change (i.e., transcriptional activation or suppression). Taken together these values predict the activation state of specific gene regulator complexes during SD (Kramer et al., 2014). In line with prior meta-analysis of SD-induced transcripts (Wang et al., 2010), Creb1 was identified as the transcriptional regulator whose downstream targets' were most consistently affected across all cytosolic (**Figure 3.6A**). *Creb1* transcript itself was not

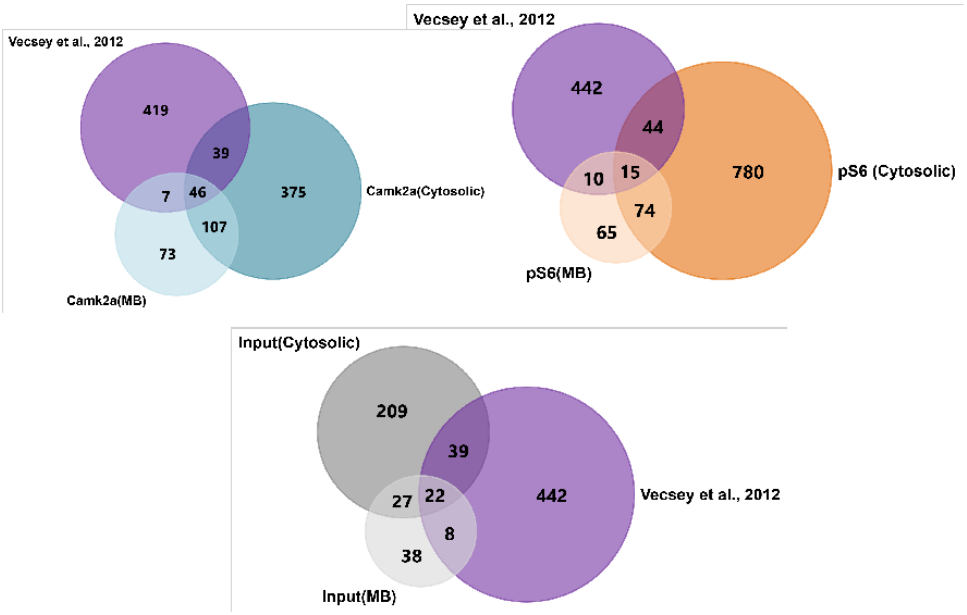


**Supplemental Figure S3.2 Overlap of SD-altered transcripts with previously-characterized SD-altered mRNAs.** Venn diagrams indicate degree of overlap for transcripts altered by SD in the present study and those previously reported for whole hippocampus following SD (Vecsey et al., 2012).

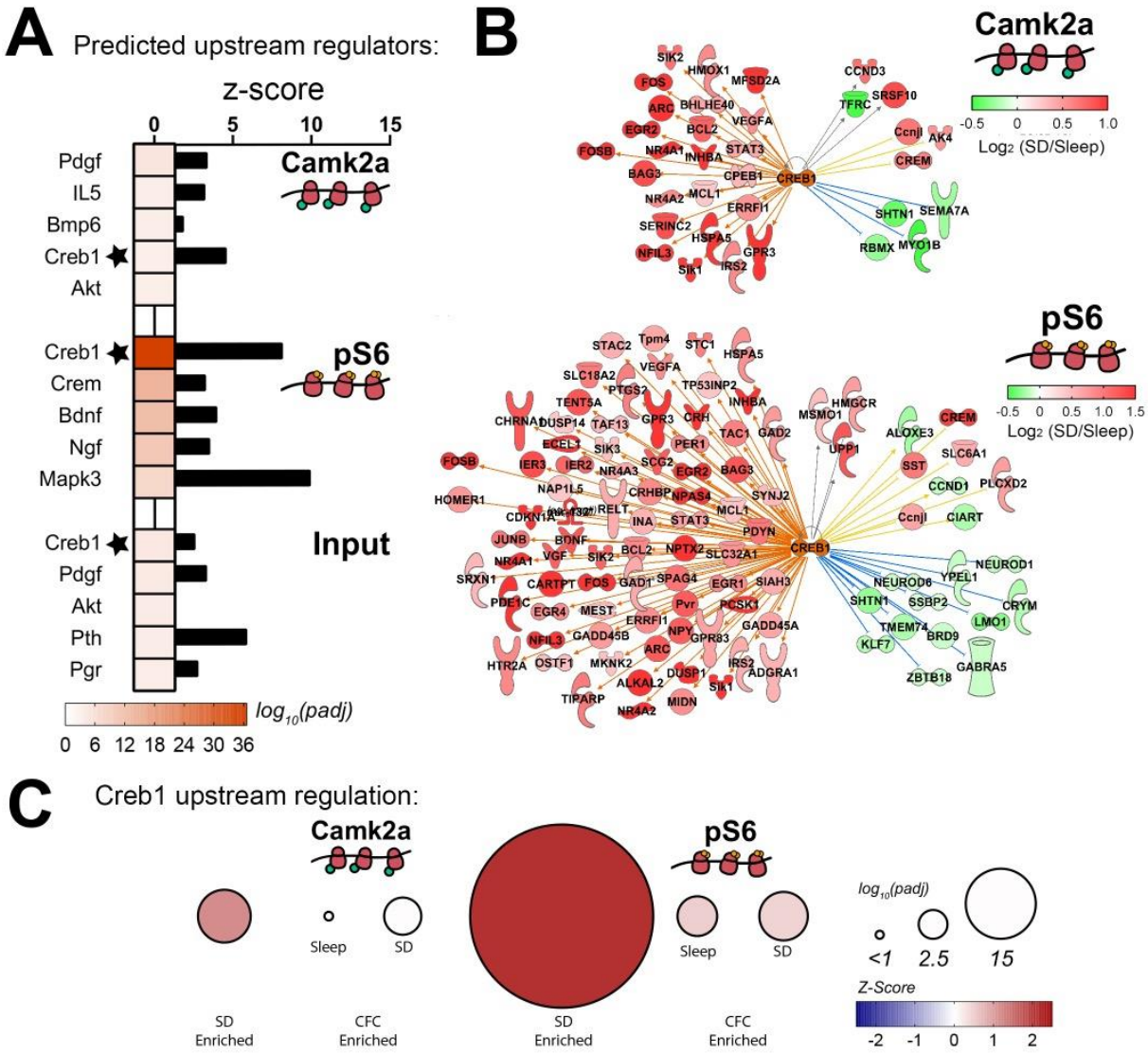


**Figure 3.6 Creb1 target transcripts are upregulated on cytosolic ribosomes after SD. (A)** Z-scores for the 5 upstream transcriptional regulators whose target transcripts were most significantly affected by SD, ranked by $p_{adj}$ values. **(B)** Networks of Creb1 transcriptional targets altered by SD in Camk2a+ (***top***) and pS6+ (***bottom***) neurons. Color of arrows from Creb1 to transcripts indicates the predicted direction of transcriptional regulation - orange (with red transcript symbols) denotes transcripts predicted to be upregulated by Creb1 which are upregulated following SD; blue (with green transcript symbols) indicates transcripts predicted to be repressed by Creb1 which are repressed by SD; yellow indicates SD-related changes that do not match predicted regulation by Creb1; grey indicates undermined effects of Creb1 on transcript levels. **(C)** Relative Creb1 network regulation $p_{adj}$ values and z-scores are plotted for transcripts altered on cytosolic ribosomes by SD, CFC + Sleep, and CFC + SD in Camk2a+ and pS6+ cell populations.

increased following SD, although *Crebl2* and *Crem* mRNAs were both increased, and multiple Creb1 transcriptional targets (e.g., *Fos, Arc, FosB, Egr2, Nfil3, Nr4a2, Bag3, Irs2*) were upregulated in the cytosolic fraction of both Camk2a+ and pS6+ neuronal populations (**Figure 3.6B**) after SD.

## 3.8 CFC-Induced Changes in Cytosolic Ribosome-Associated mRNAs Are Occluded by Subsequent SD.

Hippocampal fear memory consolidation in the hours following CFC relies on both sleep (Graves et al., 2003; Ognjanovski et al., 2018; Vecsey et al., 2009) and CREB-mediated transcription (Katche et al., 2010; Rao-Ruiz et al., 2019). With Creb1 activity high during SD, we were curious what effect SD would have on the abundance of ribosome-associated transcripts involved in memory consolidation. As discussed above, few cytosolic ribosome-associated mRNAs were altered by CFC (**Figure 3.4, 3.5**). In Camk2a+ neurons, 19 cytosolic ribosome-associated transcripts were altered (compared to HC controls) in CFC + Sleep mice, whereas only 2 transcripts were altered in CFC + SD mice. Of those, most (13/19 from CFC + Sleep, 2/2 from CFC + SD) were also increased by SD alone (**Figure 3.5A**). Ribosome-associated mRNAs affected by both SD and CFC in Camk2a+ neurons included activity-dependent transcripts such as *Fosb, Arhgap39(Vilse),* and *Errfi1* (**Figure 3.5C, Yellow**). For comparison, for Input (i.e., whole hippocampus), slightly more cytosolic ribosome-associated mRNAs were altered after CFC + SD (27 transcripts) vs. CFC + Sleep (14 transcripts). Of these, 6/27 and 9/14, respectively, were similarly affected by SD alone (**Figure 3.5A**).

These initial data suggested that changes in cytosolic ribosome-associated transcripts after SD alone could occlude transcript changes triggered by CFC. To better characterize how this might affect the neurons that are most activated by CFC (which could represent CFC “engram neurons”), we compared cytosolic transcripts affected by CFC vs. SD alone in pS6+ neurons. While similar numbers of transcripts were altered by CFC followed by sleep or SD (23 vs. 22), only two transcripts (*Fosb* and *Egr3*) were similarly affected in both CFC + Sleep and CFC + SD mice (**Figure 3.5A, C**). Of the transcripts altered on cytosolic ribosomes after CFC in pS6+ neurons, several (12/23 of those affected in freely sleeping mice, 6/22 of those affected in SD mice) were also regulated by SD (**Figure 3.5A)**, including *Fosb, Egr3, Arghap39(Vilse), Gpr3, Ssh2, Inhba, Rnf19a,* and *Cdkn1a* (**Figure 3.5C, Yellow**). Because SD alters a significant number of transcripts involved in RNA splicing/processing (**Figure 3.5B**), and splice isoforms play critical roles in synaptic plasticity and memory storage (Poplawski et al., 2016), we next assessed effects of SD and CFC on differentially-spliced mRNA isoforms using transcript-level analysis (Yi et al., 2018) (**Figure 3.5C**). On cytosolic ribosomes from pS6+ neurons, both the activity-dependent splice isoform of Homer1 scaffolding protein (*Homer1a*) and the highly-stable activity-dependent splice isoform of FosB (*ΔFosb*) were increased after CFC followed by *ad lib* sleep, but not after CFC in SD mice (**Figure 3.5C**). These isoforms were also increased as a function of SD alone, suggesting another mechanism by which SD could occlude changes to pS6+ neurons initiated by learning (**Figure 3.5C, Yellow**).

To validate and extend these findings, we harvested hippocampi from CFC and HC mice following 5 h of SD or *ad lib* sleep (i.e., a later time point with respect to learning).

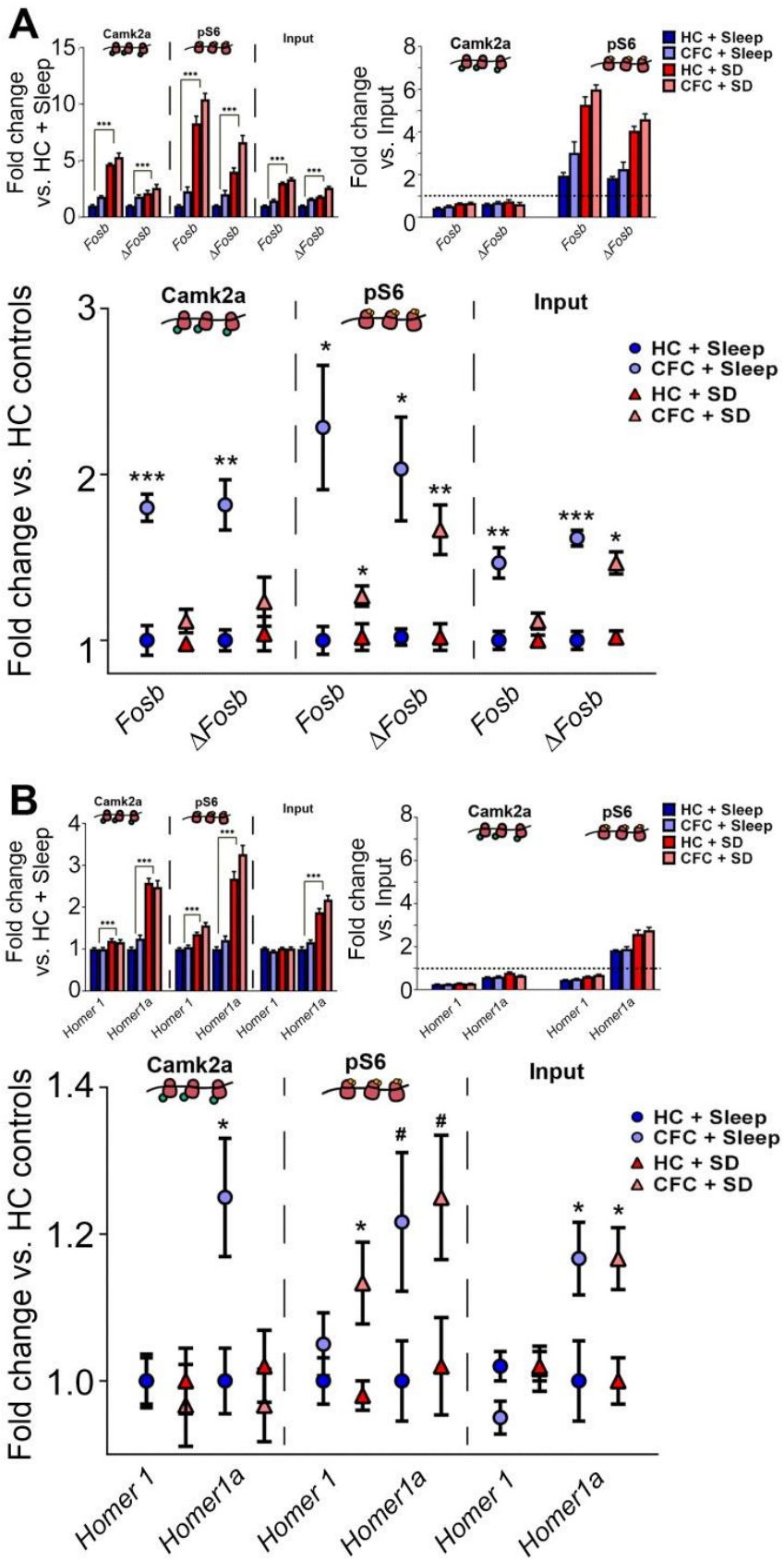


**Figure 3.7 CFC-induced alterations in Fosb and Homer1 splice variants are occluded by post-CFC SD in Camk2a+ neurons.** **(A)** *Fosb* and *ΔFosb* expression for CFC and HC mice after 5 h of subsequent sleep or SD is shown for cytosolic fractions of the 3 cell populations. ***Top, left:*** Expression in the 4 conditions relative to values from HC + Sleep mice (Two-way ANOVA, CFC/SD, df = 18, *** p-value < 0.001). ***Top, right:*** Relative enrichment/de-enrichment for *Fosb* and *ΔFosb* in Camk2a+ and pS6+ neurons, relative to Input, for the 4 conditions. ***Bottom:*** Expression of Fosb and *ΔFosb* following CFC conditions relative to same-state (SD or Sleep) home-cage (HC) conditions (t-test, $n$ = 5/group[HC], $n$ = 6/group[CFC]) #, * , ** , and *** indicate $p < 0.1$, $p < 0.05$, $p < 0.01$, and $p < 0.001$, respectively. **(B)** *Homer1* and *Homer1a* expression in cytosolic fractions in the 4 conditions, normalized as described in **(A)**.

Using qPCR, we first quantified mRNA levels for splice isoforms of *Fosb* and *Homer1* in the cytosolic fraction of whole hippocampus (Input), Camk2a+ neurons, and pS6+ neurons. Similar to what was observed after 3 h of SD, 5 h of SD increased expression of both *Fosb* and its long-lasting splice isoform *ΔFosb*, regardless of prior CFC (**Figure 3.7A, left**). Compared with Input, *Fosb* and *ΔFosb* transcripts were relatively de-enriched in Camk2a+ neurons, but highly enriched in pS6+ neurons (consistent with neural activity regulating both S6 phosphorylation and *Fosb* and *ΔFosb* transcript abundance) (**Figure 3.7A, right**). To measure CFC-driven changes in these transcripts, we normalized *Fosb* and *ΔFosb* transcripts in CFC + Sleep or CFC + SD mice to that of the corresponding HC control group. In both pS6+ neurons and Input, *ΔFosb* increased following CFC, regardless of subsequent sleep or SD. In Camk2a+ neurons, however, both *Fosb* and *ΔFosb* transcripts increased in CFC + Sleep mice, but this increase was occluded in CFC + SD mice (**Figure 3.7A, bottom**).

We also used qPCR to quantify the relative expression *Homer1* and its splice variant *Homer1a* in cytosolic fractions after CFC and 5 h subsequent sleep or SD. *Homer1* itself was modestly affected by 5 h of SD, whereas the *Homer1a* transcript was dramatically elevated, consistent with earlier findings (Mackiewicz et al., 2008; Maret et al., 2008) (**Figure 3.7B, left**). *Homer1* was de-enriched in both Camk2a+ and pS6+ neurons relative to Input, while *Homer1a* was enriched only in pS6+ neurons (consistent with regulation by neuronal activity) (**Figure 3.7B, right**). Similar to *ΔFosb*, CFC increased *Homer1a* across all cell populations in mice allowed *ad lib* sleep, but this increase was occluded in Camk2a+ neurons by SD (**Figure 3.7C, bottom**).

We quantified additional cytosol-enriched transcripts for proteins with known functions in hippocampal plasticity and memory, to test the effects of CFC and 5 h subsequent sleep or SD (**Figure S3.3**). These included transcripts increased in our Desq2 analysis following SD alone, and either unaffected by CFC (*Cfos, Arc*), altered only in CFC + SD mice (*Atf3*), or altered only in CFC + Sleep mice (*1700016P03Rik*). We also visualized *Egr3* which was unaffected by SD but increased by CFC in both CFC + SD and CFC + Sleep groups. All transcripts except *Egr3* were altered by 5 h SD in Camk2a+ and pS6+ neuron populations. In pS6+ neurons, *Cfos* and the lncRNA transcript *1700016P03Rik* (Aten et al., 2016; Aten et al., 2018) remained significantly elevated as a function of learning 5 h following CFC; SD either fully or partially occluded these learning-associated changes (**Figure S3.3**). No significant CFC-induced changes in these transcripts were detectable on cytosolic ribosomes from Camk2a+ neurons at 5 h post-CFC.

Taken together, these data support the hypothesis that CFC-associated changes in activity-regulated transcripts at cytosolic ribosomes are likely occluded by subsequent SD. This effect, which is most pronounced for highly-active (putative engram) hippocampal neurons, constitutes a plausible mechanism for memory consolidation disruption by SD.

## 3.9 SD Affects MB Ribosomal Transcripts Involved in Receptor-Mediated Signaling, Endoplasmic Reticulum Function, and Protein Synthesis.

Fewer mRNAs were altered as a function of SD alone on MB ribosomes compared with cytosolic ribosomes (where most observed changes were driven by SD, rather than

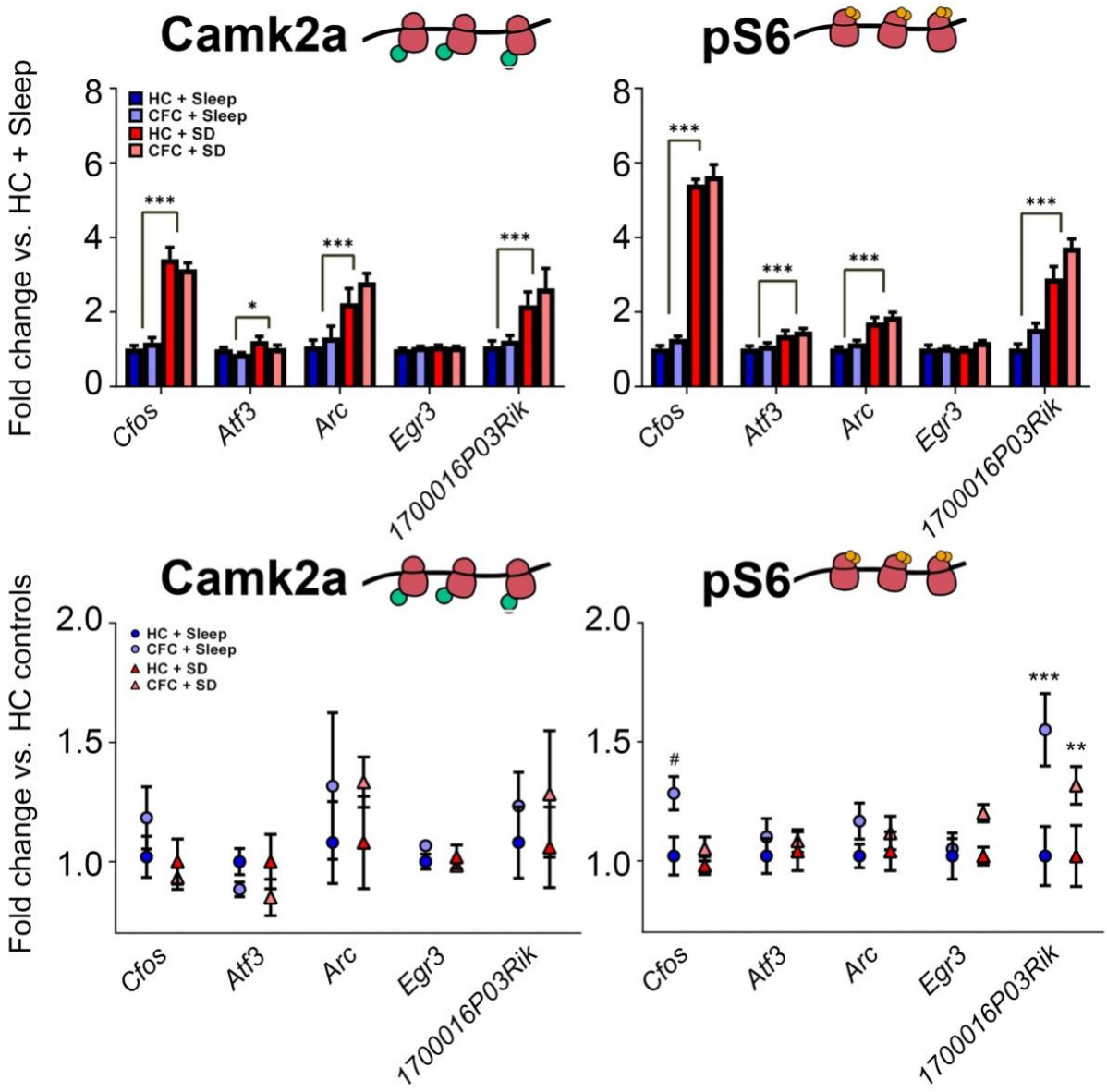


**Supplemental Figure S3.3 CFC-induced alterations in activity-dependent transcripts in Sleep and SD mice.** Expression of activity-regulated transcripts *Cfos*, *Atf3*, *Arc*, and *Erg1*) and lncRNA *1700016P03Rik* for CFC and HC mice after 5 h of subsequent sleep or SD is shown for cytosolic fractions of Camk2a+ and pS6+ neurons. ***Top:*** Expression in the 4 conditions relative to values from HC + Sleep mice (Two-way ANOVA, CFC/SD, df = 18) #, * , ** , and *** indicate $p < .10$, $p < 0.05$, $p < 0.01$, and $p < 0.001$, respectively. ***Bottom:*** Expression for the CFC conditions relative to same-state (SD of Sleep) HC conditions.

CFC) (**Figure 3.4, Figure 3.8A**). Changes in MB ribosomal transcripts due to SD were also dwarfed by more numerous changes to MB ribosome-associated transcripts following CFC. These changes differed substantially between Camk2a+ neurons, pS6+ neurons, and Input, thus canonical pathways represented by transcripts altered in the three populations by SD also differed. Critically, no canonical pathways were significantly enriched by SD-induced transcript changes in either Camk2a+ neurons or Input. On MB ribosomes from both Input and Camk2a+ cell populations, SD-altered transcripts included components of cellular pathways that were significantly affected in SD-regulated transcripts on cytosolic ribosomes (see **Figure 3.5B**), and with transcripts affected by SD in prior whole hippocampus transcriptome studies (Naidoo et al., 2005; Tudor et al., 2016; Vecsey et al., 2012). These included components of the AMPK (*Chrm5, Irs2, Pfkfb3, Ppm1f, Prkab2, Prkag2, Smarcd2*), IGF-1 (*Elk1, Rasd1*), IL-3 (*Crkl, Foxo1*), relaxin (*Gnaz, Pde4b, Smpdl3a*), and neuregulin (*Errfi1*) signaling pathways in Camk2+ neurons, and components of glucocorticoid receptor signaling (*Elk1, Gtf2e2, Prkab2, Prkag2, Rasd1, Smarcd2, Taf12, Fos, Krt77, Ptgs2, Tsc22d3*), unfolded protein response (*Hspa5, Pdia6*), and endoplasmic reticulum stress (Calr, *Xbp1*) pathways in both Camk2a+ neurons and Input. Critically, however, only 30 (6%) of the 511 mRNAs previously reported to be altered by SD in whole hippocampus (Vecsey et al., 2012) overlapped with SD-affected mRNAs in the MB fraction of whole hippocampus (i.e., Input; **Figure S3.2**). This suggests that even within these common identified cellular pathways, individual transcripts altered by SD in on MB ribosomes may differ substantially from those reported previously.

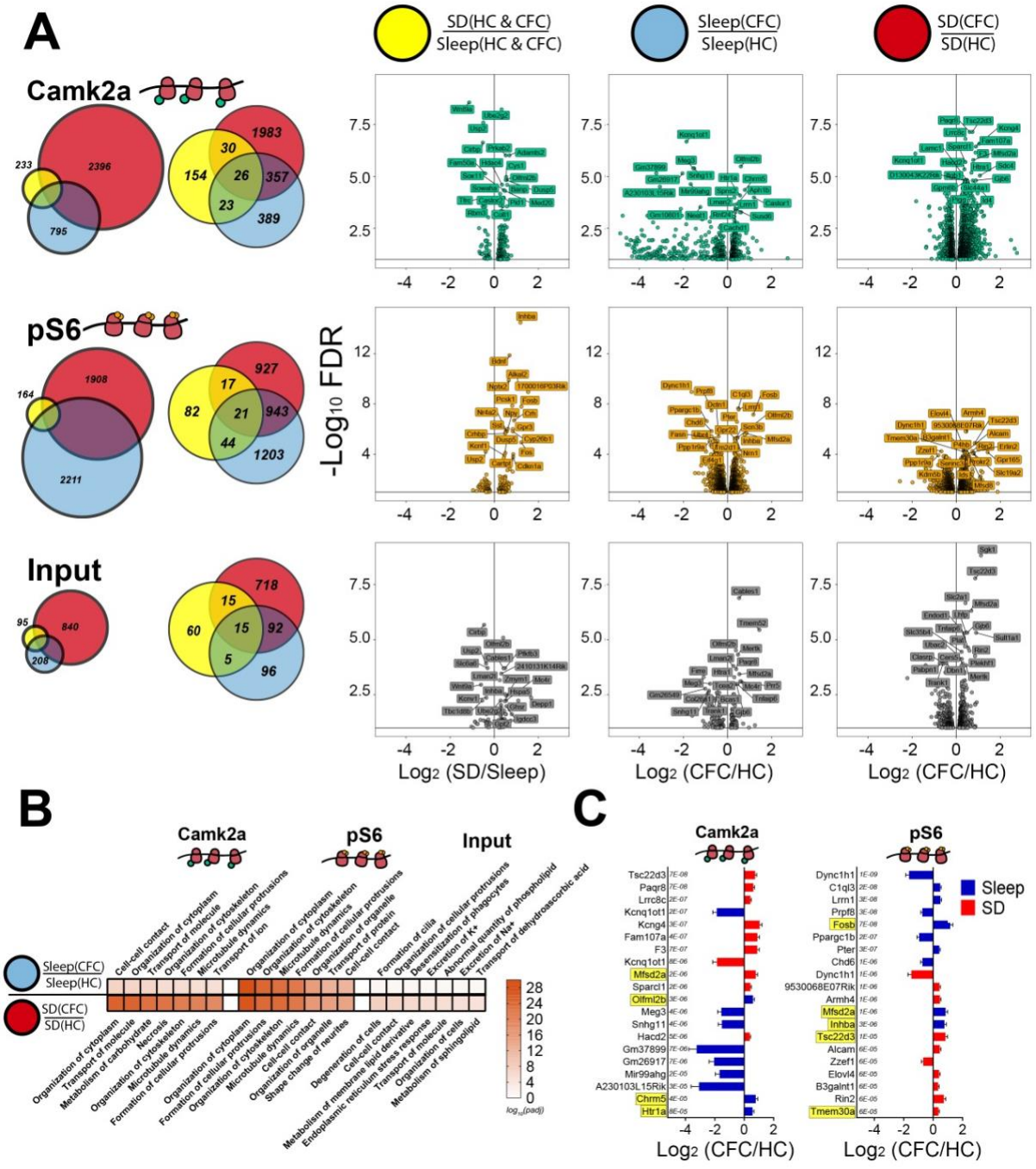


**Figure 3.8 Transcripts altered by CFC on MB ribosomes encode regulators of neuronal morphology, intracellular trafficking, and lncRNAs. (A)** ***Left*****:** Proportional and overlapping Venn diagrams of transcripts significantly altered by SD, CFC + Sleep, and CFC + SD in MB fractions from Camk2a+ neurons, pS6+ neurons, and Input. ***Right:*** Volcano plots of Deseq2 results for transcripts measured in each condition. **(B)** The 7 most-significant molecular functions (ranked by $p_{adj}$ value) for transcripts altered by CFC + Sleep (***top***) and CFC + SD (***bottom***) in Camk2a+ neurons, pS6+ neurons, and Input. **(C)**The 10 transcripts most significantly affected in CFC + Sleep (blue) and CFC + SD (red) conditions for Camk2a+ and pS6+ neurons, ranked by $p_{adj}$ value. Transcripts that were also significantly altered as a function of SD alone are highlighted in yellow.

In contrast to SD-driven changes in Camk2a+ neurons and Input, SD-altered transcripts from pS6+ neurons' MB ribosomes significantly enriched for several canonical pathways. These included the neurotrophin/TRK (*Atf4, Bdnf, Fos, Ngf, Plcg1, Spry2*), corticotropin releasing hormone (*Crh, Vegfa*), ERK5 (*Il6st, Rasd1*), and EIF2 (*Eif2b3, Hspa5, Ptbp1, Rpl37a*) signalling pathways and the human embryonic stem cell pluripotency pathway (*Bmp2, Inhba, Wnt2*). Thus the major pathways affected by SD among MB ribosome-associated transcripts comprise receptor signalling pathways, protein synthesis regulation, and endoplasmic reticulum function.

## 3.10 Learning-Related Changes in MB Ribosomal Transcripts Diverge Based on Subsequent Sleep or SD.

In contrast to the sparsely expressed CFC-driven transcript changes observed on cytosolic ribosomes, the majority of transcript changes on MB ribosomes were driven by CFC (**Figure 3.4, Figure 3.8A**). Critically, learning-induced changes in MB-fraction transcripts diverged in all cell populations, depending on whether CFC was followed by 3 h of *ad lib* sleep or 3 h of SD. In contrast to the high degree of overlap between SD-driven and CFC-driven transcript changes in the cytosol, on MB ribosomes, mRNAs affected by SD showed significantly less proportional overlap (2-10%) with CFC-induced changes (**Figure 3.8A**). These data suggest that translational profiles of MB ribosomes are most selectively affected by prior learning, but that the specific mRNAs associated with MB ribosomes also vary dramatically as a function of post-learning sleep or SD.

We first characterized the cellular and molecular functions of MB ribosomal mRNAs altered as a function of CFC and subsequent sleep or SD. For Camk2a+ and

pS6+ neurons, the most enriched functional categories largely overlapped, and represented similar molecular categories in CFC + Sleep and CFC + SD mice - including organization of cytoplasm, organization of cytoskeleton, microtubule dynamics, cell-cell contact, and formation of protrusions (**Figure 3.8B**). In contrast, few of these categories were enriched in Input MB fractions. There, the most enriched functional categories for transcripts altered by CFC + Sleep included excretion of sodium and potassium, formation of cilia, organization of cellular protrusions, desensitization of phagocytes, and abnormal quantity of phospholipid. Alterations in Input mRNAs following CFC + SD also enriched for functional categories not represented in neuronal MB fractions, including cell degeneration, metabolism of membrane lipid derivative, metabolism of sphingolipid, endoplasmic reticulum stress response. Together, these data suggest that CFC may alter similar membrane-associated cellular functions in Camk2a+ and pS6+ neuronal populations, regardless of subsequent sleep or SD. In contrast, CFC may have distinct and pronounced effects on membrane-associated functions in other hippocampal cell types (e.g., glia), and that these effects may diverge based on the animal's sleep state.

To further characterize changes in MB-associated ribosomal transcripts following learning, we first compared the most significantly altered mRNAs (based on adjusted *p* value) in Camk2a+ and pS6+ neurons following CFC in sleeping and SD conditions (**Figure 3.8C**). At Camk2a+ neurons' MB ribosomes, CFC + Sleep led to increased abundance for mRNAs encoding transmembrane receptors (*Chrm5, Htr1a*) and dramatically decreased abundance for multiple lncRNAs including *Kcnq1ot1*, *Meg3*, *Mir99ahg* and unannotated transcripts (e.g., *Gm37899*, *Gm26917*) (**Figure 3.8C**). Many other lncRNAs showed reduced abundance on MB ribosomes following CFC (including

*Neat1*, *Malat1*, *Mirg*, and *Ftx*). With the exception of *Mirg* and *Ftx*, these lncRNAs were also significantly reduced following CFC + SD. CFC + SD led to the most significant transcript increases on MB ribosomes for *Lrrc8c* (encoding an acid sensing, volume-regulated anion channel), and anti-adhesive extracellular molecules (*Sparcl1/Hevin*), adhesion molecules (*F3/Contactin1*), transmembrane receptors (*Paqr8*), potassium modifiers (*Kcng4*), endoplasmic reticulum-tethered lipid synthesis molecules (*Hacd2*), and actin regulators (*Fam107a*).

In highly active (pS6+) neurons, *Dync1h1* was the most significantly altered transcript following CFC, and was dramatically reduced in both freely-sleeping and SD mice (**Figure 3.8C**). *Dync1h1* encodes the main retrograde motor protein in eukaryotic cells, supporting retrograde transport in axons and dendrites (Schiavo et al., 2013). To a lesser extent, its abundance was also significantly reduced on MB ribosomes from Camk2a+ neurons. *Dync1h1* was not reduced as a function of SD itself in either neuron population, suggesting that decreases in *Dync1h1* are specific to the post-learning condition.

We next constructed canonical pathway networks affected by CFC + Sleep or CFC + SD, to visualize the signaling and metabolic pathways differently altered in the two conditions. Canonical pathways are represented as hubs and connected through commonly transcript components. Here, hub sizes were weighted by their corresponding *p* value and shaded to indicate their z-score (blue indicating a decrease in the pathway following CFC, whereas red indicates an increase) (**Figure 3.9**). Network comparisons of MB ribosome-associated transcript changes in Camk2a+ neurons revealed overlapping hubs significant in both CFC + Sleep (**Figure 3.9, Top Left**) and CFC + SD conditions

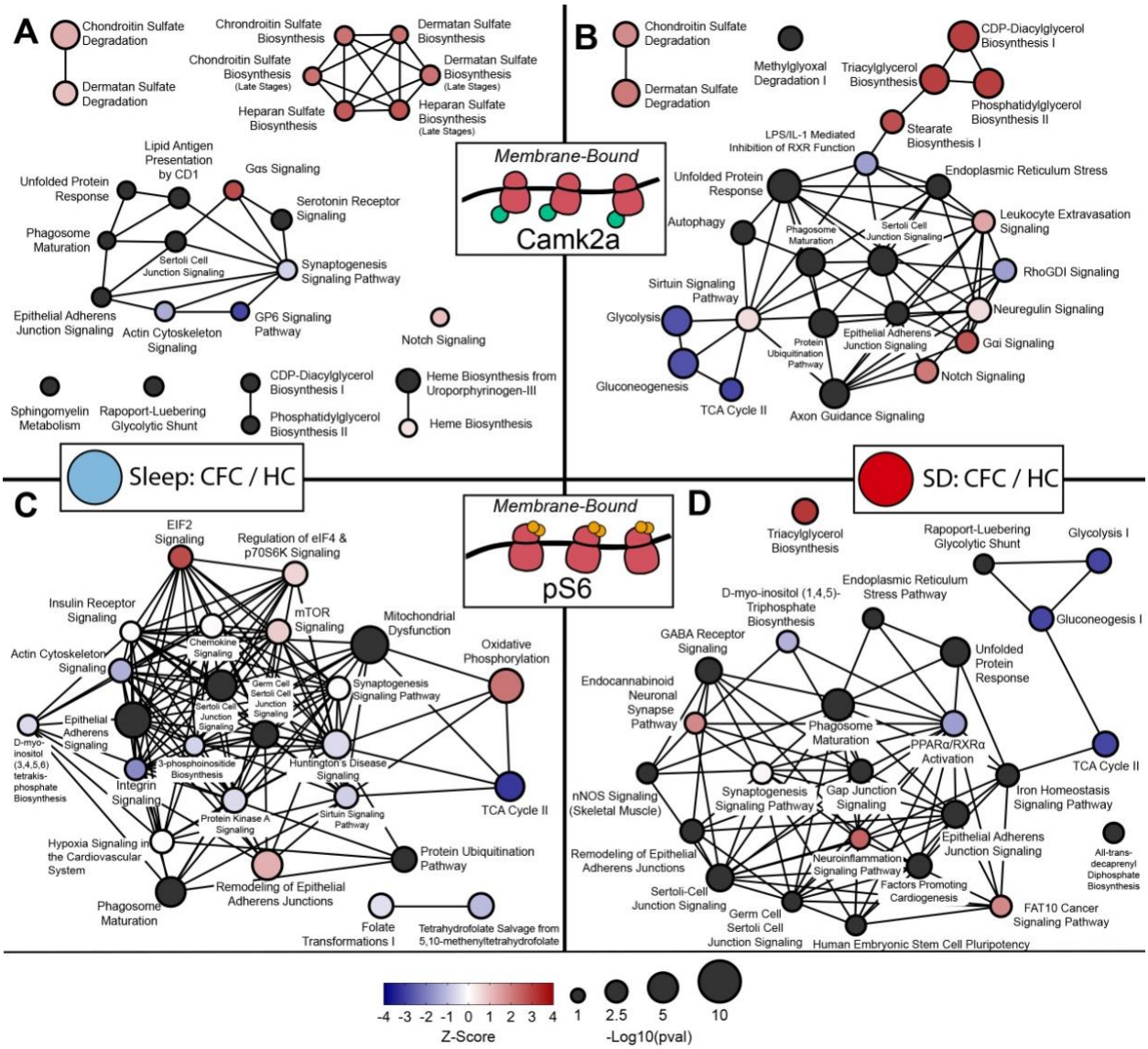


**Figure 3.9 MB ribosomal transcript networks affected by CFC vary as a function of subsequent sleep or SD.** Canonical pathway network analysis of transcripts altered on MB ribosomes from Camk2a+ (***top***) or pS6+ (***bottom***) neurons following CFC + Sleep (***left***) or CFC + SD (***right***). Hub size and color denote $p_{adj}$ value and z-score, respectively, in each condition, while connecting lines indicate commonly expressed genes between hubs.

(**Figure 3.9, Top Right**). These hubs represented chondroitin sulfate degradation, unfolded protein response, notch signaling, phagosome maturation, sertoli cell junction signaling, and epithelial adherens signaling canonical pathways. However, the significance values for these pathway hubs (like the number of transcripts altered in Camk2a+ neurons after CFC) were markedly higher in SD mice relative to sleeping mice. For example, the overlap and centrality of sertoli cell junction signaling, phagosome maturation, and epithelial adherens junction signaling pathways suggest common transcripts altered in both freely-sleeping and SD mice after CFC. Upon closer inspection, while some tubulin transcripts were decreased following CFC in both Sleep and SD groups (*Tuba1a, Tuba1b*), a large number of tubulin-encoding mRNAs were decreased only after SD (*Tuba4a, Tubb5, Tubb2a, Tubb3, Tubb4a, Tubb4b, Tubg1*). Similarly, while unfolded protein response-related transcripts were moderately elevated following CFC + Sleep (*Calr, Mbtps1, P4hb, Sel1l, Syvn1*), substantially more mRNAs associated with the unfolded protein response were increased after CFC + SD (*Amfr, Calr, Canx, Cd82, Cebpz, Dnajc3, Edem1, Eif2ak3, Hsp90b1, Hspa5, Mapk8, Mbtps1, Nfe2l2, Os9, P4hb, Sel1l, Syvn1, Ubxn4,* and *Xbp1*).

In Camk2a+ neurons, CFC + SD also altered the expression of MB ribosome-associated mRNAs linked to metabolic pathways that were unaffected in the CFC + Sleep group **(Figure 3.9A**). For example, CFC + SD increased abundance of transcripts related to lipid (triacylglycerol, phosphatidylglycerol, cdp-diacylglycerol) biosynthesis, including mRNAs encoding 1-acylglycerol-3-phosphate O-acyltransferases (*Agpat2, Agpat3, Agpat4*), ELOVL fatty acid elongases (*Elvol1, Elovl2, Elovl6*), and phospholipid phosphatases (*Plpp3*). CFC + SD also decreased the abundance of transcripts related to

glucose metabolic pathways (glycolysis, gluconeogenesis, and TCA Cycle), including *Aldoa, Adloc, Eno1, Eno2, Gapdh, Gpi1, Pfkl,* and *Pkm*. Taken together with results shown in **Figure 3.8**, these data indicate that Sleep and SD lead to divergent changes in the bioenergetic responses of Camk2a+ neurons following learning.

We performed a similar canonical pathway network analysis on transcripts altered on MB ribosomes from pS6+ neurons following CFC (**Figure 3.9, Bottom**). Many of the same pathways altered by CFC in Camk2a+ neurons (in both Sleep and SD conditions) were also observed in pS6+ neurons - including sertoli cell junction signaling, epithelial adherens signaling, and phagosome maturation - suggesting some overlap. Pathways affected in the CFC + SD condition in Camk2a+ neurons included lipid and carbohydrate pathways affected in pS6+ neurons. Interestingly, in the CFC + Sleep condition (where CFM is being consolidated), there was an increased abundance of MB ribosome-associated transcripts representing protein translation regulatory pathways (eIF2, regulation of eIF4 & p70S6K, and mTOR signaling pathways). This change, critically, was not present in CFC + SD mice. In both sleeping and SD mice, MB ribosomal transcripts which decreased in abundance after CFC included eukaryotic initiation factors (*Eif3a, Eif3c, Eif3l, Eif4a1, Eif4g1, Eif4g3*), *mTOR,* and *Tsc1*. However, in mice allowed post-CFC sleep, transcripts related to the small ribosomal subunit were elevated in pS6+ neurons, including *Rps12, Rps14, Rps17, Rps19, Rps20, Rps21, Rps23, Rps24, Rps26, Rps28, Rps29, Rps6.* This suggests that following CFC, sleep may promote an increase in overall protein synthesis capacity, which occurs in the most active hippocampal neurons. The fact that these changes occur selectively on MB ribosomes suggest that this increased synthetic capacity may be cell compartment-specific.

## 3.11 Discussion

Our present RNAseq results demonstrate not only that ribosome-associated transcripts are altered in the hippocampus as a function of 1) learning and/or 2) sleep vs. sleep loss, but also as a function of 3) the cell population being profiled, and 4) the subcellular location of the ribosomes. We find that the latter aspect (i.e., location of ribosomes within the cell) is a major contributor to the observed effects of learning and subsequent sleep or SD on hippocampal ribosome transcript profiles. Neuronal ribosomes have long been known to segregate by cell compartment, present either as “free-floating” (i.e., cytosolic) or MB complexes which are easily separated by centrifugation (Andrews and Tata, 1971). These populations are known to engage in compartmentalized translation of mRNAs. The advent of TRAP has yielded new insights into the specialized functions of ribosomes in different cellular compartments. Cytosolic ribosomes are known to process mRNAs encoding proteins with functions in the cytosolic compartment, including transcription factors and kinases. MB ribosomes translate mRNAs encoding secreted or integral membrane proteins. Available data, from non-neural cell types, suggest that the two translational environments are biochemically distinct and can be differentially regulated (for example, by cellular stress) (Reid and Nicchitta, 2015). Where ribosomes have been isolated from subcellular compartments in neurons (e.g. in Purkinje neurons) (Kratz et al., 2014), MB ribosome fractions have been shown to enrich for endoplasmic reticulum-associated ribosomes and for ribosomes in the dendritic compartment engaged in local translation. Our present findings reflect this, demonstrating that the transcript profiles of MB and cytosolic ribosomes among hippocampal neurons are highly distinctive (**Figure 3.1-3.3, Figure S3.1**).

Many forms of hippocampus-dependent memory are disrupted (in human subjects and animal models) by either pre- or post-learning sleep loss (Havekes and Abel, 2017; Krause et al., 2017; Puentes-Mestril and Aton, 2017; Rasch and Born, 2013). Indeed, sleep loss seems to disrupt plasticity mechanisms within the hippocampus more dramatically than in other brain areas (Delorme et al., 2019; Raven et al., 2019). The underlying mechanisms by which sleep loss leads to these changes (and disrupts memory mechanisms) have remained elusive. Transcriptome profiling of the effects of sleep loss alone on the hippocampus has indicated that SD increases expression of genes involved in transcriptional activation, and downregulates expression of genes involved in transcriptional repression, ubiquitination, and translation (Vecsey et al., 2012). While neither our cytosolic, MB, or Input hippocampal fractions showed a large degree of overlap with transcripts affected in prior studies (**Figure S3.2**), we do find that the same cellular pathways are affected in the cytosolic fraction (**Figure 3.5B**). Our present data add to this by demonstrating that in both whole hippocampus, and in either Camk2a+ or pS6+ hippocampal neurons, the majority of purely SD-induced changes to transcripts are present in the cytosolic fraction, and on cytosolic ribosomes (**Figure 3.4B, Figure 3.5**). While SD-driven mRNA changes also occur on MB ribosomes, these changes, in comparison, are relatively few in number (**Figure 3.4B, Figure 3.8**). Pathways affected by SD - across neuronal populations and both subcellular compartments - were those linked to regulation of transcription (consistent with prior findings) (Vecsey et al., 2012) and the AMPK, IL-3, IGF-1, and PDGF signaling pathways. Critically, AMPK (Chikahisa et al., 2009) and IGF-1 signaling (Chennaoui et al., 2014) have been implicated in homeostatic sleep responses (changes in sleep architecture of brain oscillations)

following SD. Thus it is tempting to speculate that sleep loss could lead to subsequent changes in sleep brain dynamics through changes in intracellular signaling in neurons.

However, two unanswered questions are 1) which SD-associated changes in specific transcripts' synthesis or translation provide a plausible mechanism to disrupt hippocampal memory consolidation, and 2) what cell types within the hippocampus are critically affected by SD following learning. This study aimed to address this in the context of a form of hippocampus-dependent memory consolidation (contextual fear memory; CFM) which is critically dependent on post-learning sleep. Work from our lab and others has shown that disruption of sleep within the first few hours following CFC is sufficient to disrupt CFM consolidation (Graves et al., 2003; Ognjanovski et al., 2018). While some of systems-level mechanisms occurring during post-CFC sleep have been implicated in the consolidation process (Boyce et al., 2016; Ognjanovski et al., 2018; Ognjanovski et al., 2014; Ognjanovski et al., 2017; Xia et al., 2017)), almost nothing is known about the cellular mechanisms mediating sleep (or SD) effects on CFM consolidation. We were surprised that very few transcript changes were induced on cytosolic ribosomes by CFC, in comparison with the large number of cytosolic ribosomal mRNAs affected by SD alone. However, of those transcripts altered by CFC, almost all 1) were similarly affected in either CFC + Sleep or CFC + SD conditions, and 2) were similarly altered by SD (**Figure 3.5C**). This makes sense in light of the fact that many cytosolic ribosomal mRNAs altered after CFC are transcribed or translated in an activity-dependent manner. We found that CFC increased the expression of activity-dependent genes in both total hippocampal mRNA (Input) and in the most activated neurons (pS6+) in both Sleep and SD mice. Importantly, post-CFC SD occluded learning-induced changes in cytosolic ribosomal transcripts

present in excitatory Camk2a+ hippocampal neurons. These included increases in Fosb (and its highly stable isoform ΔFosb) and Homer1 (and its short isoform Homer1a) (**Figure 3.7, Figure S3.3**). These transcript isoforms encode proteins that are critically linked to synaptic plasticity and memory (Clifton et al., 2019; Eagle et al., 2015). The timing with which SD occludes changes in their abundance (3-5 h following CFC) coincides a critical window for post-CFC sleep, essential for CFM consolidation (Graves et al., 2003; Ognjanovski et al., 2018). Thus this could represent a plausible mechanism for memory disruption by sleep loss.

In contrast to the relative paucity of transcripts altered on cytosolic ribosomes by prior learning, CFC affected a surprisingly large number of mRNAs on MB ribosomes (**Figure 3.4B, Figure 3.8A**). In general, CFC induced changes in MB ribosome-associated transcripts encoding proteins associated with neuronal structural remodeling - from cellular pathways involved in cytoskeletal remodeling, intracellular transport, and cell-cell interactions (**Figure 3.8B**). Some changes were also highly surprising and unexpected - for example, the significant reduction in ribosome-associated lncRNAs on MB ribosomes in Camk2a+ neurons after CFC (**Figure 3.8C**). Critically, the precise transcripts and (in some cases) the cellular pathways altered after CFC diverged dramatically based on whether learning was followed by sleep or SD (**Figures 3.8-3.9**). These differences provide a wealth of information with regard to potential mechanisms for SD-related disruption of CFM. For example, our present findings suggest that in non-neuronal cell types in the hippocampus, CFC induces a unique set of transcript changes (which are present in the MB fraction of Input, but are absent from MB fractions of neuronal ribosomes. Increased abundance of transcripts related to energy metabolism,

particularly those encoding mitochondrial proteins, glucose transporters, and proteins related to glycogen metabolism are commonly observed following SD (Cirelli et al., 2004; Mackiewicz et al., 2007; Vecsey et al., 2012) . Unlike previous reports, our data suggest that in Camk2a+ neurons, cellular metabolic/energetic pathways may be selectively disrupted when CFC is followed by SD, but not when CFC is followed by sleep (**Figures 3.8-3.9**). Thus, it may be that SD disrupts CFM consolidation by increasing the metabolic demands on the hippocampus.

In the most active (pS6+) neurons, CFC + Sleep leads to regulation of numerous pathways linked to protein synthesis regulation, including a widespread increase in MB ribosomal mRNAs encoding the translational machinery itself. This change is not seen when sleep is followed by SD. Thus it is tempting to speculate that in the neurons most active following memory encoding (putative “engram neurons”), long lasting changes to membrane associated protein synthesis may play a critical role in subsequent consolidation. Neuropharmacological studies have suggested that disruption of either cAMP signaling and protein synthesis in the hippocampus by SD may prevent memory consolidation (Abel et al., 1997; Bourtchouladze et al., 1998; Tudor et al., 2016; Vecsey et al., 2009). Our present data demonstrate that CFC may initiate changes to these pathways in specific hippocampal cell types, which are facilitated long-term by subsequent sleep.

Recently, TRAP has been used to characterize compartment-specific ribosomal transcripts of amygdala-projecting cortical axons during cued fear memory consolidation (Ostroff et al., 2019). However, the methods used in this study (as is true for most transcriptome and TRAP studies) would primarily report transcript changes associated

with cytosolic, rather than MB ribosomes. Here we show that the vast majority of changes due to learning itself are expressed at MB ribosomes (**Figure 3.4B, Figure 3.8**) - with surprisingly few CFC-induced changes to cytosolic ribosome-associated mRNAs (**Figure 3.5**). Recent comparisons of hippocampal ribosome-associated and total mRNA abundance suggests that cytosolic and MB ribosome-associated mRNAs are distinctly regulated with regard to translation efficiency (Cho et al., 2015). Thus understanding the effects of both learning and subsequent sleep on structures like the hippocampus will require further investigation into their effects on translation happening at the membrane.

How universal are these sleep-dependent mechanisms for memory consolidation? While this question is presently unanswered, consolidation of various types of memory, across species, share common cellular substrates (Kandel et al., 2014), with post-learning mRNA translation being a vital element. Changes in the activity patterns of neurons and the activation of particular intracellular pathways during post-learning sleep share common features, across brain structures and species (Puentes-Mestril and Aton, 2017; Puentes-Mestril et al., 2019). Our present findings have illustrated a number of sleep-dependent post-learning cellular processes which affect pathways vital for learning and memory. Future studies will determine whether these processes underlie sleep-dependent memory consolidation events in the other brain circuits, following diverse forms of learning.

## 3.12 References

Abel, T., Nguyen, P.V., Barad, M., Deuel, T.A., Kandel, E.R., and Bourtchouladze, R. (1997). Genetic demonstration of a role for PKA in the late phase of LTP and in hippocampus-based long-term memory. Cell 88, 615-626.

Andrews, T.M., and Tata, J.R. (1971). Protein Synthesis by Membrane-Bound and Free Ribosomes of the Developing Rat Cerebral Cortex Biochem J 124, 883-889.

Aten, S., Hansen, K.F., Hoyt, K.R., and Obrietan, K. (2016). The miR-132/212 locus: a complex regulator of neuronal plasticity, gene expression and cognition. RNA Dis 3.

Aten, S., Hansen, K.F., Snider, K., Wheaton, K., Kalidindi, A., Garcia, A., Alzate-Correa, D., Hoyt, K.R., and Obrietan, K. (2018). miR-132 Couples the Circadian Clock to Daily Rhythms of Neuronal Plasticity and Cognition Learn Mem 25, 214-229.

Biever, A., Valjent, E., and Puighermanal, E. (2015). Ribosomal Protein S6 Phosphorylation in the Nervous System: From Regulation to Function. Front Mol Neurosci 8.

Bourtchouladze, R., Abel, T., Berman, N., Gordon, R., Lapidus, K., and Kandel, E.R. (1998). Different training procedures recruit either one or two critical periods for contextual memory consolidation, each of which requires protein synthesis and PKA. Learn Mem 5, 365-374.

Boyce, R., Glasgow, S.D., Williams, S., and Adamantidis, A. (2016). Causal evidence for the role of REM sleep theta rhythm in contextual memory consolidation. Science 352, 812-816.

Bruning, F., Noya, S.B., Bange, T., Koutsouli, S., Rudolph, J.D., Tyagarajan, S.V., Cox, J., Mann, M., Brown, S.A., and Robles, M.S. (2019). Sleep-wake Cycles Drive Daily Dynamics of Synaptic Phosphorylation Science 366.

Chennaoui, M., Drogou, C., Sauvet, F., Gomez-Merino, D., Scofield, D.E., and Nindl, B.C. (2014). Effect of acute sleep deprivation and recovery on Insulin-like Growth Factor-I responses and inflammatory gene expression in healthy men. European Cytokine Network 25.

Chikahisa, S., Fujiki, N., Kitaoka, K., Shimizu, N., and Sei, H. (2009). Central AMPK Contributes to Sleep Homeostasis in Mice Neuropharmacology 57, 369-374.

Cho, J., Yu, N.-K., Choi, J.-H., Sim, S.-E., Kang, S.-J., J., Kwak, C., Lee, S.-W., Kim, J.-I., Choi, D.I., Kim, V.H., et al. (2015). Multiple repressive mechanisms in the hippocampus during memory formation. Science 350, 82-87.

Cirelli, C., Gutierrez, C.M., and Tononi, G. (2004). Extensive and divergent effects of sleep and wakefulness on brain gene expression. Neuron 41, 35-43.

Cirelli, C., Pfister-Genskow, M., McCarthy, D., Woodbury, R., and Tononi, G. (2009). Proteomic profiling of the rat cerebral cortex in sleep and waking. Arch Ital Biol 147, 59-68.

Clifton, N.E., Trent, S., Thomas, K.L., and Hall, J. (2019). Experience-Dependent Induction of Hippocampal ΔFosB Controls Learning Mol Neuropsychiatry 5, 147-161.

Daumas, S., Halley, H., Frances, B., and Lassalle, J.M. (2005). Encoding, consolidation, and retrieval of contextual memory: differential involvement of dorsal CA3 and CA1 hippocampal subregions. Learn Mem 12, 375-382.

Delorme, J.E., Kodoth, V., and Aton, S.J. (2019). Sleep loss disrupts Arc expression in dentate gyrus neurons. Neurobiol Learn Mem 160, 73-82.

Dennis Jr., G., Sherman, B.T., Hosack, D.A., Yang, J., Gao, W., Lane, H.C., and Lempicki, R.A. (2003). DAVID: Database for Annotation, Visualization, and Integrated Discovery. Genome Biology 4.

Eagle, A.L., Gajewski, P.A., Yang, M., Kechner, M.E., Al Masraf, B.S., Kennedy, P.J., Wang, H., Mazei-Robinson, M.S., and Robison, A.J. (2015). Experience-Dependent Induction of Hippocampal ΔFosB Controls Learning J Neurosci 35, 13773-13783.

Gafford, G.M., Parsons, R.G., and Helmstetter, F.J. (2011). Consolidation and reconsolidation of contextual fear memory requires mammalian target of rapamycin-dependent translation in the dorsal hippocampus. Neuroscience 182.

Graves, L.A., Heller, E.A., Pack, A.I., and Abel, T. (2003). Sleep deprivation selectively impairs memory consolidation for contextual fear conditioning. Learn Mem 10, 168-176.

Havekes, R., and Abel, T. (2017). The tired hippocampus: the molecular impact of sleep deprivation on hippocampal function. Curr Opin Neurobiol 44, 13-19.

Havekes, R., and Aton, S.J. (2020). Impacts of Sleep Loss Versus Waking Experience on Brain Plasticity: Parallel or Orthogonal? Trends in Neuroscience 43, 385-393.

Havekes, R., Park, A.J., Tudor, J.C., Luczak, V.G., Hansen, R.T., Ferri, S.L., Bruinenberg, V.M., Poplawski, S.G., Day, J.P., Aton, S.J., et al. (2016). Sleep deprivation causes memory deficits by negatively impacting neuronal connectivity in hippocampal area CA1. eLife 5, pii: e13424.

Igaz, L.M., Vianna, M.R., Medina, J.H., and Izquierdo, I. (2002). Two time periods of hippocampal mRNA synthesis are required for memory consolidation of fear-motivated learning. J Neurosci 22, 6781-6789.

Jiang, Y., Gong, N.N., Hu, X.S., Ni, M.J., Pasi, R., and Matsunami, H. (2015). Molecular profiling of activated olfactory neurons identifies odorant receptors for odors in vivo. Nat Neurosci 18, 1446-1454.

Kandel, E.R. (2012). The molecular biology of memory: cAMP, PKA, CRE, CREB-1, CREB-2, and CPEB. Mol Brain 5.

Kandel, E.R., Dudai, Y., and Mayford, M.R. (2014). The Molecular and Systems Biology of Memory. Cell 157, 163-186.

Katche, C., Bekinschtein, P., Slipczuk, L., Goldin, S., Izquierdo, I., Cammarota, M., and Medina, J.H. (2010). Delayed wave of c-Fos expression in the dorsal hippocampus involved specifically in persistence of long-term memory storage. PNAS 107, 349-354.

Knight, Z.A., Tan, K., Birsoy, K., Schmidt, S., Garrison, J.L., Wysocki, R.W., Emiliano, A., Ekstrand, M.I., and Friedman, J.M. (2012). Molecular profiling of activated neurons by phosphorylated ribosome capture. Cell 151, 1126-1137.

Kramer, A., Green, J., Pollard Jr., J., and Tugendreich, S. (2014). Causal Analysis Approaches in Ingenuity Pathway Analysis Bioinformatics 30, 523-530.

Kratz, A., Beguin, P., Kaneko, M., Chimura, T., Suzuki, A.M., Matsunaga, A., Kato, S., Bertin, N., Lassmann, T., Vigot, R., et al. (2014). Digital expression profiling of the compartmentalized translatome of Purkinje neurons. Genome Res 24, 1396-1410.

Krause, A.J., Simon, E.B., Mander, B.A., Greer, S.M., Saletin, J.M., Goldstein-Piekarski, A.N., and Walker, M.P. (2017). The sleep-deprived human brain. Nat Rev Neurosci 18, 404-418.

Liao, Y., Smyth, G.K., and Shi, W. (2013). featureCounts: an efficient general purpose program for assigning sequence reads to genomic features. Bioinformatics 30, 923-930.

Love, M.I., Huber, W., and Anders, S. (2014). Moderated estimation of fold change and dispersion for RNA-seq data with DESeq2. Genome Biology 15.

Luo, J., Phan, T.X., Yang, Y., Garelick, M.G., and Storm, D.R. (2013). Increases in cAMP, MAPK Activity, and CREB Phosphorylation during REM Sleep: Implications for REM Sleep and Memory Consolidation. J Neurosci 33, 6460-6468.

Mackiewicz, M., Paigen, B., Naidoo, N., and Pack, A.I. (2008). Analysis of the QTL for sleep homeostasis in mice: Homer1a is a likely candidate. Physiol Genomics 33, 91-99.

Mackiewicz, M., Shockley, K.R., Romer, M.A., Galante, R.J., Zimmerman, J.E., Naidoo, N., Baldwin, D.A., Jensen, S.T., Churchill, G.A., and Pack, A.I. (2007). Macromolecule biosynthesis - a key function of sleep. Physiol Genomics 31, 441-457.

Maret, S., Dorsaz, S., Gurcel, L., Pradervand, S., Petit, B., Pfister, C., Hagenbuchle, O., O'Hara, B.F., Franken, P., and Tafti, M. (2008). Homer1a is a core brain molecular correlate of sleep loss. Proc Natl Acad Sci USA 104, 20090-20095.

McDermaid, A., Monier, B., Zhao, J., Liu, B., and Ma, Q. (2019). Interpretation of differential gene expression results of RNA-seq data: review and integration. Briefings in Bioinformatics 20, 2044-2054.

Naidoo, N., Giang, W., Galante, R.J., and Pack, A.I. (2005). Sleep deprivation induces the unfolded protein response in mouse cerebral cortex. J Neurochem 92, 1150-1157.

Noya, S.B., Colamea, D., Bruning, F., Spinnler, A., Mircsof, D., Opitz, L., Mann, M., Tuagarajen, S.K., Robles, M.S., and Brown, S.A. (2019). The Forebrain Synaptic Transcriptome Is Organized by Clocks but Its Proteome Is Driven by Sleep Science 366.

Ognjanovski, N., Broussard, C., Zochowski, M., and Aton, S.J. (2018). Hippocampal Network Oscillations Rescue Memory Consolidation Deficits Caused by Sleep Loss. Cereb Cortex 28, 3711-3723.

Ognjanovski, N., Maruyama, D., Lashner, N., Zochowski, M., and Aton, S.J. (2014). CA1 hippocampal network activity changes during sleep-dependent memory consolidation. Front Syst Neurosci 8, 61.

Ognjanovski, N., Schaeffer, S., Mofakham, S., Wu, J., Maruyama, D., Zochowski, M., and Aton, S.J. (2017). Parvalbumin-expressing interneurons coordinate hippocampal network dynamics required for memory consolidation. Nature Communications 8, 15039.

Ostroff, L.E., Santini, E., Sears, R., Deane, Z., Kanadia, R.N., LeDoux, J.E., Lhakhang, T., Tsirigos, A., Heguy, A., and Klann, E. (2019). Axon TRAP reveals learning-associated alterations in cortical axonal mRNAs in the lateral amgydala. eLife 8.

Pereira, L.M., de Castro, C.M., Guerra, L.T.L., Queiroz, T.M., Marques, J.T., and Pereira, G.S. (2019). Hippocampus and Prefrontal Cortex Modulation of Contextual Fear Memory Is Dissociated by Inhibiting De Novo Transcription During Late Consolidation Mol Neurobiol 56, 5507-5519.

Poirrier, J.-E., Guillonneu, F., Renaut, J., Sergeant, K., Luxen, A., Maquet, P., and Leprince, P. (2008). Proteomic changes in rat hippocampus and adrenals following short-term sleep deprivation. Proteome Science 6.

Poplawski, S.G., Peixoto, L., Porcari, G.S., Wimmer, M.E., McNally, A.G., Mizuno, K., Giese, K.P., S., C., Koberstein, J.N., Risso, D., et al. (2016). Contextual Fear Conditioning Induces Differential Alternative Splicing. Neurobiol Learn Mem 134, 221-235.

Puentes-Mestril, C., and Aton, S.J. (2017). Linking network activity to synaptic plasticity during sleep: hypotheses and recent data. Frontiers in Neural Circuits 11, doi: 10.3389/fncir.2017.00061.

Puentes-Mestril, C., Roach, J., Niethard, N., Zochowski, M., and Aton, S.J. (2019). How rhythms of the sleeping brain tune memory and synaptic plasticity. Sleep 42, pii: zsz095.

Rao-Ruiz, P., Couey, J.J., Marcelo, I.M., Bouwkamp, C.G., Slump, D.E., Matos, M.R., van der Loo, R.J., Martins, G.J., van den Hout, M., van Icken, W.F., et al. (2019). Engram-specific Transcriptome Profiling of Contextual Memory Consolidation Nat Communications 10.

Rasch, B., and Born, J. (2013). About sleep's role in memory. Physiol Rev 93, 681-766.

Raven, F., Meerlo, P., Van der Zee, E.A., Abel, T., and Havekes, R. (2019). A brief period of sleep deprivation causes spine loss in the dentate gyrus of mice. Neurobiol Learn Mem 160, 83-90.

Reid, D.W., and Nicchitta, C.V. (2015). Diversity and selectivity in mRNA translation on the endoplasmic reticulum. Nat Rev Mol Cell Biol 16.

Ren, J., Zhang, M.-J., Li, T.-M., Zhang, J.-E., Lin, R., Chen, S., Luo, M., and Dong, M.-Q. (2016). Quantitative Proteomics of Sleep-Deprived Mouse Brains Reveals Global Changes in Mitochondrial Proteins. PLoS One 11.

Sanz, E., Bean, J.C., Carey, D.P., Quintana, A., and McKnight, G.S. (2019). RiboTag: Ribosomal Tagging Strategy to Analyze Cell-Type-Specific mRNA Expression In Vivo. Curr Protoc Neurosci 88, e77.

Sanz, E., Yang, L., Su, T., Morris, D.R., McKnight, G.S., and Amieux, P.S. (2009). Cell-type-specific isolation of ribosome-associated mRNA from complex tissues. Proc Natl Acad Sci U S A 106, 13939-13944.

Schiavo, G., Greensmith, L., Hafezparast, M., and Fisher, E.M.C. (2013). Cytoplasmic dynein heavy chain: the servant of many masters. Trends in Neuroscience 36, 641-651.

Shigeoka, T., Jung, J., Holt, C.E., and Jung, H. (2018). Axon-TRAP-RiboTag: Affinity Purification of Translated mRNAs from Neuronal Axons in Mouse In Vivo. In RNA Detection (Methods in Molecular Biology) (New York: Humana Press), pp. 85-94.

Spano, G.M., Banningh, S.W., Marshall, W., de Vivo, L., Bellesi, M., Loschky, S.S., Tononi, G., and Cirelli, C. (2019). Sleep Deprivation by Exposure to Novel Objects Increases Synapse Density and Axon-Spine Interface in the Hippocampal CA1 Region of Adolescent Mice. J Neurosci 39, 6613-6625.

Tudor, J.C., Davis, E.J., Peixoto, L., Wimmer, M.E., van Tilborg, E., Park, A.J., Poplawski, S.G., Chung, C.W., Havekes, R., Huang, J., et al. (2016). Sleep deprivation impairs memory by attenuating mTORC1-dependent protein synthesis. Sci Signal 9.

Vecsey, C.G., Baillie, G.S., Jaganath, D., Havekes, R., Daniels, A., Wimmer, M., Huang, T., Brown, K.M., Li, X.Y., Descalzi, G., et al. (2009). Sleep deprivation impairs cAMP signalling in the hippocampus. Nature 461, 1122-1125.

Vecsey, C.G., Hawk, J.D., Lattal, K.M., Stein, J.M., Fabian, S.A., Attner, M.A., Cabrera, S.M., McDonough, C.B., Brindle, P.K., Abel, T., et al. (2007). Histone deacetylase inhibitors enhance memory and synaptic plasticity via CREB:CBP-dependent transcriptional activation. J Neurosci 27, 6128-6140.

Vecsey, C.G., Peixoto, L., Choi, J.H., Wimmer, M., Jaganath, D., Hernandez, P.J., Blackwell, J., Meda, K., Park, A.J., Hannenhalli, S., et al. (2012). Genomic analysis of sleep deprivation reveals translational regulation in the hippocampus. Physiol Genomics 44, 981-991.

Wang, H., Liu, Y., Briesemann, M., and Yan, J. (2010). Computational analysis of gene regulation in animal sleep deprivation. Physiol Genomics 42 427-436.

Xia, F., Richards, B.A., Tran, M.M., Josselyn, S.A., Takehara-Nishiuchi, K., and Frankland, P.W. (2017). Parvalbumin-positive interneurons mediate neocortical-hippocampal interactions that are necessary for memory consolidation. eLife 6, e27868.

Yi, L., Pimentel, H., Bray, N.L., and Pachter, L. (2018). Gene-level differential analysis at transcript-level resolution. Genome Biology 19.

# Chapter IV. Sleep Loss Disrupts Hippocampal Memory Consolidation via an Acetylcholine- and Somatostatin Interneuron-Mediated Inhibitory Gate

## 4.1 Abstract

Sleep loss profoundly disrupt consolidation of hippocampus-dependent memory, in both human subjects and animal models. To better characterize the effects of sleep loss on the hippocampal circuit, we quantified activity-dependent phosphorylation of ribosomal subunit S6 (pS6) across the dorsal hippocampus. We find that pS6 expression in enhanced in the dentate gyrus (DG) in the hours following learning a hippocampus-dependent task (single-trial contextual fear conditioning; CFC). pS6 expression throughout the hippocampus is disrupted by brief sleep deprivation (SD) – a manipulation which disrupts contextual fear memory (CFM). This suggests that network activity is reduced during SD relative to sleep. To characterize cell populations affected by SD, we used translating ribosome affinity purification (TRAP) to isolate cell type-specific transcripts associated with pS6-ribosomes in active neurons. TRAP-seq was used to profile pS6-associated transcripts enriched after SD vs. sleep. Cell type-specific enrichment analysis (CSEA) of these transcripts revealed that somatostatin-expressing (SST+) interneurons, and cholinergic and orexinergic inputs to hippocampus, are selectively activated after SD. We used TRAP of ribosome-associated transcripts in hippocampal SST+ interneurons (SST-TRAP) to verify this result and identify mechanisms mediating SST+ interneuron activation during SD. We next used

pharmacogenetics to mimic the effects of SD, selectively activating hippocampal SST+ interneurons while mice slept in the hours following CFC. We find that activation of SST interneurons is sufficient to disrupt CFM consolidation, by gating activity in surrounding neurons. Pharmacogenetic inhibition of cholinergic input to the hippocampus from the medial septum (MS) promoted CFM consolidation and disinhibited neurons in the DG, increasing pS6 expression. This suggests that state-dependent gating of SST interneurons activity is mediated by cholinergic input. Together these data provide evidence for an inhibitory gate on hippocampal information processing, which is activated by sleep loss.

## 4.2 Introduction

Hippocampal plasticity and memory storage are gated by vigilance states. In both human subjects and animal models, sleep loss disrupts consolidation of multiple types of hippocampus-dependent memories (Abel et al., 2013; Havekes and Abel, 2017). This effect has been extensively studied in mice, where as little as a few hours of experimental sleep deprivation (SD) can disrupt hippocampally-mediated consolidation of object-place memory (Havekes et al., 2016; Prince et al., 2014; Vecsey et al., 2009) and contextual fear memory (CFM) (Graves et al., 2003; Ognjanovski et al., 2018). Recent work has characterized biochemical pathways involved in memory consolidation which are disrupted in the hippocampus by SD (Aton et al., 2009b; Havekes et al., 2016; Tudor et al., 2016; Vecsey et al., 2009). However, much less is known about how SD affects the hippocampal microcircuit, or its function.

SD disrupts patterns of hippocampal network activity which are associated with memory consolidation. For example, SD interferes with the increases in the occurrence of hippocampal network oscillations, increased stability of spike timing relationships between CA1 neurons, and increase neuronal firing rates within CA1 during CFM consolidation (Ognjanovski et al., 2018). However, the reason that these learning-induced network activity changes are disrupted by post-learning SD is unknown. Recent work has demonstrated that activity-dependent regulation of protein translation machinery within the dorsal hippocampus is essential for sleep-dependent memory consolidation (Tudor et al., 2016). SD interferes with biochemical pathways which drive increased protein synthesis following learning (Tudor et al., 2016; Vecsey et al., 2012).

To better characterize the link between neuronal activity and protein synthesis in the hippocampus during CFM consolidation, we characterized the activity-dependent phosphorylation of ribosomal subunit S6 (pS6). We find that CFC increases pS6 phosphorylation at a terminal serine residue (pS6 Ser242-244), and that SD reduces pS6 Ser242-244 throughout the dorsal hippocampus. To identify the cell populations expressing pS6 after sleep vs. SD, we used a pSer242-244 as an affinity tag for translating ribosome affinity purification (pS6 TRAP). We then identified modules of cell-type specific transcripts with expression correlated to wake time in sleeping and SD mice, and verified these findings with qPCR. These analyses indicate that SD selectively activates (i.e., leads to increased pS6 expression in) hippocampal SST+ interneurons, and orexinergic (lateral hypothalamic) and cholinergic (MS) neurons which send input to the hippocampus. We used TRAP in SST+ interneurons (SST-TRAP) to verify that activity-dependent transcripts are increased in these neurons with SD. To assess how

increased activity in the hippocampus SST+ interneuron population during SD affects memory consolidation, we used pharmacogenetics to selectively activate these neurons in the hours following CFC. We find the mimicking the effects of SD on SST+ interneuron activity is sufficient for disruption of CFM consolidation in freely-sleeping mice. Lastly, we tested the hypothesis that state-dependent regulation of the dorsal hippocampal network is mediated by changes in activity of MS cholinergic neurons. We find that pharmacogenetic inhibition of cholinergic input to hippocampus following CFC promotes CFM consolidation, and increases pS6 expression in dorsal hippocampus. Together, these data provide evidence for a state-dependent gate on network activity in the hippocampus, regulated by SST+ interneurons and MS cholinergic input, which causes SD-induced disruption of memory consolidation.

## 4.3 Materials & Methods

### Mouse husbandry, handling, and behavioral procedures

All animal husbandry and experimental procedures were approved by the University of Michigan Institutional Animal Care and Use Committee (PHS Animal Welfare Assurance number D16-00072 [A3114-01]). Mice were maintained on a 12 h:12 h light:dark cycle with *ad lib* access to food.

For behavioral experiments, 3-4 month old C57Bl6/J mice (Jackson) or transgenic mice on a C57Bl6/J background (see below) were individually housed with beneficial enrichment one week prior to experimental procedures, and were habituated to experimenter handling (5 min/day) for five days prior to experimental procedures. At lights on (ZT0), animals were either left in their home cage (HC) or underwent single-trial

contextual fear conditioning (CFC). During CFC, mice were place in a novel conditioning chamber (Med Associates), and were allowed to explore the chamber freely for 2.5 min, after which they received a 2-s, 0.75 mA foot shock through the chamber's grid floor. Mice remained in their conditioning chamber for an additional 28 s, after which they were then returned to their home cage. Mice were then either were permitted *ad lib* sleep (Sleep) or were sleep-deprived (SD) by gentle handling (Durkin et al., 2017; Ognjanovski et al., 2018) over the next 3-5 h.

**Translating Ribosome Affinity Purification (TRAP)**

For pS6 RNA-sequencing (TRAP-seq) experiments, 3-4 month old C57Bl/6J mice were randomly assigned to one of four groups: HC + Sleep ($n$ = 8), HC + SD ($n$ = 7), CFC + Sleep ($n$ = 8), CFC + SD ($n$ = 8). Beginning at ZT3, animals were euthanized with an i.p injection of pentobarbital (Euthasol) and hippocampi were dissected in cold dissection buffer (1x HBSS, 2.5 mM HEPES [pH 7.4], 4 mM $NaHCO_3$, 35 mM glucose, 100μg/ml cycloheximide). Hippocampal tissue was then transferred to a glass dounce homogenizer containing homogenization buffer (10 mM HEPES [pH 7.4], 150 mM KCl, 10 mM $MgCl_2$, 2 mM DTT, cOmplete™ Protease Inhibitor Cocktail [Sigma-Aldrich, 11836170001], 100 U/mL RNasin® Ribonuclease Inhibitors [Promega, N2111], and 100 μg/mL cycloheximide) and manually homogenized on ice. Homogenate was transferred to 1.5 ml LoBind tubes (Eppendorf) and centrifuged at 4°C at 1000 g for 10 min. The resulting supernatant was transferred to a new tube, and 10% NP40 was added to the samples (90μL), and incubated 5 min on ice. Samples were centrifuged at 4°C at maximum speed for 10 min, 500μL supernatant transferred to a new LoBind tube, and

incubated with anti-pS6 244-247 (ThermoFisher 44-923G; Knight et al., 2012). Antibody binding of the homogenate-antibody solution occurred over 1.5 h at 4°C with constant rotation. For affinity purification, 200 µl of Protein G Dynabeads (ThermoFisher, 10009D) were washed 3 times in 0.15M KCl IP buffer (10 mM HEPES [pH 7.4], 150 mM KCl, 10 mM MgCl 2 , 1% NP-40) and incubated in supplemented homogenization buffer (+10% NP-40). Following this step, supplemented buffer was removed, homogenate-antibody solution was added directly to the Dynabeads, and the solution was incubated for 1 h at 4°C with constant rotation. During the final wash, beads were placed onto the magnet and moved to room temperature. After removing the supernatant, RNA was eluted by vortexing the beads vigorously in 350 µl RLT (Qiagen, 79216). Eluted RNA was purified using RNeasy Micro kit (Qiagen).

SST-Ribo mice were generated by crossing *SST-IRES-CRE* (B6N.Cg-Sst$^{tm2.1(SST-cre)Zjh}$; Jackson) mice to the RiboTag$^{fl/fl}$ (B6N.129-Rpl22$^{tm1.1Psam}$/J; Jackson) mouse line to generate mice expressing HA-tagged Rpl22 protein in SST interneurons. For SST-TRAP, ribosomes and associated transcripts were affinity purified by incubating homogenate with 1/40 (10 µl) anti-HA antibody (Abcam, ab9110) (Shigeoka et al., 2018).

**RNA sequencing and data analysis**

RNA-Seq was carried out at the University of Michigan's DNA sequencing core. cDNA libraries were prepared by the core using Takara's SMART-seq v4 Ultra Low Input RNA Kit (Takara 634888) and sequenced on Illumina's NovaSeq 6000 platform. Sequencing reads (50 bp, paired end) were mapped to *Mus musculus* using Star v2.6.1a and quality checked with Multiqc(v1.6a0). Reads mapped to unique transcripts were

counted with featureCounts (Liao et al., 2014). For weighted gene co-expression network analysis (WGCNA) analysis, raw counts for pS6 data was filtered to keep genes with at least 30 total reads across the 30 samples. The filtered reads were normalized using the DESeq2 variance stabilizing transformation (vst) function (Love et al., 2014) and filtered to keep genes with a variance larger than 0.03 among the 30 samples. The 1662 genes were retained and used for the network analysis in WGCNA (Langfelder and Horvath, 2008).

For cell type-specific expression analysis (CSEA), genes from the Brown and Magenta clusters were combined and uploaded into the CSEA Tool (http://genetics.wustl.edu/jdlab/csea-tool-2/), selecting Candidate Gene List from: Mice (Xu et al., 2014). Results for cell-types enriched in our pS6 clusters were analyzed at the most stringent specificity index ($p$SI < 0.0001). Observing significant values in cholinergic (+Chat), orexinergic (Hcrt+), and GABAergic (Pnoc+, Cort+) neurons, we plotted genes from the highest and second highest specificity index. To analyze how SD promotes pS6 enrichment of these cell type-specific transcripts, we calculated the $Log_2FC$ values of combined CFC and HC mice and assessed the effect of SD over sleep control mice (Love et al., 2014).

**Quantitative PCR (qPCR)**

RNA from TRAP experiments was quantified by spectrophotometry (Nanodrop Lite, ThermoFisher). 50ng of RNA was reverse transcribed using iScript cDNA Synthesis (Bio-Rad, Catalog: 1708890) or SuperScript IV Vilo Master Mix (Invitrogen, Catalog: 11756060). qPCR was performed on diluted cDNA that employed either Power SYBR

Green PCR Mix (Invitrogen 4367659) or TaqMan Fast Advanced Master Mix (Invitrogen, Catalog: 4444557). Primers were designed using Primer3(v. 0.4.0) and confirmed with NCBI primer Basic Local Alignment Search Tool (BLAST). qPCR reactions were measured using a CFX96 Real-Time System, in 96-well reaction plates (Bio-Rad). For pS6- and SST-TRAP experiments, housekeeping genes for data normalization were determined by assessing the stability values prior to analysis (Andersen et al., 2004). Analyses compared *Pgk1*, *Gapdh*, *Actg1*, *Tuba4a*, *Tbp*, and *Hprt.* Results from both analyses independently found *Gapdh* and *Pgk1* to be the most stable and least altered housekeeping transcripts following SD or CFC. Therefore expression was normalized to the geometric mean of *Gapdh* and *Pgk1.* To assess differences in transcript abundance between groups, values were expressed as fold changes normalized to the mean values for mice in the HC + Sleep group. To measure relative enrichment of mRNA in pS6-TRAP or SST-TRAP experiments, each sample was normalized to the geometric mean of *Pgk1* and *Gapdh* housekeeping transcripts and then normalized to the corresponding Input sample (TRAP Enrichment = 2^(ΔCt_target - ΔCt_housekeeping).

**Immunohistochemistry and protein expression analysis**

Mice were injected with euthasol and perfused with cold 1xPBS followed by 4% paraformaldehyde. Brains were extracted and submerged in ice-cold fixative for 24hrs and transferred to 30% sucrose solubilized in 1xPBS. 50µm-thick coronal sections were cut on a cryostat. Tissue was blocked for 2-hours in 1% NGS and 0.3% Triton X-100 followed by 2-3 days of 4C° incubation in 1xPBS (5% NGS, 0.3% Triton X-100) with primary antibody(ies): pS6 S235-236 (Cell Signaling, Catalog: 4858, 1:500), pS6 S244-

247(ThermoFisher, Catalog: 44-923G, 1:500), SST (Millipore, MAB354, 1:200), Pvalb (Synaptic Systems, Catalog: 195004, 1:500), cFos (Abcam, Catalog: 190289, 1:500), Arc (Synaptic Systems, 156004, 1:500) by constant rotation. Sections were then washed 3x in 1xPBS (1% NGS, 0.2% Triton X-100) and incubated for 1hr in 1xPBS (5% NGS, 0.3% TX-100) and secondary antibody: Fluorescein (FITC) AffiniPure Goat Anti-Rabbit IgG (Jackson, Catalog: 111-095-003, 1:200), Donkey anti-Rat IgG Alexa Fluor 488 (ThermoFisher, A-21208), Goat Anti-Guinea Pig IgG Alexa Fluor 555 (Abcam, Catalog: ab150186, 1:200), Goat anti-Rabbit IgG Alexa Fluor 633 (ThermoFisher, Catalog: A-21070, 1:200). Tissue was then washed 3x in 1xPBS (1% NGS, 0.2% Triton X-100), 3x in 1xPBS, and then mounted on coverslips and embedded in ProLong Gold Antifade Mountant (ThermoFisher, Catalog: P10144).

For optical density (OD) calculations, 4 fluorescent microscope images were taken from each brain and analyzed in Fiji. A scorer blind to experimental condition collected optical density values from CA1 and CA3 pyramidal cell layers as well as background. For analysis, equally sized regions of interest (ROIs) were obtained for each image. OD values were background subtracted and normalized to HC + Sleep control groups. For DG cell counts, pS6 co-localization, and SST/PVALB quantification, images were captured using a 20x objective lens on a Leica SP5 laser scanning confocal microscope. Z-projected images were analyzed in MIPAR image analysis software in their raw grayscale format (Sosa et al., 2014) For DG cell counts, a non-local means filter was used to reduce image noise and an adaptive threshold applied to identify cell counts whose mean intensity values were 200% its surroundings. Colocalization and mean fluorescence intensity were determined by adaptive thresholding of fluorescent signals, quantifying

percentage overlap of ROI obtained from both signals and mean fluorescent intensity values of underlying fluorescent signals.

**AAV virus injections, pharmacogenetic manipulations, and CFM testing**

At age 3-4 months, male *SST-IRES-CRE* (B6N.Cg-Sst$^{tm2.1(SST-cre)Zjh}$) or *Chat-CRE* (B6.FVB(Cg)-Tg(Chat-cre)GM53Gsat/Mmucd, MMRRC) mice underwent bilateral dorsal hippocampus or MS viral transduction. *SST-IRES-CRE* mice were transduced with either hM3dq-mCherry (pAAV-hSyn-DIO-hM3D(Gq)-mCherry, University of Pennsylvania Vector Core, Lot: V55836) or (as a control) an mCherry reporter (EF1A-DIO-mCherry, University of Pennsylvania Vector Core, Lot: PBK273-9). For both vectors, 1 µl of virus was injected using a 33-gauge beveled syringe needle into the dorsal hippocampus each hemisphere at a rate of 4 nL/s (2.1 mm posterior, 1.6 mm lateral, 2.1 mm ventral to Bregma). *Chat*-CRE mice were injected with hM4Di-mCitrine (AAV8 hSyn-DIO-HA-hM4D(Gi)-P2a-Citrine, University of Pennsylvania Vector Core, Lot: PBK399-9). 1 µl of virus was injected into the medial septum (0.75 mm anterior, 0.0 mm lateral, 4.0 mm ventral to Bregma).

After 2-4 weeks of postoperative recovery and daily handling as described above, mice underwent single-trial CFC at ZT0. Immediately after CFC, mice were injected i.p. with either 0.3 mg/kg clozapine N-oxide (CNO; Tocris, Catalog: 4936, Lot: 13D/233085) in 0.5% DMSO and saline, or 0.5% DMSO vehicle (VEH). All mice were then returned to their home cage for ad lib sleep, and were returned to the CFC context for CFM testing. Mice were video monitored and context-specific freezing behavior was quantified by a scorer blinded to experimental conditions as described previously (Ognjanovski et al.,

2018; Ognjanovski et al., 2014; Ognjanovski et al., 2017). To verify effects of pharmacogenetic manipulations on the hippocampal network, 2 weeks following CFM tests, mice were administered CNO (or VEH) at lights on, and were allowed 3 h *ad lib sleep* prior to perfusion for immunohistochemical analysis of activity-dependent cFos or pS6 expression.

### 4.4 Learning increases and sleep loss decreases phosphorylation of S6 in the hippocampus

Since brief sleep deprivation (SD) of only a few hours is sufficient to disrupt many forms of hippocampus-dependent memory consolidation in mice (Graves et al., 2003; Havekes et al., 2016; Ognjanovski et al., 2018; Prince et al., 2014; Vecsey et al., 2009), we first characterized the effects of 3-h SD on S6 phosphorylation. Following 5 days of habituation to handling, beginning at lights on (ZT0), mice either had continuous SD by gentle handling or were allowed *ad lib* sleep (Sleep) prior to sacrifice at ZT3 (**Figure 4.1A**). Because S6 is sequentially phosphorylated at five serine residues, we first quantified phosphorylation using an antibody recognizing the initial Ser235-236 phosphorylation sites (pS6 235-236). Consistent with previous reports (Tudor et al., 2016), 3-h SD did not alter either the number of pS6(Ser235-236)+ neurons in the dentate gyrus (DG) or the intensity of pS6 235-236 staining in the pyramidal cell body layers of CA1 or CA3 (**Figure 4.1C**). We then quantified phosphorylation at the terminal S6 sites (Ser244-247; hereafter referred to simply as pS6). in SD mice, we observed a significant decrease in the number of pS6+ neurons in the dentate gyrus, and reduced intensity of pS6+ staining in pyramidal cell body layers of CA1 and CA3 (**Figure 4.1B, C**). In contrast,

neocortical regions adjacent the dorsal hippocampus (i.e., primary somatosensory cortex) showed increased numbers of pS6+ neurons at both sites after 3-h SD (**Figure S4.2**). Because S6 phosphorylation is neuronal activity-driven (Pirbhoy et al., 2016) we also tested whether pS6+ neurons co-expressed the activity-regulated protein Arc. Consistent with our previous findings (Delorme et al., 2019), 3-h SD reduced numbers of both Arc+ and pS6+ neurons in the DG. Arc and pS6 were co-localized to a similar extent in DG of both Sleep and SD mice (**Figure 4.1D**), with 80% of Arc+ DG neurons, on average, being pS6+, and 60% of pS6+ DG neurons being Arc+.

We next tested whether hippocampal S6 phosphorylation was affected by learning a hippocampus-dependent memory task. Mice underwent single-trial contextual fear conditioning (CFC; in which exploration of a novel chamber is paired with a foot shock) or, for comparison, were left in their home cage (HC) at lights on. After this, both CFC and HC mice were either allowed *ad lib* sleep, or had SD by gentle handling in their home cage. In freely-sleeping mice, CFC increased the number of pS6+ DG neurons at both 30 min and 3 h post-CFC, relative to HC controls (two-way ANOVA: main effect of time, $F = 50.63$, $p < 0.001$; main effect of learning, $F = 33.59$, $p < 0.001$; time × learning interaction, $F = 2.22$, $p = 0.16$) (**Figure S4.1**). In contrast, CFC did not alter pS6 expression CA1 or CA3 of freely-sleeping mice, relative to HC controls. Consistent with greater pS6 expression in the hippocampus after periods rich in sleep, pS6+ neurons increased between the two timepoints (ZT0 vs. ZT3) in both HC + Sleep and CFC + Sleep mice (**Figure S4.1**). 3-h SD disrupted pS6 expression in the hippocampus following CFC, with fewer pS6+ neurons in the DG and reduced pS6+ expression in CA1 (**Figure 4.1C**).

Taken together, these data suggest that learning increases and SD reduces S6 phosphorylation in the hippocampus.

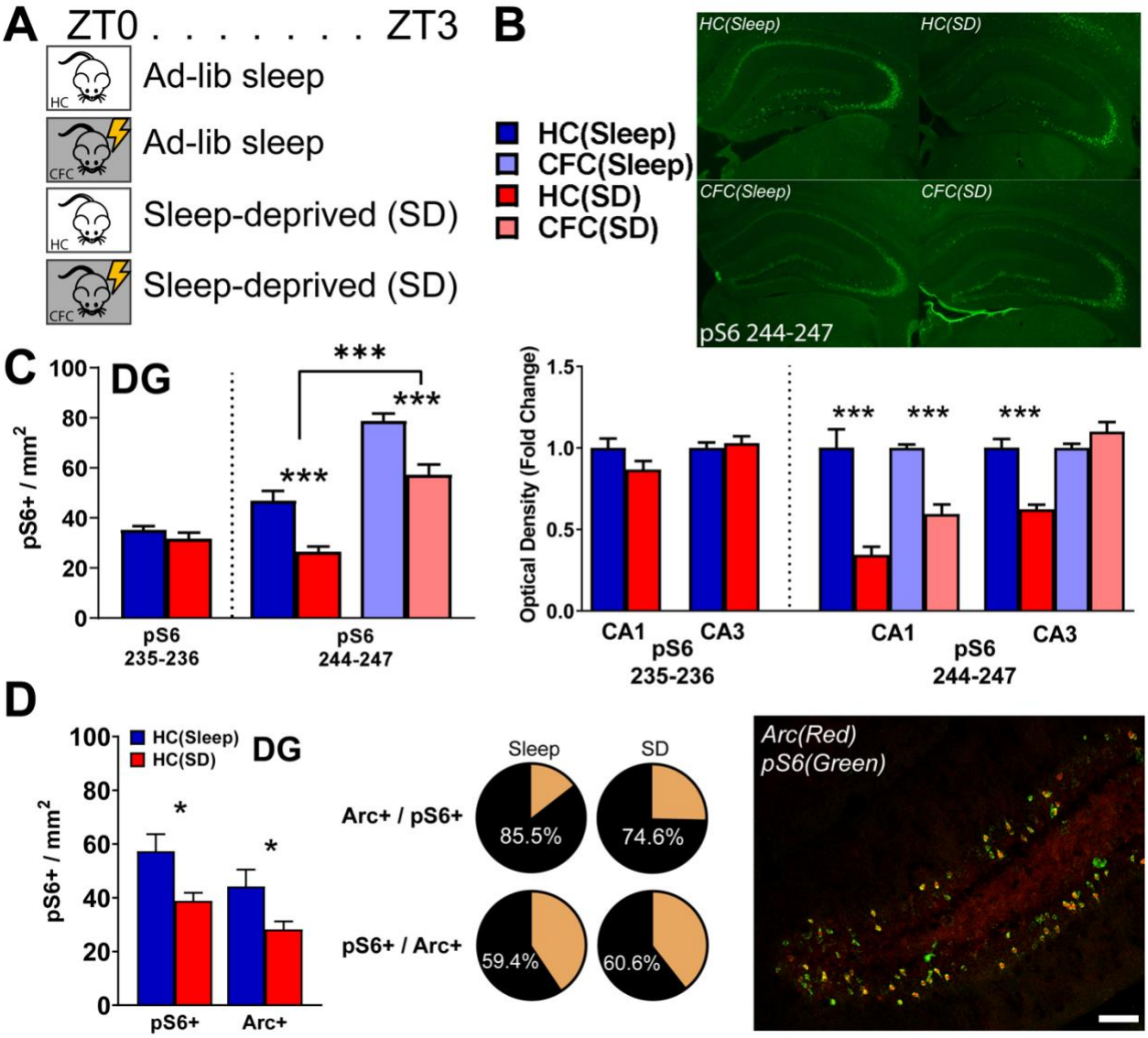


**Figure 4.1 Hippocampal S6 phosphorylation increases after learning and is reduced by sleep deprivation (SD).** ***A)*** Experimental paradigm. Mice underwent single-trial contextual fear conditioning (CFC) at ZT0, or were left in their home cage (HC). Over the next 3 h, mice in CFC and HC groups were then permitted *ad lib* sleep (Sleep) or were sleep-deprived (SD) by gentle handling. ***B)*** Fluorescent images of pS6 (S244-247) staining in the hippocampus in HC + Sleep and HC + SD mice. ***C) Left:*** pS6+ neurons in DG were counted with S6 phosphorylation at either S235-236 or S244-247 sites. SD selectively reduced S244-247 pS6+ neurons in both HC ($n$ = 5/group) and CFC ($n$ = 5/group) mice. CFC increased the number of pS6+ neurons (two-way ANOVA: main effect of CFC, $F = 87.09$, $p < 0.001$; main effect of SD, $F = 38.94$, $p < 0.001$; CFC × SD interaction, *N.S.*). ***Right:*** pS6 expression in pyramidal cell layers CA1/CA3 was quantified as background subtracted optical density. SD values were calculated as the fold change relative to the Sleep condition HC + Sleep or CFC + Sleep , respectively. pS6 (S244-247) OD was reduced in both CA1 ($p < 0.001$, Student's t-test) and CA3 ($p < 0.001$) after SD in HC mice. After CFC, SD reduced pS6 expression in CA1 neurons ($p < 0.001$) following SD. ***D*** pS6 and Arc colocalization in HC + Sleep and HC + SD mice ($n$ = 5/group). 3-h SD reduced both Arc+ ($p <$

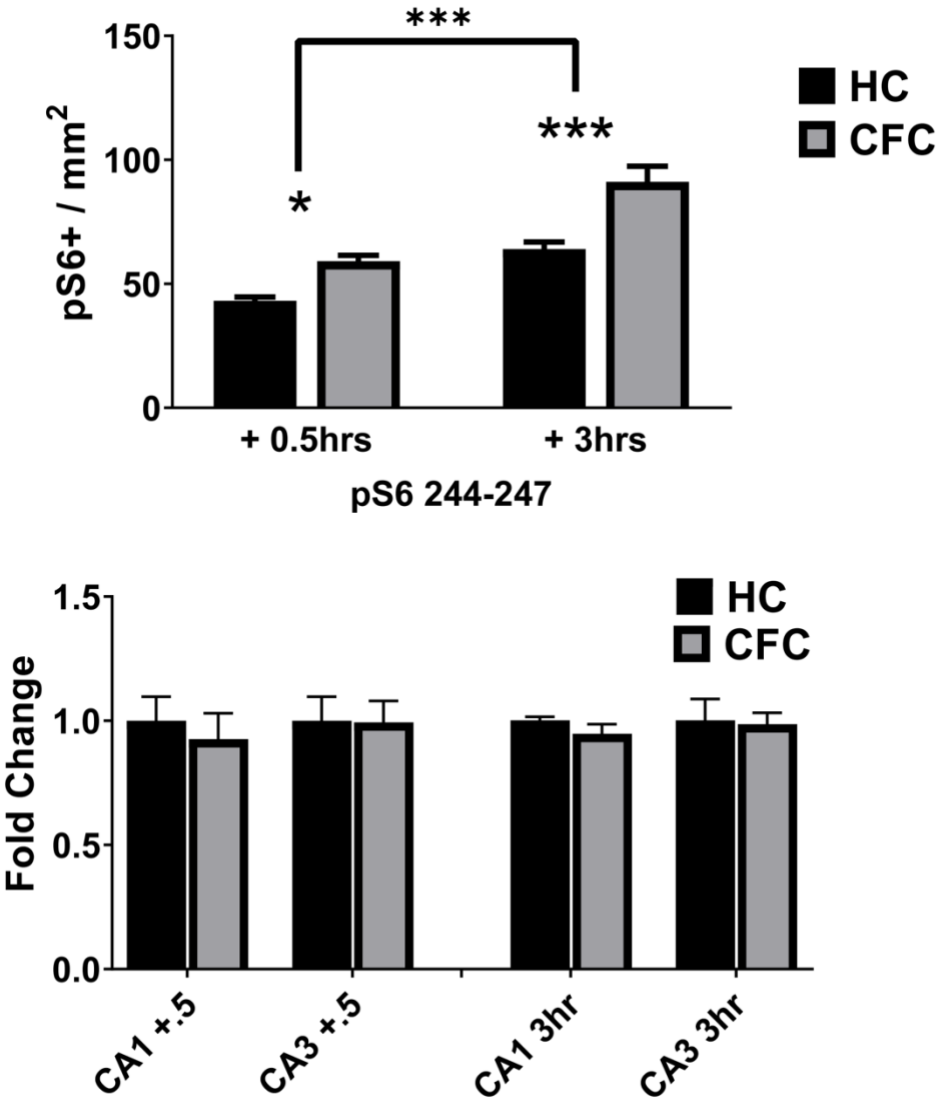


0.05, Student's t-test) and pS6+ ($p < 0.05$) neurons in DG. ~80% of Arc+ DG neurons expressed pS6+; ~60% of pS6+ neurons expressed Arc.

**Supplemental Figure 4.1 CFC-driven increases in hippocampal pS6 expression.** ***Top:*** CFC (at ZT0) increased the number of pS6+ (S244-247) DG neurons at ZT0.5 h ($p < 0.05$, Holm-Sidak *post hoc* test) and ZT3 ($p < 0.001$, Holm-Sidak *post hoc* test). Both HC and CFC mice had greater numbers of pS6+ neurons at ZT3 (two-way ANOVA: main effect of time, $F = 50.63$, $p < 0.001$; main effect of CFC, $F = 33.59$, $p < 0.001$ ; time × CFC interaction, *N.S.*), likely reflecting the effect of sleep time between the time points. ***Bottom:*** pS6 expression was unchanged by CFC in CA1 and CA3 pyramidal regions.

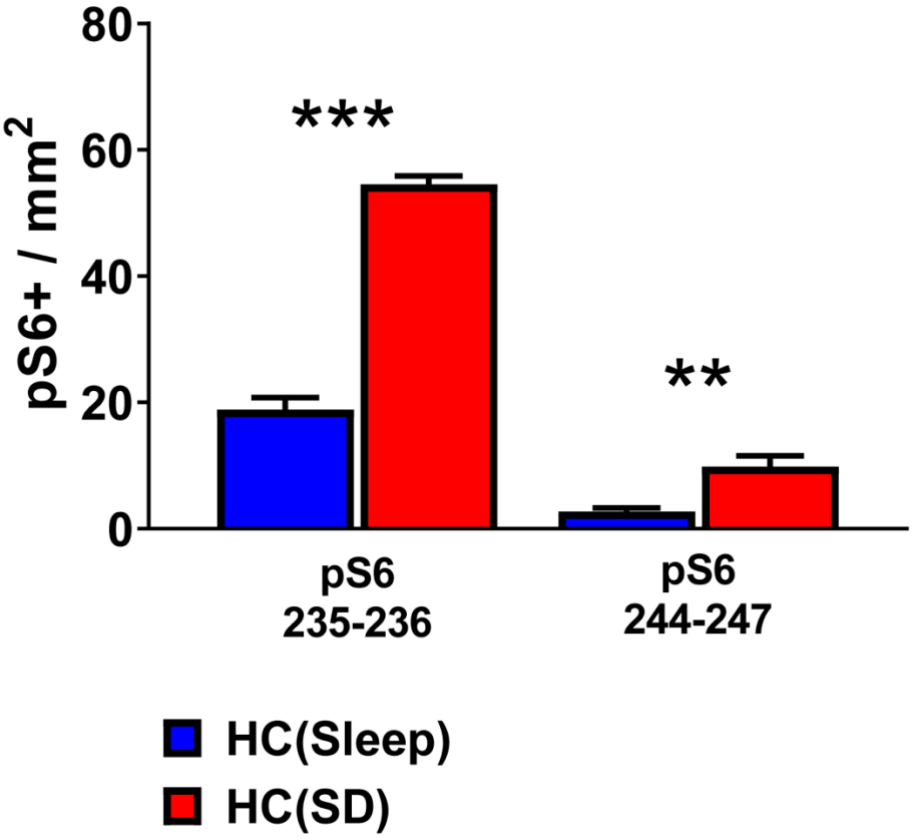


**Supplemental Figure S4.2 SD increases S6 phosphorylation in the neocortex.** pS6 (S235-236 and S244-247) expression in neocortical regions dorsal hippocampus (i.e., primary somatosensory cortex). SD increased the numbers of pS6+ neurons using antibodies targeting pS6 S235-236 ($p < 0.0001$, Student's t-test) and S244-247 ($p < 0.01$).

## 4.5 Identification of hippocampal cell types with altered S6 phosphorylation during SD

We next used an unbiased RNA-seq approach to identify cells in which pS6 expression differs between Sleep and SD. Using pS6 as an affinity tag to isolate ribosomes and associated transcripts in active cells, we performed pS6 translating ribosome affinity purification (pS6-TRAP) (Knight et al., 2012). Hippocampi were collected from CFC and HC mice after 3 h *ad lib* sleep or SD. Ribosome-associated transcripts were then isolated by pS6-TRAP for RNA-seq. To identify clusters of co-regulated transcripts in our RNA-seq data (such as might be expected for genetically-defined cell types), we used weighted gene correlation network analysis (WGCNA) (Langfelder and Horvath, 2008) on transcripts with a variance greater than 0.03 ($n$ = 1662 transcripts). WCGNA yielded 10 clusters (modules) of highly correlated transcripts in our data, and a separate (Gray) cluster representing unassigned (uncorrelated) transcripts (**Figure 4.2A**). To determine which modules' expression varied as a function of Sleep vs. SD, we correlated the level of expression of module eigengenes with the percent of time mice spent awake over the 3 h prior to sacrifice (Sleep = 25.6 ± 2.2%, SD = 100 ± 0.0% [mean ± SEM]). Results from the analysis revealed two significantly correlated eigengene clusters (Brown, Magenta) whose expression negatively correlated with sleep time (**Figure 4.2A**). Since these represented sub-clusters of the same module, we combined them for further analysis (Brown/Magenta cluster).

Since our data suggested that the population of pS6+ neurons in the hippocampus may differ in freely-sleeping and SD mice (**Figure 4.1**), we used cell type-specific expression analysis (CSEA) (Xu et al., 2014) to quantify cell type-specifying transcripts

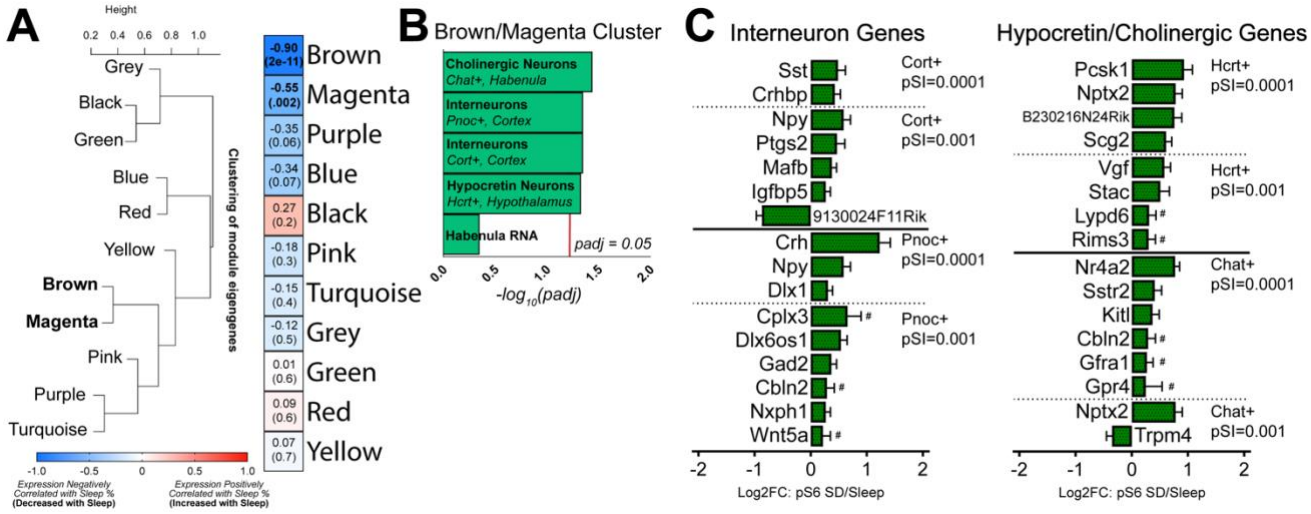


**Figure 4.2 Phosphorylated ribosome capture following SD enriches transcripts specific to GABAergic, cholinergic, and orexinergic neurons.** ***A) Left:*** Weighted gene co-expression analysis (WGCNA) identified modules of similarly correlated pS6 transcripts. Each module is identified with a color name, Grey represents transcripts not assigned to a co-expression module. ***Right****:* Correlation between eigengene expression in each module and total sleep time prior to sacrifice (*R*- and *p*-values for Pearson correlation in parentheses for each module). ***B)*** Transcripts in the Brown/Magenta module with expression correlated to sleep time were used for cell type-specific expression analysis (CSEA). The Brown/Magenta transcripts showed significant overlap with mRNAs enriched most selectively ($p$SI < 0.0001) in cholinergic (Epi.ChAT, $p_{adj}$ = 0.036), orexinergic (Hyp.Hcrt, $p_{adj}$ = 0.047), and GABAergic (Ctx.Pnoc, $p_{adj}$ = 0.045; Ctx.Cort, $p_{adj}$ = 0.045) neuron populations. ***C)*** Deseq2 $Log_2FC$ (SD/Sleep) values from Brown/Magenta transcripts identified by CSEA. All genes are statistically significant ($p_{adj}$ < 0.1) unless otherwise indicated (# indicates $p_{adj}$ > 0.1).

represented in the Brown/Magenta cluster, which were significantly affected by SD. CSEA was used to generate a $p_{adj}$ value for overlap between transcripts in Brown/Magenta cluster and known cell type-specific enriched transcripts of a particular specificity index *p* value (*p*SI) (based on a multiple comparisons-corrected Fisher's exact test). Using the most stringent CSEA (*p*SI < 0.0001), we identified Brown/Magenta cluster transcripts as mRNAs expressed most selectively in cholinergic (Chat+) neurons ($p_{adj}$ = 0.036), orexinergic (Hcrt+) neurons ($p_{adj}$ = 0.047), and Pnoc+ and Cort+ interneurons ($p_{adj}$ = 0.045) (**Figure 4.2B,C**). This suggests that after SD, pS6 is associated with more transcripts from hippocampal neurons similar to these neuron types, despite the fact that overall pS6 expression is reduced after SD. The former likely reflects transcripts present in orexinergic inputs to the hippocampus from lateral hypothalamus and cholinergic input from the medial septum, respectively - both of which are more active during active wake vs. sleep (Kiyashchenko et al., 2002; Teles-Grilo Ruivo et al., 2017). With respect to the latter finding, overlap between the Brown/Magenta cluster and transcripts expressed selectively in Cort+ and Pnoc+ interneurons (Doyle et al., 2008; Taniguchi et al., 2011) included transcripts encoding interneuron-specific transcription factors (*Dlx1*) and secreted neuropeptides somatostatin (*Sst*), neuropeptide Y (*Npy*), and corticotrophin-releasing hormone (*Crh*).

## 4.6 Hippocampal somatostatin interneurons and cholinergic inputs show increased activity during brief SD

SST and NPY neuropeptides are co-expressed in dendritic-targeting interneurons in DG, CA3, and CA1, which play a role in gating neighboring neuronal activity (Kosaka et al., 1998; Pelkey et al., 2017; Stefanelli et al., 2016). To confirm enrichment of *Sst,*

*Npy,* and other CSEA-identified transcripts in the pS6+ cell population after SD, we carried out a second experiment in which CFC and HC mice either were allowed 5 h of *ad lib* sleep or underwent 5-h SD. pS6-TRAP was followed by quantitative PCR (qPCR) to measure cell type-specific transcripts from the hippocampus. We found that independent of prior training (CFC or HC), SD caused similar enrichment for transcripts present in GABAergic neurons in pS6-TRAP. While *Gad67* and *Pvalb* transcripts were only moderately increased following 5-h SD, *Sst* and *Npy* showed large increases (**Figure 4.3A**). SD also increased *Cht* expression in both CFC and HC mice. These data support our unbiased CSEA-based finding of increased abundance of SST-expressing (SST+) interneuron and cholinergic neuron markers in the SD pS6+ population.

Because these data suggest that despite reduced total activation of hippocampal neurons during SD, SST+ interneurons in the hippocampus are more activated, we next quantified expression of activity markers in SST+ interneurons directly. We used TRAP to isolate mRNAs associated with translating ribosomes in this cell population using *SST-IRES-CRE* transgenic mice expressing hemagglutinin (HA)-tagged Rpl-22 (RiboTag) in a Cre-dependent manner (Sanz et al., 2019). Ribosome-associated transcripts from the hippocampus of these mice, isolated following a 3-h period of sleep or SD, were quantified with qPCR. We first verified enrichment of cell type-specific (i.e., SST+ interneuron-specific) mRNAs, by comparing transcript levels from TRAP vs. Input (whole hippocampus) mRNA. SST TRAP significantly de-enriched glial (G*fap, Mbp*) and excitatory neuron (*Vlugt1*, *Vglut2*) selective transcripts, and significantly enriched for SST+ interneuron-expressed transcripts *Gad1, Vgat, Sst, Npy, and Crhbp* (**Figure 4.3B**). We then tested whether 3-h SD increased the expression of activity-regulated transcripts

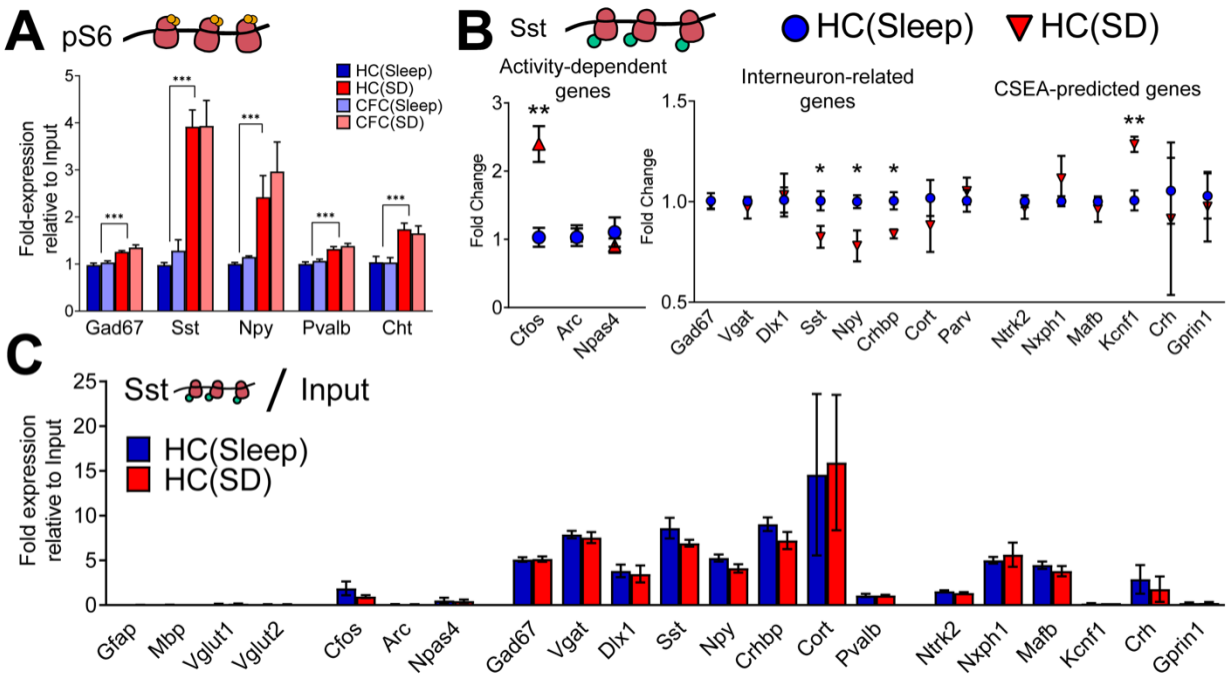


**Figure 4.3 SD increases activity in SST+ interneurons.** ***A)*** qPCR data for pS6-associated transcripts from CFC (*n* = 6/group) or HC (*n* = 5/group) mice with 5 h subsequent *ad lib* sleep or SD (two-way ANOVA: main effect of SD, $p < 0.001$; main effect of CFC, *N.S.*; CFC × SD interaction, *N.S.*). ***B)*** Expression of cell type-specific markers in mRNA from SST-TRAP vs. Input. SST de-enriched transcripts expressed in glial cells, and preferentially enriched transcripts expressed in SST (GABAergic) interneurons. These enrichment values did not differ between HC+ Sleep (*n* = 5) and HC + SD (*n* = 4) mice. ***C)*** Changes in expression of activity-regulated, interneuron-specific , and CSEA-predicted transcripts associated with SST+ ribosomes following 3-h of ad lib sleep or SD. Sleep vs. SD, ***, **, and * indicate $p < 0.001$, $p < 0.01$, and $p < 0.05$, respectively, Student's t-test.

in SST+ interneurons, and found that *Cfos* (but not *Npas4* or *Arc*), was significantly elevated at SST+ interneurons' ribosomes after SD (**Figure 4.3C**). We also tested whether SD-driven increases in *Sst*, *Npy*, and *Crhbp* in pS6+ TRAP were due to increased expression levels within SST+ interneurons. Using qPCR for these neuropeptide transcripts in mRNA isolated using SST TRAP pulldown, we found that following 3-h SD, *Sst*, *Npy*, and *Crhbp* transcripts were all *less abundant*, rather than more abundant (**Figure 4.3C**). The same change was not present in Input (whole hippocampus) mRNA, where expression of *Sst, Npy,* and *Crhbp* mRNAs were all unchanged by SD (**Figure S4.3**). We also used qPCR to quantify expression of other cell type-specific transcripts identified in pS6+ TRAP by WCGNA/CSEA. Of the transcripts tested, we found that SD increased expression of *Kcnf1*, encoding the voltage-gated potassium channel subunit Kv2.1 in SST+ interneurons (**Figure 4.3C**). Critically, greater expression of *Kcnf1* is correlated with reduced action potential threshold and increased neuronal firing rate (Bomkamp et al., 2019). Taken together, these data support the conclusion that SD-induced increases in *Sst*, *Npy*, and *Crhbp* transcripts in pS6-TRAP reflect increases in the activity, and thus pS6 expression, within SST+ interneurons.

To further validate increases in SST+ interneuron activity after SD, we examined SD-driven changes in pS6 expression in SST+ and parvalbumin-expressing (PV+) interneurons in the dorsal hippocampus using immunohistochemistry (**Figure 4.4A**). As observed previously (**Figure 4.1**), 3-h SD reduced the total number pS6+ neurons in the DG (**Figure 4.4B**). However, at the same time, 3-h SD increased pS6 expression among SST+ interneurons in the DG, and showed a strong trend for increased expression in CA3 SST+ interneurons (**Figure 4.4C**). Overall numbers of SST+ interneurons were similar

between Sleep and SD mice, and consistent with qPCR results from SST TRAP, the intensity of SST staining among SST+ interneurons was decreased after SD (**Figure S4.4**).

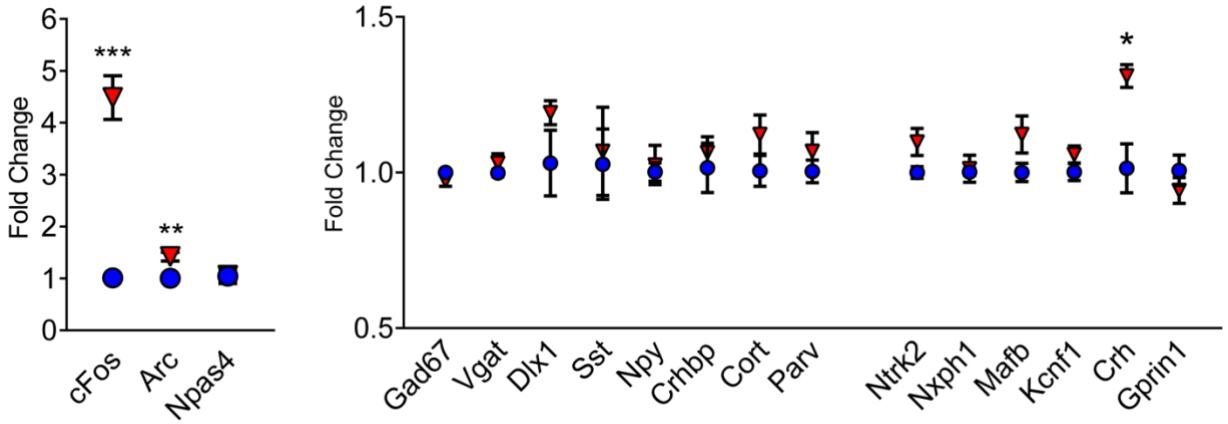


**Supplemental Figure 4.3 Whole hippocampus gene expression following 3 h SD or ad lib sleep.** qPCR data for activity-dependent, GABAergic, and CSEA-predicted transcripts in whole hippocampus (Input) following 3h of SD ($n$ = 4) or Sleep ($n$ = 5). Sleep vs SD, ***, **, and * indicated $p < 0.001$, $p < 0.01$, and $p < 0.05$, respectively, Student's t-test.

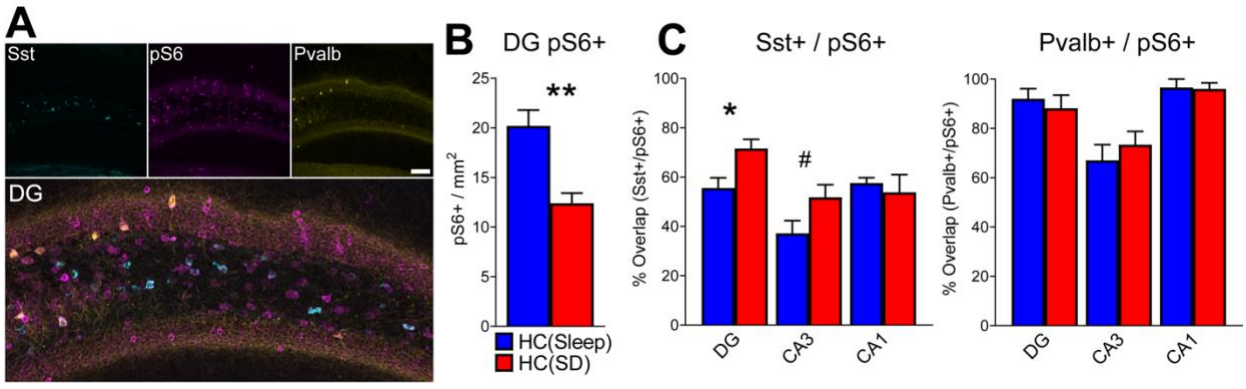


**Figure 4.4 DG SST+ interneurons show increased pS6 expression following SD.** ***A)*** Representative images showing expression of SST, PV, and pS6 in DG (scale bar = 100 μm). ***B)*** DG pS6+ neurons decreased following 3-h SD ($p < 0.01$, Student's t-test, $n = 5$ mice/group) ***C)*** pS6 colocalization in SST+ and PV+ DG interneurons was compared for HC mice after 3-h SD or *ad lib* sleep. SD elevated pS6 expression in SST interneurons in the DG hilus ($p < 0.05$, Student's t-test) and trended in CA3 ($p < 0.1$). pS6 expression in PV+ interneurons was unaffected by SD. Sleep vs SD, ***, **, * , and # indicated $p < 0.001$, $p < 0.01$, $p < 0.05$, and $p < 0.1$ respectively, Student's t-test.

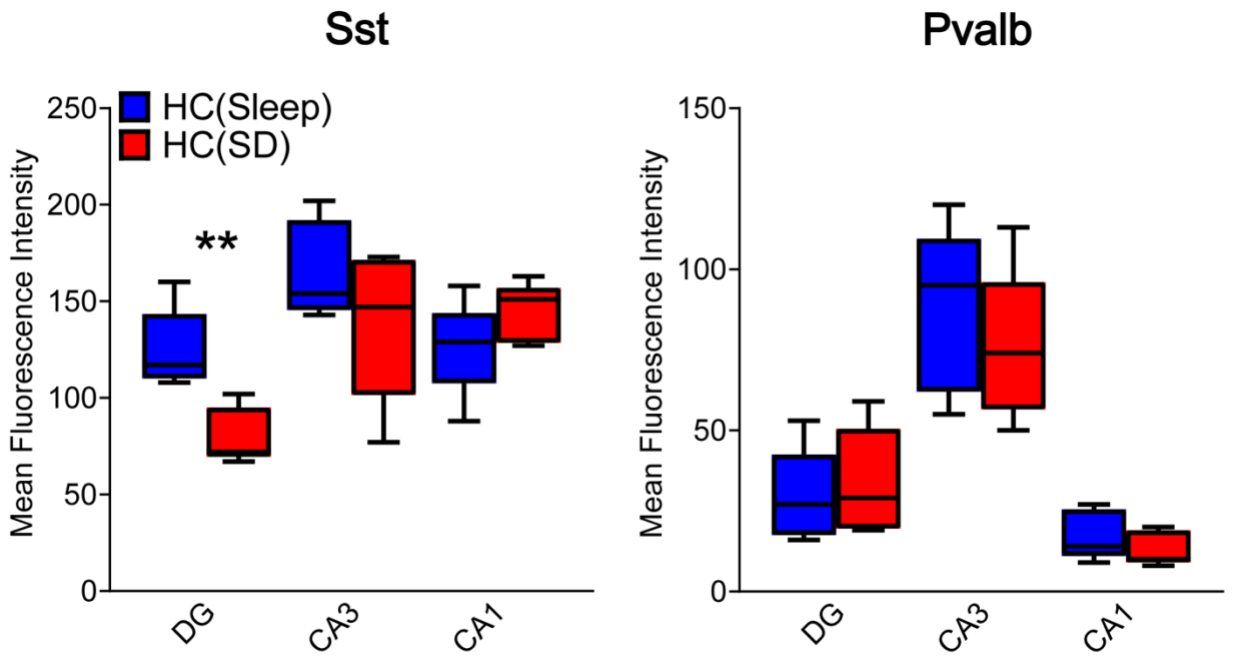


**Supplemental Figure 4.4 Mean fluorescence intensity values for somatostatin (SST) and paravalbumin (PV).** Mean fluorescence intensity values for SST and PV following 3 h of *ad lib* sleep ($n$ = 5) or SD ($n$ = 5). 3 h SD reduced SST staining intensity in DG neurons (Student's t-test, $p < 0.01$). Values listed indicate the average number (and intensity) of SST+ or PV+ neurons counted per region.

## 4.7 Mimicking SD-driven increases in SST+ interneuron activity in the hippocampus disrupts sleep-dependent memory consolidation

Because the SD-associated increase in SST+ interneuron activity has the potential to profoundly suppress surrounding hippocampal network activity (Raza et al., 2017; Stefanelli et al., 2016), we next tested how this process affects sleep-dependent memory consolidation. To test this, we transduced the dorsal hippocampus of *SST-IRES-CRE* mice with an AAV vector to express either the activating DREADD hM3Dq-mCherry or mCherry alone in a Cre-dependent manner (**Figure 4.5A**). To test how activating SST+ interneurons affects memory consolidation, hM3Dq-mCherry- and mCherry-expressing mice ($n$ = 5 and 4, respectively) underwent single-trial CFC at lights on, after which they were immediately injected with clozapine-N-oxide (CNO; 3 mg/kg), and returned to their home cage for *ad lib* sleep. 24 h later, at lights on, mice were returned to the CFC context to assess CFM. Mice expressing hM3Dq showed significant decreases in context-specific freezing compared to mCherry-expressing control mice ($p$ < 0.001, Student's t-test). (**Figure 4.5B**). To confirm effects of CNO administration on SST+ interneuron and surrounding neuronal activity, hM3Dq- and mCherry-expressing mice were injected with CNO at lights on and allowed 3 h *ad lib* sleep in their home cage prior to sacrifice. hM3Dq-mCherry-expressing DG neurons showed a significantly higher level of cFos expression at this time point (hM3Dq: 68.0 ± 15.9% vs. mCherry: 2.0 ± 1.4%; $p$ < 0.01 Student's t-test) **(Figure 4.5C)**. To assess effects of CNO on SST+ interneuron-mediated inhibition in the DG, we quantified cFos expression in surrounding non-transduced neurons. hM3Dq expression significantly reduced numbers of cFos+ neurons in the surrounding DG relative to mCherry-expressing control mice ($p$ < .05, Student's t-test) **(Figure 4.5C)**.

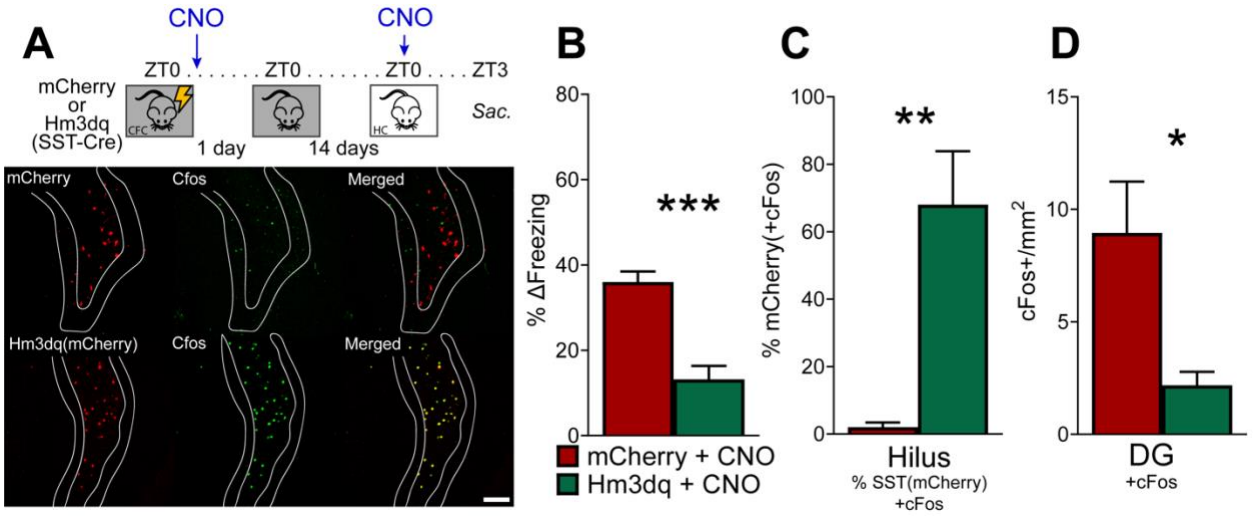


**Figure 4.5 Mimicking SD effects on activity in SST+ interneurons impairs sleep-dependent memory consolidation.** ***A) Top:*** Experimental design: *SST-IRES-CRE* mice expressing either mCherry (*n* = 4) or hM3Dq-mCherry (*n* = 5) in dorsal hippocampus underwent single-trial CFC at lights on, and then were immediately administered CNO (0.3 mg/kg, i.p.) and allowed *ad lib* sleep in their home cage. 24 h later, all mice were returned to the CFC context for assessment of contextual fear memory (CFM). Two-weeks following CFM tests, mice were again injected with CNO at lights on and allowed 3 h *ad lib* sleep prior to sacrifice for immunohistochemistry. ***Bottom:*** Confocal images of mCherry and cFos expression in the DG granule cell layer (white outlines) and hilar SST+ interneurons. ***B)*** hM3Dq- expressing mice showed significant reductions in CFM (measured as % time freezing, compared with mCherry control mice ($p < 0.001$, Student's t-test). ***C)*** Expression of cFos in mCherry+ SST interneurons was significantly higher in the hilus of hM3Dq-expressing mice than in mCherry control mice ($p < 0.01$, Student's t-test). **D)** Expression of Cfos+ in surrounding DG neurons was reduced in hM3Dq-expressing mice ($p < 0.05$, Student's t-test).

Together, these data show that sleep-dependent consolidation of CFM can be disrupted via activation of SST+ interneurons, which have strong inhibitory effects on the surrounding hippocampal network.

## 4.8 Reducing cholinergic input to hippocampus improves sleep-dependent memory consolidation and increases hippocampal pS6 expression

Cholinergic input from MS selectively increases activity and structural plasticity in SST+ interneurons, via muscarinic receptor activation (Gais and Born, 2004; Hajos et al., 1998; Lovett-Barron et al., 2014; Rasch et al., 2006; Raza et al., 2017; Schmid et al., 2016). Because acetylcholine release in the hippocampus is higher overall during wake vs. sleep (Teles-Grilo Ruivo et al., 2017), a reasonable assumption is that this drives higher SST+ interneuron activity during SD. We tested whether altering medial septum (MS) cholinergic input to the hippocampus following CFC affected CFM consolidation. To do this, we transduced the MS of *Chat-CRE* mice with an AAV vector to express the inhibitory DREADD hM4Di in a Cre-dependent manner. Immunohistochemistry confirmed hM4Di-mCherry labeling of ChAT+ terminals in the DG **(Figure 4.6A**), consistent with previous reports (Raza et al., 2017). Transduced mice underwent single-trial CFC at lights on, after which they were immediately injected with either CNO or vehicle (VEH) ($n$ = 10 mice/group), and were returned to their home cages for *ad lib* sleep. 24 h later, at lights on, mice were returned to the CFC context to assess CFM. Mice administered CNO showed significant increases in context-specific freezing compared to vehicle-treated mice ($p < 0.05$, Student's t-test) (**Figure 4.6B**). To characterize the effects of reduced MS cholinergic input on network activity in the hippocampus, hM4Di-expressing mice were

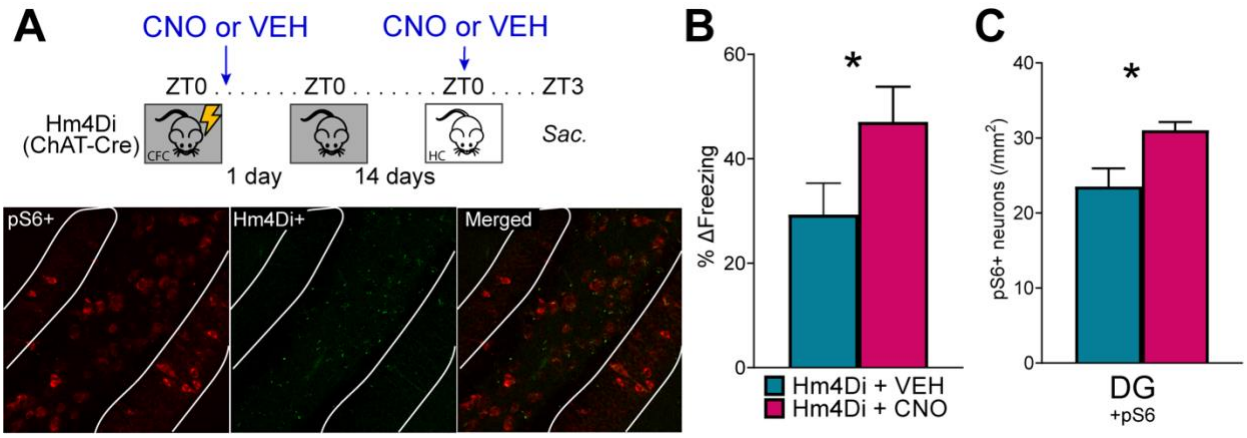


**Figure 4.6 Reduced cholinergic input to the hippocampus increases DG network activity and improves sleep-associated memory consolidation.** ***A) Top:*** Experimental design: *Chat-CRE* mice expressing hM4Di-expressing mice underwent single-trial CFC at lights on, after which they were immediately administered CNO (0.3 mg/kg, i.p.) or vehicle (VEH) (*n* = 10/group), and allowed *ad lib* sleep in their home cage. 24 h later, mice were returned to the CFC context for a CFM test. Two weeks later, at lights on, mice again received CNO or VEH (*n* = 5/group) and were allowed 3 h *ad lib* sleep prior to sacrifice. ***Bottom:*** Representative images of transgene expressing cholinergic terminals in DG and pS6+ expression in the DG granule cell layer (GCL, white lines) and hilus. ***B)*** CFM performance 24 h post-CFC was better in CNO-treated, relative to VEH-treated mice (*p*-value < 0.05, Student's t-test). ***C)*** CNO-treated mice had higher numbers of pS6+ DG neurons after 3 h of *ad lib* sleep (*p*-value < 0.05, Student's t-test).

treated with CNO or VEH at lights on, and allowed 3 h *ad lib* sleep. Inhibition of cholinergic MS neurons in CNO-treated mice increased numbers of pS6+ neurons in DG relative to VEH-injected mice ($n$ = 5 mice/group, $p < 0.05$, Student's t-test) (**Figure 4.6C**). These data suggest that MS cholinergic input to the hippocampus may mediate the state-dependent gating of hippocampal network activity in the same way that somatostatin does, thus acting a brake on memory consolidation mechanism.

## 4.9 Discussion

Here we present converging lines of evidence that indicate SD disrupts activity in the dorsal hippocampus, and disrupts memory consolidation, via a SST+ interneuron-mediated inhibitory gate. First, we find that, similar to *Arc* mRNA and Arc protein (Delorme et al., 2019), activity-dependent expression of pS6 in dorsal hippocampus increases across a brief period of sleep (**Figure S4.1**), but is reduced by a period of SD (**Figure 4.1**). This effect of SD is enhanced by prior learning (**Figure 4.1**, **Figure S4.1**), and seems to occur selectively in the hippocampus - it is not seen in the neocortex (**Figure S4.2**). We find that under SD conditions, pS6 expression in SST+ interneurons (but not other cell types) is increased, rather than decreased (**Figure 4.4**). Using pS6 itself as an affinity tag, we took an unbiased TRAP-seq approach to characterize cell types active in the hippocampus during sleep vs. SD. We found that transcripts upregulated on pS6+ ribosomes after SD included those with expression unique to specific interneuron subtypes (*e.g*., *Sst*, *Npy*, and *Crhbp*), and markers of cholinergic and orexinergic neurons (*e.g*., *Cht*) (**Figure 4.2**, **Figure 4.3**). Hippocampal SST+ interneurons are enriched in the same interneuron-specific markers identified as increasing in abundance after SD with

pS6 TRAP-seq (**Figure 4.3B**). SD-driven changes in their expression appear to be caused by greater activity in these neurons as a function of SD (**Figure 4.3, Figure S4.3**).

Previous reports have shown that SST+ interneurons gate DG network activity during memory acquisition, and that their activation likewise gates initial learning (Raza et al., 2017; Stefanelli et al., 2016). Considering we observe fewer activated DG neurons expressing either Arc or pS6 after SD (**Figure 4.1**), one possibility is that by driving higher firing activity in SST+ interneurons, SD may disrupt memory consolidation by acting as an inhibitory gate – i.e., limiting activity in the surrounding network. Within the hippocampus, SST+ interneurons target both neighboring pyramidal cells and other interneuron types (such as PV+ interneurons) for inhibition (Bloss et al., 2016; Harris et al., 2018; Katona et al., 1999; Katona et al., 2014; Pelkey et al., 2017; Somogyi et al., 2013). Our present data demonstrate that activation of SST+ interneurons is sufficient to disrupt activity-regulated gene expression in neighboring neurons, and CFM consolidation (**Figure 4.5**). Because selective activation of SST+ interneurons in the hippocampus is characteristic of SD, we conclude that this mechanism may explain the sleep-dependence of CFM consolidation (Graves et al., 2003; Ognjanovski et al., 2018; Vecsey et al., 2009). It may also explain other effects of SD on the dorsal hippocampal network, including disruption of long-term potentiation (LTP) (Havekes et al., 2016; Vecsey et al., 2009), reduction of plasticity-associated gene expression (Delorme et al., 2019), and decreases in dendritic spine density on pyramidal neurons (Havekes et al., 2016; Raven et al., 2019). CFM consolidation itself relies on intact network activity in dorsal hippocampus (Daumas et al., 2005), and is associated with increased network activity in structures such as CA1 (Ognjanovski et al., 2018; Ognjanovski et al., 2014),

and regularization of spike-timing relationships during post-CFC sleep (Ognjanovski et al., 2018; Ognjanovski et al., 2014; Ognjanovski et al., 2017). Thus disruption of network activation via activation of an inhibitory circuit element during SD is likely to interfere with consolidation mechanisms. Critically, SST+ interneurons may act as a gate on the hippocampal network, inhibiting sharp-wave ripple oscillations (Katona et al., 2014; Klausberger and Somogyi, 2008) and hippocampal-cortical communication (Abbas et al., 2018; Haam et al., 2018). Both of these features correlate with sleep-dependent consolidation of CFM (Ognjanovski et al., 2017; Xia et al., 2017).

Increased representation of cholinergic and orexinergic cell type-specific transcripts with SD using pS6-TRAP (**Figure 4.2**) is consistent with increased activity in lateral hypothalamic (orexinergic) and MS (cholinergic) inputs to dorsal hippocampus during wake (Kiyashchenko et al., 2002; Teles-Grilo Ruivo et al., 2017). Does activation of cholinergic or orexinergic inputs to the hippocampus likewise contribute to disruption of CFM consolidation? And do these modulators drive selective activation of hippocampal SST+ interneurons during SD?

Behavioral data from both human subjects (Gais and Born, 2004; Rasch et al., 2006) and animal models (Inayat et al., 2020) demonstrate that reduced acetylcholine signaling is essential for the benefits of sleep for memory consolidation (Gais and Born, 2004; Rasch et al., 2006; Schmid et al., 2016). Our present data (**Figure 4.6**) are consistent with reductions in MS cholinergic input to the hippocampus being vital for sleep-dependent CFM consolidation. Available data suggest that these effects could be mediated by cholinergic regulation of SST+ interneurons. Our present data demonstrate that pS6 expression in the hippocampus is augmented when MS cholinergic input is

reduced (**Figure 4.6**), consistent with disinhibition. Others have found that stimulation of septohippocampal cholinergic neurons causes GABAergic inhibition of DG granule cells, mediated by cholinergic receptors on hilar (SST- and NPY-expressing) interneurons (Pabst et al., 2016). In contrast, while less is known about the role of orexinergic signaling in memory consolidation, available data suggests that orexin can promote, rather than inhibit, consolidation (Mavanji et al., 2017). Moreover, orexinergic input to the hippocampus appears to activate glutamatergic neurons to a greater extent that GABAergic neurons (Stanley and Fadel, 2011).

An outstanding question is whether SD-associated, selective activation of SST+ interneurons is driven mainly by network interactions (e.g., input from MS cholinergic interneurons) or cell-autonomous mechanisms (e.g. cell-type specific changes in expression of proteins that alter intrinsic excitability and neuronal firing). Our present data do not discriminate between these two mechanisms, but provide circumstantial evidence of both (**Figure 4.3** and **Figure 4.6**, respectively). A second outstanding question is whether these mechanisms are unique to the hippocampus, or whether similar selective activation of SST+ interneurons is associated with SD in other structures, such as the neocortex. Recent findings from calcium imaging studies of mouse neocortex have demonstrated higher activity of SST+ interneurons in superficial cortical layers during wake vs. NREM sleep (Niethard et al., 2017; Niethard et al., 2016). This effect (which would lead to reductions in dendrite-targeted inhibition during sleep) may be related to the recent finding of dendritic calcium spikes in these cortical layers during NREM oscillations (Seibt et al., 2017). Critically, activation of SST+ interneurons in neocortex during active wake is driven by cholinergic signaling (Munoz et al., 2017). While this

mechanism serves effective circuit-level information processing during brief periods of arousal, one possibility is that extended wake may act as a gate, preventing information processing altogether - as we see evidence for here. Together, these findings suggest that a similar mechanism may underlie SD-induced disruption of memory consolidation mechanisms outside of the hippocampus (Puentes-Mestril and Aton, 2017), as well. Prior work has identified a number of intracellular pathways as being critical targets for SD-mediated disruption of memory in the hippocampus (Havekes et al., 2016; Tudor et al., 2016; Vecsey et al., 2009) and neocortex (Aton et al., 2009a; Dumoulin et al., 2015; Seibt et al., 2012). Our present data indicate that microcircuit regulation of brain activity is another SD-driven mechanism underlying the disruption of memory consolidation by sleep loss.

## 4.10 References


Abbas, A.I., Sundiang, M.J.M., Henoch, B., Morton, M.P., Bolkan, S.S., Park, A.J., Harris, A.Z., Kellendonk, C., and Gordon, J.A. (2018). Somatostatin Interneurons Facilitate Hippocampal-Prefrontal Synchrony and Prefrontal Spatial Encoding Neuron *100*, 926-939.

Abel, T., Havekes, R., Salatin, J.M., and Walker, M.P. (2013). Sleep, Plasticity and Memory from Molecules to Whole-Brain Networks. Curr Biol *23*, R774-788.

Andersen, C.L., Jensen, J.L., and Orntoft, T.F. (2004). Normalization of Real-Time Quantitative Reverse Transcription-PCR Data: A Model-Based Variance Estimation Approach to Identify Genes Suited for Normalization, Applied to Bladder and Colon Cancer Data Sets. Cancer Research *64*, 5245-5250.

Aton, S.J., Seibt, J., Dumoulin, M., Jha, S.K., Steinmetz, N., Coleman, T., Naidoo, N., and Frank, M.G. (2009a). Mechanisms of sleep-dependent consolidation of cortical plasticity. Neuron *61*, 454-466.

Aton, S.J., Seibt, J., and Frank , M.G. (2009b). Sleep and memory. In Encyclopedia of Life Science (Chichester: John Wiley and Sons, Ltd.).

Bloss, E.B., Cembrowski, M.S., Karsh, B., Colonell, J., Fetter, R.D., and Spruston, N. (2016). Structured Dendritic Inhibition Supports Branch-Selective Integration in CA1 Pyramidal Cells. Neuron *89*, 1016-1030.

Bomkamp, C., Tripathy, S.J., Bengtsson Gonzalez, C., Hjerling-Leffler, J., Craig, A.M., and Pavlidis, P. (2019). Transcriptomic correlates of electrophysiological and morphological diversity within and across excitatory and inhibitory neuron classes. PLoS Computational Biology *15*.

Daumas, S., Halley, H., Frances, B., and Lassalle, J.M. (2005). Encoding, consolidation, and retrieval of contextual memory: differential involvement of dorsal CA3 and CA1 hippocampal subregions. Learn Mem *12*, 375-382.

Delorme, J.E., Kodoth, V., and Aton, S.J. (2019). Sleep loss disrupts Arc expression in dentate gyrus neurons. Neurobiol Learn Mem *160*, 73-82.

Doyle, J.P., Dougherty, J.D., Heiman, M., Schmidt, E.F., Stevens, T.R., Ma, G., Bupp, S., Shrestha, P., Shah, R.D., Doughty, M.L.*, et al.* (2008). Application of a Translational Profiling Approach for the Comparative Analysis of CNS Cell Types. Cell *135*, 749-762.

Dumoulin, M.C., Aton, S.J., Watson, A.J., Renouard, L., Coleman, T., and Frank, M.G. (2015). Extracellular Signal-Regulated Kinase (ERK) Activity During Sleep Consolidates Cortical Plasticity In Vivo. Cereb Cortex *25*, 507-515.

Durkin, J., Suresh, A.K., Colbath, J., Broussard, C., Wu, J., Zochowski, M., and Aton, S.J. (2017). Cortically coordinated NREM thalamocortical oscillations play an essential, instructive role in visual system plasticity. Proceedings National Academy of Sciences *114*, 10485-10490.

Gais, S., and Born, J. (2004). Low acetylcholine during slow-wave sleep is critical for declarative memory consolidation. PNAS *101*, 2140-2144.

Graves, L.A., Heller, E.A., Pack, A.I., and Abel, T. (2003). Sleep deprivation selectively impairs memory consolidation for contextual fear conditioning. Learn Mem *10*, 168-176.

Haam, J., Zhou, J., Cui, G., and Yakel, J.L. (2018). Septal cholinergic neurons gate hippocampal output to entorhinal cortex via oriens lacunosum moleculare interneurons. Proc Natl Acad Sci USA *115*, E1886-1895.

Hajos, N., E.C., P., Acsady, L., Levey, A.I., and Freund, T.F. (1998). Distinct Interneuron Types Express m2 Muscarinic Receptor Immunoreactivity on Their Dendrites or Axon Terminals in the Hippocampus Neuroscience *82*, 355-376.

Harris, K.D., Hochgerner, H., Skene, N.G., Magno, L., Katona, L., Bengtsson Gonzales, C., Somogyi, P., Kessaris, N., Linnarsson, S., and Hjerling-Leffler, J. (2018).

Classes and continua of hippocampal CA1 inhibitory neurons revealed by single-cell transcriptomics. PLoS Biology *16*, e2006387.

Havekes, R., and Abel, T. (2017). The tired hippocampus: the molecular impact of sleep deprivation on hippocampal function. Curr Opin Neurobiol *44*, 13-19.

Havekes, R., Park, A.J., Tudor, J.C., Luczak, V.G., Hansen, R.T., Ferri, S.L., Bruinenberg, V.M., Poplawski, S.G., Day, J.P., Aton, S.J.*, et al.* (2016). Sleep deprivation causes memory deficits by negatively impacting neuronal connectivity in hippocampal area CA1. eLife *5*, pii: e13424.

Inayat, S., Qandeel, Nasariahangarkoaee, M., Singh, S., McNaughton, B.L., Whishaw, I.Q., and Mohajerani, M.H. (2020). Low acetylcholine during early sleep is important for motor memory consolidation. Sleep *43*.

Katona, I., Acsady, L., and Freund, T.F. (1999). Postsynaptic targets of somatostatin-immunoreactive interneurons in the rat hippocampus. Neuroscience *88*, 37-55.

Katona, L., Lapray, D., Viney, T.J., Oulhaj, A., Borhegyi, Z., Micklem, B.R., Klausberger, T., and Somogyi, P. (2014). Sleep and Movement Differentiates Actions of Two Types of Somatostatin-Expressing GABAergic Interneuron in Rat Hippocampus Neuron *82*, 872-886.

Kiyashchenko, L.I., Mileykovskiy, B.Y., Maidment, N., Lam, H.A., Wu, M.-F., John, J., Peever, J., and Siegel, J.M. (2002). Release of Hypocretin (Orexin) during Waking and Sleep States. JNeurosci *22*, 5282-5286.

Klausberger, T., and Somogyi, P. (2008). Neuronal Diversity and Temporal Dynamics: The Unity of Hippocampal Circuit Operations Science *321*, 53-57.

Knight, Z.A., Tan, K., Birsoy, K., Schmidt, S., Garrison, J.L., Wysocki, R.W., Emiliano, A., Ekstrand, M.I., and Friedman, J.M. (2012). Molecular profiling of activated neurons by phosphorylated ribosome capture. Cell *151*, 1126-1137.

Kosaka, T., Wu, J.-Y., and Benoit, R. (1998). GABAergic neurons containing somatostatin-like immunoreactivity in the rat hippocampus and dentate gyrus. Experimental Brain Res *71*, 388-398.

Langfelder, P., and Horvath, S. (2008). WGCNA: an R package for weighted correlation network analysis. BMC Bioinformatics *9*.

Liao, Y., Smyth, G.K., and Shi, W. (2014). featureCounts: An Efficient General Purpose Program for Assigning Sequence Reads to Genomic Features Bioinformatics *30*, 329-330.

Love, M.I., Huber, W., and Anders, S. (2014). Moderated estimation of fold change and dispersion for RNA-seq data with DESeq2. Genome Biology *15*.

Lovett-Barron, M., Kaifosh, P., Kheirbek, M.A., Danielson, N., Zaremba, J.D., Reardon, T.R., Turi, G.F., Hen, R., Zemelman, B.V., and Losonczy, A. (2014). Dendritic Inhibition in the Hippocampus Supports Fear Learning Science *343*, 857-863.

Mavanji, V., Butterick, T.A., Duffy, C.M., Nixon, J.P., Billington, C.J., and Kotz, C.M. (2017). Orexin/hypocretin treatment restores hippocampal-dependent memory in orexin-deficient mice. Neurobiol Learn Mem *146*, 21-30.

Munoz, W., Tremblay, R., Levenstein, D., and Rudy, B. (2017). Layer-specific modulation of neocortical dendritic inhibition during active wakefulness. Science *355*, 954-959.

Niethard, N., Burgalossi, A., and Born, J. (2017). Plasticity during Sleep Is Linked to Specific Regulation of Cortical Circuit Activity. Front Neural Circuits *11*.

Niethard, N., Hasegawa, M., Itokazu, T., Oyanedel, C.N., Born, J., and Sato, T.R. (2016). Sleep-Stage-Specific Regulation of Cortical Excitation and Inhibition. Curr Biol *26*, 2739-2749.

Ognjanovski, N., Broussard, C., Zochowski, M., and Aton, S.J. (2018). Hippocampal Network Oscillations Rescue Memory Consolidation Deficits Caused by Sleep Loss. Cereb Cortex *28*, 3711-3723.

Ognjanovski, N., Maruyama, D., Lashner, N., Zochowski, M., and Aton, S.J. (2014). CA1 hippocampal network activity changes during sleep-dependent memory consolidation. Front Syst Neurosci *8*, 61.

Ognjanovski, N., Schaeffer, S., Mofakham, S., Wu, J., Maruyama, D., Zochowski, M., and Aton, S.J. (2017). Parvalbumin-expressing interneurons coordinate hippocampal network dynamics required for memory consolidation. Nature Communications *8*, 15039.

Pabst, M., Braganza, O., Dannerberg, H., Hu, W., Pothmann, L., Rosen, J., Mody, I., van Loo, K., Deisseroth, K., Becker, A.J.*, et al.* (2016). Astrocyte Intermediaries of Septal Cholinergic Modulation in the Hippocampus. Neuron *90*, 853-865.

Pelkey, K.A., Chittajallu, R., Craig, M.T., Tricoire, L., Wester, J.C., and McBain, C.J. (2017). Hippocampal GABAergic Inhibitory Interneurons. Physiol Rev *97*, 1619-1747.

Pirbhoy, P.S., Farris, S., and Steward, O. (2016). Synaptic activation of ribosomal protein S6 phosphorylation occurs locally in activated dendritic domains. Learn Mem *23*, 255-269.

Prince, T.M., Wimmer, M., Choi, J., Havekes, R., Aton, S., and Abel, T. (2014). Sleep deprivation during a specific 3-hour time window post-training impairs hippocampal synaptic plasticity and memory. Neurobiol Learn Mem *109*, 122-130.

Puentes-Mestril, C., and Aton, S.J. (2017). Linking network activity to synaptic plasticity during sleep: hypotheses and recent data. Frontiers in Neural Circuits *11*, doi: 10.3389/fncir.2017.00061.

Rasch, B.H., Born, J., and Gais, S. (2006). Combined blockade of cholinergic receptors shifts the brain from stimulus encoding to memory consolidation. Journal of Cognitive Neuroscience *18*, 793-802.

Raven, F., Meerlo, P., Van der Zee, E.A., Abel, T., and Havekes, R. (2019). A brief period of sleep deprivation causes spine loss in the dentate gyrus of mice. Neurobiol Learn Mem *160*, 83-90.

Raza, S.A., Albrecht, A., Caliskan, G., Muller, B., Demiray, Y.E., Ludewig, S., Meis, S., Faber, N., Hartig, R., Schraven, B*., et al.* (2017). HIPP neurons in the dentate gyrus mediate the cholinergic modulation of background context memory salience. Nat Communications *8*.

Sanz, E., Bean, J.C., Carey, D.P., Quintana, A., and McKnight, G.S. (2019). RiboTag: Ribosomal Tagging Strategy to Analyze Cell-Type-Specific mRNA Expression In Vivo. Curr Protoc Neurosci *88*, e77.

Schmid, L.C., Mittag, M., Poll, S., Steffen, J., Wagner, J., Geis, H.-R., Schwarz, I., Schmidt, B., Schwarz, M.K., Remy, S*., et al.* (2016). Dysfunction of Somatostatin-Positive Interneurons Associated With Memory Deficits in an Alzheimer's Disease Model Neuron *92*, 114-125.

Seibt, J., Dumoulin, M., Aton, S.J., Coleman, T., Watson, A., Naidoo, N., and Frank, M.G. (2012). Protein synthesis during sleep consolidates cortical plasticity in vivo. Curr Biol *22*, 676-682.

Seibt, J., Richard, C.J., Sigl-Glockner, U., Takahashi, N., Kaplan, D.I., Doron, G., de Limoges, D., Bocklisch, C., and Larkum, M.E. (2017). Cortical dendritic activity correlates with spindle-rich oscillations during sleep in rodents. Nat Commun *8*, 1838.

Shigeoka, T., Jung, J., Holt, C.E., and Jung, H. (2018). Axon-TRAP-RiboTag: Affinity Purification of Translated mRNAs from Neuronal Axons in Mouse In Vivo. In RNA Detection (Methods in Molecular Biology) (New York: Humana Press), pp. 85-94.

Somogyi, P., Katona, L., Klausberger, T., Lasztoczi, B., and Viney, T.J. (2013). Temporal redistribution of inhibition over neuronal subcellular domains underlies state-dependent rhythmic change of excitability in the hippocampus. Philos Trans R Soc Lond B Biol Sci *369*, 20120518.

Sosa, J.M., Huber, D.E., Welk, B., and H.L., F. (2014). Development and application of MIPAR™: a novel software package for two- and three-dimensional microstructural characterization. Integrating Materials and Manufacturing Innovation *3*, 123-140.

Stanley, E.M., and Fadel, J.R. (2011). Aging-related alterations in orexin/hypocretin modulation of septo-hippocampal amino acid neurotransmission. Neuroscience *195*, 70-90.

Stefanelli, T., Bertollini, C., Luscher, C., Muller, D., and Mendez, P. (2016). Hippocampal Somatostatin Interneurons Control the Size of Neuronal Memory Ensembles. Neuron *89*, 1074-1085.

Taniguchi, H., He, M., Wu, P., Kim, S., Paik, R., Sugino, K., Kvitsani, D., Fu, Y., Lu, J., Lin, Y.*, et al.* (2011). A Resource of Cre Driver Lines for Genetic Targeting of GABAergic Neurons in Cerebral Cortex. Neuron *71*, 995-1013.

Teles-Grilo Ruivo, L.M., Baker, K.L., Conway, M.L., Isaac, J.T.R., Lowry, J.P., and Mellor, J.R. (2017). Coordinated Acetylcholine Release in PrefrontalCortex and Hippocampus Is Associated with Arousal and Reward on Distinct Timescales. Cell Reports *18*, 905-917.

Tudor, J.C., Davis, E.J., Peixoto, L., Wimmer, M.E., van Tilborg, E., Park, A.J., Poplawski, S.G., Chung, C.W., Havekes, R., Huang, J.*, et al.* (2016). Sleep deprivation impairs memory by attenuating mTORC1-dependent protein synthesis. Sci Signal *9*, ra41.

Vecsey, C.G., Baillie, G.S., Jaganath, D., Havekes, R., Daniels, A., Wimmer, M., Huang, T., Brown, K.M., Li, X.Y., Descalzi, G.*, et al.* (2009). Sleep deprivation impairs cAMP signalling in the hippocampus. Nature *461*, 1122-1125.

Vecsey, C.G., Peixoto, L., Choi, J.H., Wimmer, M., Jaganath, D., Hernandez, P.J., Blackwell, J., Meda, K., Park, A.J., Hannenhalli, S.*, et al.* (2012). Genomic analysis of sleep deprivation reveals translational regulation in the hippocampus. Physiol Genomics *44*, 981-991.

Xia, F., Richards, B.A., Tran, M.M., Josselyn, S.A., Takehara-Nishiuchi, K., and Frankland, P.W. (2017). Parvalbumin-positive interneurons mediate neocortical-hippocampal interactions that are necessary for memory consolidation. eLife *6*, e27868.

Xu, X., Wells, A.B., O'Brien, D.R., Nehorai, A., and Dougherty, J.D. (2014). Cell Type-Specific Expression Analysis to Identify Putative Cellular Mechanisms for Neurogenetic Disorders. J Neurosci *34*, 1420-1431.

# Chapter V. Discussion

## 5.1 Summary & Future Directions

Sleep is known to play a critical role in multiple forms of learning and memory. Less understood are the cellular and circuit level mechanisms supporting consolidation during sleep. The present work addresses these questions within the context of a well-studied form of hippocampus-mediated memory consolidation (CFC/CFM), using genetic tools developed for use in mice.

Previous work has suggested that sleep preferentially drives protein translation [1, 2] thereby supporting hippocampal memory consolidation [3]. In **Chapter 2**, we provided the first demonstration that SD may have differential effects on translation of plasticity-associated mRNAs in the hippocampus vs. cortex. Specifically, we found that expression of Arc, which is necessary for many forms of synaptic plasticity, is reduced in DG of the dorsal hippocampus after SD, while its abundance simultaneously increases in neocortex [4].

In **Chapter 3**, we identified differences in hippocampal ribosome-associated mRNAs in Sleep or SD mice following CFC. To capture which mRNAs are selectively translated following CFC, we used translating ribosome affinity purification (TRAP) to immunoprecipitate cytosolic and membrane-bound (MB) ribosomes from both excitatory (Camk2a+) and activated (pS6+) neurons (**Figure 3.1**). Our sequencing results revealed that cytosolic ribosomes encoded mainly cytosol-localized transcripts (e.g., transcription factors, kinases, RNA polymerase-related genes) whereas MB ribosomal transcripts

enriched for subcellularly trafficked mRNAs (e.g. transmembrane receptors, secreted molecules, endoplasmic reticulum genes) (**Figure 3.2, 3.3**). This confirmed previous reports that have shown MB-ribosomes preferentially immunoprecipitate endoplasmic reticulum-bound ribosomes and enrich in secretory-pathway associated mRNAs [5]. Using this strategy, we quantified mRNAs associated with two differentially localized ribosome pools (cytosolic, MB) in hippocampal excitatory (Camk2a+) and activated (pS6+) neurons.

Results from our sequencing experiments found that SD strongly increased the expression of cytosolic mRNAs involved in synaptic plasticity but were mostly unaffected by CFC (**Figure 3.4, Figure 3.5**). MB ribosomes, in contrast, displayed significant differences in bound transcripts following CFC but were relatively unaltered by SD (**Figure 3.8**). Interestingly, differences in transcripts bound to MB ribosomes was influenced by an animals behavioral state if learning preceded it. In hippocampal excitatory (Camk2a+) neurons, 2,396 MB ribosome-associated transcripts were altered in SD mice whereas only 840 were changed mice permitted sleep (**Figure 3.4**). Although CFC altered similar MB transcripts following CFC, SD displayed unique alterations in transcripts coding for lipid biosynthesis and carbohydrate metabolism (**Figure 3.8, 3.9**). Our data suggests that CFC may induce a metabolic burden that is exacerbated by SD. Moreover, this difference was only observed in MB ribosomes, suggesting that the metabolic demand may occur in a trafficked region of the neuron (e.g., axon or dendrites). Recent reports have shown that ~67% of forebrain-derived synaptoneurosome mRNAs are regulated by the circadian clock while their translation is dependent on subsequent

sleep [6]. Future directions will need to address how mRNAs are trafficked during sleep and through what mode of regulation impaired.

There has been significant debate regarding the contributions of sleep to the synaptic consolidation of previously learned memories [7]. Previous microarray studies have found that sleep-deprivation promotes the expression of activity-dependent plasticity genes both in the neocortex [8] and hippocampus [9] (**Figure 2.1**). Similarly, we also observed increased expression of plasticity genes in whole hippocampus, excitatory neurons, and activated neurons, particularly in the cytosolic fraction (**Figure 3.4, Figure 3.5**). Consistent with waking being associated with changes in synaptic plasticity, the most consistently altered upstream regulator present across all cell populations was CREB (**Figure 3.6**). CREB (cAMP-response element binding protein) is a transcription factor activated by neuronal activity and subsequent second messenger signals. CREB plays a critical role in coordinating waves of gene transcription to increase both the intrinsic excitability and synaptic strength of CREB-expressing neurons. Furthermore, CREB has been shown to be involved in multiple forms of hippocampus-dependent memories including contextual fear conditioning, inhibitory avoidance training, and different forms of spatial memory [21].

Thus during SD, CREB-mediated transcription promotes the expression of synaptic plasticity genes which are also involved in memory encoding. Less understood are the transcripts that persist late into the consolidation phase and may be preferentially translated during sleep. To identify such transcripts, we assessed the impact of CFC in Sleep and SD rodents separately. At cytosolic Camk2a+ ribosomes, we observed 21 genes altered by CFC in rodents allowed to sleep whereas only 2 transcripts were

different in SD mice (**Figure 3.5**). Indeed, 70% of the transcripts altered by CFC were also altered by SD. Our analysis identified two activity-dependent splice isoforms (*ΔFosB* and *Homer1a*), whose expression remained elevated at 3- and 5-h following CFC in both Sleep and SD rodents. Results demonstrated that *ΔFosb* and *Homer1a* were detectable in both activated (pS6+) neurons and whole hippocampal mRNA (Input+) **Figure 3.7**). Critically, in excitatory hippocampal neurons (Camk2a+), expression of *ΔFosb* and *Homer1a* was readily observable in mice permitted to sleep and completely occluded in SD mice (**Figure 3.7**). Our data supports the idea that the allocation of memories to neural circuits is supported by reduced expression of plasticity genes during subsequent sleep. Experiments testing the role of *ΔFosb* in CFC have found that both blocking and over-expression of *ΔFosb* in the dorsal hippocampus is sufficient to impair recall [10]. It may be that 5-h SD is sufficient to impair to the sparse allocation of plasticity genes necessary for accurate memory retrieval.

In **Chapter 4**, we used data from our TRAP experiment to profile cells differentially activated by SD. WGCNA-derived clusters of pS6-TRAPed transcripts revealed an enrichment of GABAergic genes (*Gad1, Dlx1, Nxhp1*) as well as co-expressed neuropeptide transcripts (*Sst, Crhbp, Crh, Npy*) in SD mice (**Figure 4.2**). These results led us to hypothesize that hippocampal somatostatin (SST) interneurons are activated by SD. SST neurons are a subgroup of dendrite-projecting GABAergic neurons and include oriens-lacunosum/moleculare (O-LM) cells, bistratified cells, and long-range projecting cells [11]. Previous experiments in the mouse hippocampus have shown that SST S6 phosphorylation is positively correlated with increased activity and memory formation [12].

To assess the influence of SD on SST activity, we performed qPCR on SST-derived ribosomes. We observed significant elevations in the activity-dependent gene *cFos* and the potassium voltage-gated channel member (*Kcnf1*), linking intracellular activity to SD (**Figure 4.3**). Since intracellular activity was elevated in SST interneurons and elevated expression of cFos is linked to increased CREB transcription, we decided to look at other CREB targets including the neuropeptides *Sst, Npy,* and *Crhbp* [13]. Surprisingly, we observed reduced levels of *Sst, Npy,* and *Crhbp* at SST-ribosomes (**Figure 4.3**). Results from SST interneurons mirror SD effects observed in pyramidal neurons of the hippocampus. Sequencing results consistently reveal CREB-based transcriptional programs are heightened during wake while intracellular levels of the cAMP are higher in sleep [14] and phosphorylated CREB is higher during REM sleep [15].

To test the location of elevated SST activity during SD, we performed pS6+/SST co-localization experiments and observed elevated pS6+ SST interneurons in the hilus of the hippocampus (**Figure 4.4**). Hilar somatostatin interneurons have been studied extensively and are referred to as hilar perforant path associated neurons (HIPP cells) [16]. HIPP cells project to the distal dendrites of granule neurons and can inhibit activity through both GABA and SST release [17]. Previous research has demonstrated that HIPP cells control the size of DG memory ensembles. Chemogenetically increasing activity in this population decreases cFos+ neurons in the DG, similar to what we observed following 3 h of SD in Arc+ (**Figure 2.3**, **Figure 2.4**), and pS6+ (**Figure 4.1, Figure 4.4**) DG neurons. Experiments have found that manipulating SST during CFC training was sufficient to impair memory *encoding* whereas reducing activity improved learning [18,

19]. To test whether reduced SST activity is necessary for sleep-dependent memory *consolidation*, we injected CNO immediately following CFC to maintain constitutive SST activity through the sleep period (mimicking the effects of SD). We found that mice with increased SST activity (hM3Dq) displayed reduced freezing than mCherry controls (**Figure 4.5**). Validating our manipulation two weeks following the experiment, 3hrs following injection with CNO, SST-hM3Dq mice displayed increased cFos+ SST neurons and reduced cFos+ DG neurons (**Figure 4.5**). These experiments strongly suggest that SST-HIPP cells reduce their activity during sleep to support memory consolidation. HIPP cells may serve as a gate by constitutively limiting plasticity during wake, acting to filter out irrelevant information. Indeed, SST activity in CA1 has been shown to filter out unconditioned stimulus (US) to selectively process the conditioned stimulus (CS) while encoding conditioned suppression of water licking [20]. Thus during sleep, reduced SST activity may permit sharp-wave ripple oscillations [22] and hippocampal-cortical communication [23] necessary for sleep-dependent consolidation of CFM.

In sum my thesis has investigated the cellular and circuit level mechanisms involved in sleep-dependent memory consolidation. At the cellular level, RNA-sequencing analyses of ribosome-bound transcripts found that sleep and learning alter distinct pools of ribosomes in hippocampal neurons. SD strongly influenced the expression of cytosolic synaptic plasticity genes and occluded subsequent gene expression following CFC. Future studies will need to identify the specific compartments of hippocampal circuits where ΔFosB and Homer1a are allocated and confirm the loss of signal-to-noise following extended wakefulness. In MB-transcripts, we find that CFC promulgated similar gene expression profiles in both Sleep and SD mice. Interestingly, SD mice also displayed

altered levels of biochemical genes bound to MB-ribosomes following CFC. Future studies are needed to determine which biological process are driving changes in these pathways to better understand how SD-may interfere with translation at the endoplasmic reticulum, dendrites, or axons. At the circuit level, pS6 cell type analysis revealed that hippocampal somatostatin interneurons are activated by SD. Confirming elevated activity through IHC, SST-TRAP, and pS6-profiling at 5h, hilar SST interneurons appear to be constitutively activated during wake. Increasing SST activity during sleep impaired both network activity in the dentate gyrus and CFM consolidation whereas reducing hippocampal cholinergic input increased DG network activity and improved memory retention. Thus our data suggests that cholinergic activity may serve as a brake on plasticity in the hippocampus during wake. We believe that cholinergic neuromodulation may work through SST interneurons although we were unable to provide a direct link between the two. Future studies are needed to further clarify the relationship between reduced SST activity during sleep to understand the unique systems consolidation events it supports.

## 5.2 References


1. Ramm, P., and Smith, C.T. (1990). Rates of cerebral protein synthesis are linked to slow-wave sleep in the rat. Physiol.Behav. *48*, 749-753.

2. Nakanishi, H., Sun, Y., Nakamura, R.K., Mori, K., Ito, M., Suda, S., Namba, H., Storch, F.I., Dang, T.P., Mendelson, W., et al. (1997). Positive correlations between cerebral protein synthesis rates and deep sleep in Macaca mulatta. Eur J Neurosci *9*, 271-279.

3. Tudor, J.C., Davis, E.J., Peixoto, L., Wimmer, M.E., van Tilborg, E., Park, A.J., Poplawski, S.G., Chung, C.W., Havekes, R., Huang, J., et al. (2016). Sleep deprivation impairs memory by attenuating mTORC1-dependent protein synthesis. Sci Signal *9*, ra41.

4. Delorme, J.E., Kodoth, V., and Aton, S.J. (2019). Sleep loss disrupts Arc expression in dentate gyrus neurons. Neurobiol Learn Mem *160*, 73-82.

5. Kratz, A., Beguin, P., Kaneko, M., Chimura, T., Suzuki, A.M., Matsunaga, A., Kato, S., Bertin, N., Lassmann, T., Vigot, R., et al. (2014). Digital expression profiling of the compartmentalized translatome of Purkinje neurons. Genome Res *24*, 1396-1410.

6. Noya, S.B., Colamea, D., Bruning, F., Spinnler, A., Mircsof, D., Opitz, L., Mann, M., Tuagarajen, S.K., Robles, M.S., and Brown, S.A. (2019). The Forebrain Synaptic Transcriptome Is Organized by Clocks but Its Proteome Is Driven by Sleep Science *366*.

7. Klinzing, J.G., Niethard, N., and Born, J. (2019). Mechanisms of systems memory consolidation during sleep. Nature Neuroscience *22*, 1598-1610.

8. Cirelli, C., Gutierrez, C.M., and Tononi, G. (2004). Extensive and divergent effects of sleep and wakefulness on brain gene expression. Neuron *41*, 35-43.

9. Vecsey, C.G., Peixoto, L., Choi, J.H., Wimmer, M., Jaganath, D., Hernandez, P.J., Blackwell, J., Meda, K., Park, A.J., Hannenhalli, S., et al. (2012). Genomic analysis of sleep deprivation reveals translational regulation in the hippocampus. Physiol Genomics *44*, 981-991.

10. Eagle, A.L., Gajewski, P.A., Yang, M., Kechner, M.E., Al Masraf, B.S., Kennedy, P.J., Wang, H., Mazei-Robinson, M.S., and Robison, A.J. (2015). Experience-Dependent Induction of Hippocampal ΔFosB Controls Learning J Neurosci *35*, 13773-13783.

11. Pelkey, K.A., Chittajallu, R., Craig, M.T., Tricoire, L., Wester, J.C., and McBain, C.J. (2017). Hippocampal GABAergic Inhibitory Interneurons. Physiol Rev *97*, 1619-1747.

12. Artinian, J., Jordan, A., Khlaifia, A., Honore, E., La Fontaine, A., Racine, A.S., Laplante, I., and Lacaille, J.C. (2019). Regulation of Hippocampal Memory by mTORC1 in Somatostatin Interneurons. J Neurosci *39*, 8439-8456.

13. Benito, E., Valor, L.M., Jimenez-Minchan, M., Huber, W., and Barco, A. (2011). cAMP Response Element-Binding Protein Is a Primary Hub of Activity-Driven Neuronal Gene Expression. J Neurosci *31*, 18237-18250.

14. Vecsey, C.G., Baillie, G.S., Jaganath, D., Havekes, R., Daniels, A., Wimmer, M., Huang, T., Brown, K.M., Li, X.Y., Descalzi, G., et al. (2009). Sleep deprivation impairs cAMP signalling in the hippocampus. Nature *461*, 1122-1125.

15. Luo, J., Phan, T.X., Yang, Y., Garelick, M.G., and Storm, D.R. (2013). Increases in cAMP, MAPK Activity, and CREB Phosphorylation during REM Sleep: Implications for REM Sleep and Memory Consolidation. J Neurosci *33*, 6460-6468.

16. Tallent, M.K. (2007). Somatostatin in the dentate gyrus. Prog Brain Res *163*, 265-284.

17. Barrata, M.V., Lamp, T., and Tallent, M.K. (2002). Somatostatin Depresses Long-Term Potentiation and Ca2+ Signaling in Mouse Dentate Gyrus. J Neurophys *88*, 3078-3086.

18. Stefanelli, T., Bertollini, C., Luscher, C., Muller, D., and Mendez, P. (2016). Hippocampal Somatostatin Interneurons Control the Size of Neuronal Memory Ensembles. Neuron *89*, 1074-1085.

19. Raza, S.A., Albrecht, A., Caliskan, G., Muller, B., Demiray, Y.E., Ludewig, S., Meis, S., Faber, N., Hartig, R., Schraven, B., et al. (2017). HIPP neurons in the dentate gyrus mediate the cholinergic modulation of background context memory salience. Nat Communications *8*.

20. Lovett-Barron, M., Kaifosh, P., Kheirbek, M.A., Danielson, N., Zaremba, J.D., Reardon, T.R., Turi, G.F., Hen, R., Zemelman, B.V., and Losonczy, A. (2014). Dendritic Inhibition in the Hippocampus Supports Fear Learning Science *343*, 857-863.

21. Benito, E., and Barco, A. (2010). CREB's control of intrinsic and synaptic plasticity: implications for CREB-dependent memory models 33(5), 230-240

22. Katona L., Lapray, D., Viney, T., Oulhaj, A., Borhegyi, Z., Micklem, B., Klausberger, T., and Somogyi, P. (2014). Sleep and Movement Differentiates Actions of Two Types of Somatostatin-Expressing GABAergic Interneuron in Rat Hippocampus *82*, 872-886

23. Abbas, A., Sundiang, M., Henoch, Britt., Morton, M., Bolkan, S., Park, A., Harris, A., Kellendonk, C., and Gordon, J. (2018). Somatostatin Interneurons Facilitate Hippocampal-Prefrontal Synchrony and Prefrontal Spatial Encoding, 100, 926-939